

**Copyright**

**by**

**Charles Stephen Pool**

**2010**

The Thesis committee for Charles Stephen Pool

Certifies that this is the approved version of the following thesis:

**Effect of Galvanization on the Fatigue Strength of High Mast  
Illumination Poles**

**APPROVED BY  
SUPERVISING COMMITTEE:**

**Supervisor:**

\_\_\_\_\_  
Karl H. Frank

\_\_\_\_\_  
Todd A. Helwig

\_\_\_\_\_  
Howard M. Liljestrand

**Effect of Galvanization on the Fatigue Strength of High Mast  
Illumination Poles**

by

**Charles Stephen Pool, B.S.**

**Thesis**

Presented to the Faculty of the Graduate School  
of the University of Texas at Austin  
in Partial Fulfillment  
of the Requirements  
for the Degree of

**Master of Science in Engineering**

The University of Texas at Austin  
May 2010

*I dedicate my work to:  
My sisters, who have always been there for me  
My parents, for always believing in me  
And my grandparents, for showing me what hard work can bring*

## **Acknowledgements**

I would like to begin by acknowledging the efforts of the Texas Department of Transportation, whose funding and hard work have made this project a reality. In particular I would like to thank Michael Smith, Vijayan Pillai, and Tim Bradberry for their help and dedication.

I would like to thank the researchers who paved the way ahead of me. I've learned a lot from the wisdom and hijinks of Nick Richman and Andrew Stam. Also, those that are finishing this project, James Kleineck and Luca Magenes, deserve much credit despite the fact that I told them I would not include them in my acknowledgements.

I must thank all of the lab technicians and staff at Ferguson lab, because without their help nothing would ever get done.

Finally, thanks to Dr. Frank and Dr. Helwig. You both have taught me a lot and I will always be grateful to have had such great professors as advisors. Good luck Dr. Frank in your post academia career.

Stephen  
May 2010

# **Effect of Galvanization on the Fatigue Strength of High Mast Illumination Poles**

by

Charles Stephen Pool, M.S.E

The University of Texas at Austin, 2010

SUPERVISOR: Karl H. Frank

This research investigation studied the effects of galvanization on the fatigue life of high mast illumination poles. Reports that galvanization of high masts caused initial cracks to form at the toe of the weld connecting the base plate to the shaft of the pole were first validated. The effects of these initial cracks on fatigue strength were then checked through experimental testing.

A variety of variables were tested for both their effects on the occurrences of the initial cracks and effects on fatigue life. These variables included testing galvanized against ungalvanized specimens, testing of varying fabricators and galvanizers, and testing of various types of connection details. These test results were compared against inspection results provided by Texas Department of Transportation inspectors.

Also, methods of mitigating the effects of toe cracks on the fatigue life of poles were investigated. A method for repairing specimens both in the fabrication shop and in the field were developed and tested. Both methods showed strong improvement in fatigue life of the specimens providing a possible repair solution.

# Table of Contents

<b>1 Investigation Introduction and Background</b> .....	1
1.1 Introduction.....	1
1.2 Background.....	3
1.3 Previous Research.....	8
1.3.1 Initial Fatigue Study.....	8
1.3.2 Pooled Fund Study.....	9
1.4 Literature Survey.....	13
1.4.1 Valmont Industries Paper.....	13
1.4.2 GalvaScience Paper.....	15
1.5 Research Approach.....	16
<b>2 Test Specimen Design</b> .....	17
2.1 Introduction.....	17
2.2 Naming Scheme.....	18
2.3 Typical Specimen Design.....	19
2.4 Specimens 33-3-12-TX-SG-A and 33-3-12-TX-SB-B.....	23
2.5 Specimens 33-3-12-TX-VG-A and 33-3-12-TX-VG-B.....	26
2.6 33-3-12-TXEC-SG-A and 33-3-12-TXEC-SG-B.....	28
2.7 Weld Repair Specimens.....	31
2.7.1 Shop Repair Specimen.....	33
2.7.2 Field Repair Specimen.....	36
<b>3 Testing</b> .....	39
3.1 Introduction.....	39
3.2 Non Destructive Testing.....	39
3.2.1 Magnetic Particle Testing.....	39
3.2.2 Ultrasonic Testing.....	43
3.3 Fatigue Testing.....	45
3.3.1 Test Setup.....	46

3.3.1.1 Load Box and Connection.....	49
3.3.1.2 Hydraulic and Control Systems.....	50
3.3.2 Fatigue Testing Procedure.....	51
3.3.2.1 Measurement and Inspection.....	51
3.3.2.2 Installation Procedure.....	51
3.3.2.3 Testing Loads and Displacements.....	53
3.4 Follow-up Inspection and Destructive Testing.....	55
<b>4 Testing Results.....</b>	<b>56</b>
4.1 Introduction.....	56
4.2 Specimens 33-3-12-TX-SG-A and 33-3-12-TX-SB-B.....	56
4.2.1 Ultrasonic Test Results.....	57
4.2.2 Fatigue Test Results.....	59
4.2.3 Destructive Test Results.....	61
4.2.3.1 Bend 5.....	61
4.2.3.2 Bend 12.....	64
4.2.3.3 Bend 8 and Bend 9.....	64
4.3 Specimens 33-3-12-TX-VG-A and 33-3-12-TX-VG-B.....	67
4.3.1 Ultrasonic Test Results.....	67
4.3.2 Fatigue Test Results.....	68
4.3.3 Destructive Test Results.....	73
4.4 Weld Repair Specimens.....	76
4.4.1 Ultrasonic Test Results.....	76
4.4.2 Fatigue Test Results.....	76
4.4.3 Destructive Test Results.....	79
4.5 Specimens 33-3-12-TXEC-SG-A and 33-3-12-TXEC-SG-B.....	79
4.5.1 Ultrasonic Test Results.....	79
4.5.2 Fatigue Test Results.....	81
4.5.3 Destructive Test Results.....	82
4.6 Ultrasonic Testing Results Comparison.....	83
4.6.1 Specimen Comparison.....	83
4.6.2 Detail Comparison Including TxDOT Inspections.....	84



4.7 Fatigue Test Comparisons .....	87
<b>5 Conclusions .....</b>	<b>89</b>
5.1 Ultrasonic Testing Conclusions .....	89
5.2 Fatigue Testing Conclusions .....	90
5.3 Destructive Testing Conclusions .....	90
5.3 Future Work .....	90
<b>Appendix A Recommended Installation Procedure .....</b>	<b>92</b>
<b>References .....</b>	<b>95</b>
<b>Vita.....</b>	<b>96</b>

## Chapter 1 Investigation Introduction and Background

### 1.1 Introduction

High mast illumination poles are often used to provide lighting at highway interchanges as well as sports venues, parking lots, and penitentiaries (Rios, 2007). A recent review of the Texas Department of Transportation (TxDOT) inventory of high mast illumination poles (HMIP's) has found evidence of shallow cracks between the base plate and the shaft in their in situ poles. The cracks generally have occurred at the toe of the weld connecting the shaft to the base plate as shown in Figure 1.1. No failures of a TxDOT HMIP have occurred, concerns have arisen from failures of similar poles in other states and in the private sector.

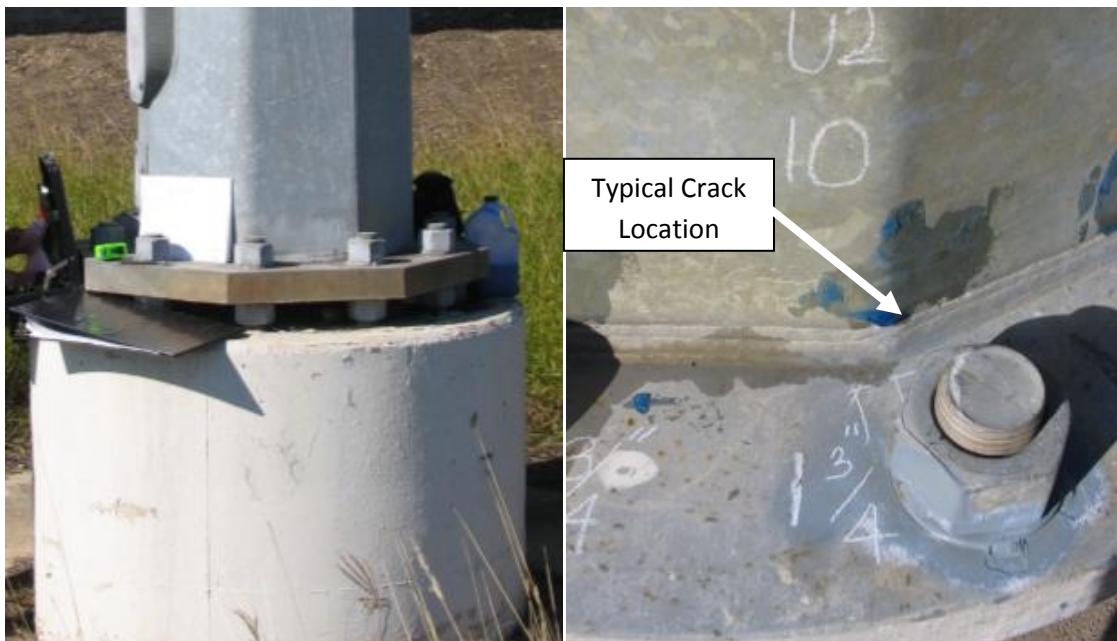


Figure 1.1 TxDOT Testing of In-Situ High Mast Illumination Pole

A primary reason for this concern is that these poles are located in congested areas with a high amount of human activity. A typical HMIP location around an interchange is shown in Figure 1.2. A failure could easily result in loss of life or a high amount of financial liability. This

concern coupled with the lack of redundancy inherent in the cantilevered poles has led to the inquiry into their safety.



Figure 1.2 Typical High Mast Towers around a Highway Interchange (Rios, 2007)

Previous investigations done at the University of Texas into cracking at the base plate in high mast illumination poles has centered on the effects of fatigue induced cracking as the initiator of failures (Stam, 2009) (Rios, 2007) (Koenigs, 2003). These investigations noticed at an early stage a lower fatigue life in specimens that had been galvanized compared to those that had not been galvanized. A link between galvanizing of the metal components and the finding of cracks at the toes of the welds before the components entered service has been previously documented (Kinstler, 2006) (Aichinger, 2006). These initial toe cracks could be an initiator for the fatigue cracks and the primary reason for the reduced fatigue life of galvanized samples.

Currently, very little research exists on the problem of cracking caused by galvanizing in high mast illumination poles, primarily due to the difficult nature inherent in investigating these cracks. There are a number of aspects that complicate the problem including the following:

- The cracks do not show up until after the galvanizing process has taken place. There are not set criteria that have been identified that regularly produce this phenomenon.
- The irregularity of the event, with the cracks showing up in one detail and not in another.
- A large number of these occurrences go unreported and undocumented, making it difficult to perform a statistical study.
- Finally, the problem is extremely complex and includes a number of variables that seem to have an affect the occurrence of cracking (Kinstler, 2006).

The goals for this investigation include determining the extent of the cracking, identifying possible causes of the cracking as well as which cracks warrant further scrutiny, and finally what should be done with the cracks. A large portion of this investigation has focused on the differences between ungalvanized and galvanized HMIP's and whether or not the galvanizing leads to a cracking problem. Also, methods for finding and categorizing cracks are investigated as a means of determining the extent of the cracking problem.

## 1.2 Background

Tall cantilevered monotube steel structures known as high masts are frequently used as an integral part of transportation networks to provide illumination over large areas. High masts such as the one shown in Figure 1.3 are generally designed to be as light as possible in order to be efficient as well as aesthetically pleasing.



Figure 1.3 Tall Cantilever Design of High Mast Illumination Pole

The design of high mast light structures is covered by *Standard Specifications for Structural Supports for Highway Signs, Luminaries, and Traffic Signals* published by the American Association of State Highway and Transportation Officials (AASHTO). Throughout this thesis, this standard for HMIP's will be referred to as the AASHTO Specification. The fatigue design in this AASHTO Specification is governed by Section 11.5 which states that all components shall be designed to accommodate fatigue stresses within their constant amplitude fatigue limits (CAFL). The CAFL represents a stress range that the structure or component of the structure can withstand for an infinite number of cycles. In theory, stress ranges over the CAFL are damaging cycles to the structure and, therefore result in a finite fatigue life to the structure. The CAFL is used for design because the number of cycles and stress ranges caused by wind loading is nearly impossible to predict, making the calculation of a finite life unreliable. A simple table listing different connection details is shown in the AASHTO Specification giving a fatigue category next to each detail. This fatigue category, signified by a letter rating, has an associated CAFL stress range that the structure should be designed not to exceed under its normal operating conditions.

Previous concerns have arisen about the possibility of the galvanizing process causing cracks in HMIP's at the location where the shaft is connected to the base plate (Kinstler, 2006) (Aichinger, 2006). More recently, TxDOT was informed by a third party of the possible existence of cracks in galvanized HMIP's before they enter service. Worried that their poles may not meet fatigue design requirements due to these cracks, TxDOT began its own internal investigation into the matter and came up with mixed results. Normal ultrasonic testing of the poles as prescribed by AWS D1.1 did not indicate the existence of these cracks. The third party explained their technique for finding the cracks, which involved different testing equipment and procedures. Through the use of this enhanced ultrasonic testing procedure TxDOT inspectors were able to find faint indications of cracking at the toe of the weld connecting the shaft of the pole to the base plate. These enhanced ultrasonic testing procedures will be further discussed in Chapter 3. A typical ultrasonic inspection is shown in Figure 1.4. No other form of testing was able to verify these findings, so research on the fatigue performance of the poles was initiated at the University of Texas.



Figure 1.4 Ultrasonic Testing Performed by a TxDOT Inspector

Concurrent with the research being done by the University of Texas, TxDOT has begun an effort to take an inventory of in-service poles throughout the state to determine the extent of cracking. Table 1.1 shows the most current assessment of TxDOT HMIP's. This table represents only a small sample of their population of poles, but it begins to offer insight into possible variables that may affect the likelihood of cracks.

HMIP Weld Toe Crack Survey		X	Cracks found										
		√	No cracks found										
12 Sided													
Dimensions				No Ground Sleeve					Ground Sleeve				
Height	Thick (in)	Dia. (in)	Dia/Th	Location	No. of HMIPs UTd	Cracked Poles No.	% Cracked	% Bends Cracked	Location	No. of HMIPs	Cracked Poles No.	% Cracked	
80 mph	100'	0.313 (5/16)	24.625	78.67412	Shop				Shop				
					Lab				Lab				
					Field	3	2	67	8.3	Field			
	125'	0.313 (5/16)	28.25	90.25559	Shop				Shop				
					Lab				Lab				
					Field	3	1	33	11.1	Field	1	1	100
	150'	0.313 (5/16)	32.625	104.2332	Shop				Shop	2	2	100	21
					Lab	4	4	100	54	Lab			
					Field	13	13	100	52	Field	1	1	100
	175'	0.375 (3/8)	36.25	96.66667	Shop				Shop				
					Lab				Lab				
					Field	17	9	53	58	Field	1	1	100
100 mph	100'	0.375 (3/8)	25.5	68	Shop				Shop				
					Lab				Lab				
					Field				Field				
	125'	0.438 (7/16)	29.125	66.49543	Shop				Shop				
					Lab				Lab				
					Field	26	0	0	0	Field			
	150'	0.438 (7/16)	33.75	77.05479	Shop				Shop				
					Lab				Lab				
					Field	12	5	42	6.24	Field	4	2*	50
	175'	0.5 (1/2)	37.375	74.75	Shop	10	0	0	0	Shop			
					Lab				Lab				
					Field				Field				

\* Two HMIPs with required 7/16" ground sleeves did not crack. Two HMIPs mis fabricated with 3/8" ground sleeves cracked.

Table 1.1 Survey of High Mast Illumination Pole Performed by Texas Department of Transportation (provided by TxDOT)

Figure 1.5 identifies the typical nomenclature that is used to identify elements on the pole shaft. The term "bend" references a location of cold working on the pole shaft, done to give the pole its polygonal shape. A "flat" is the area in between the bends. The location of a longitudinal weld seam is also considered a bend, despite the fact that it does not undergo cold working.

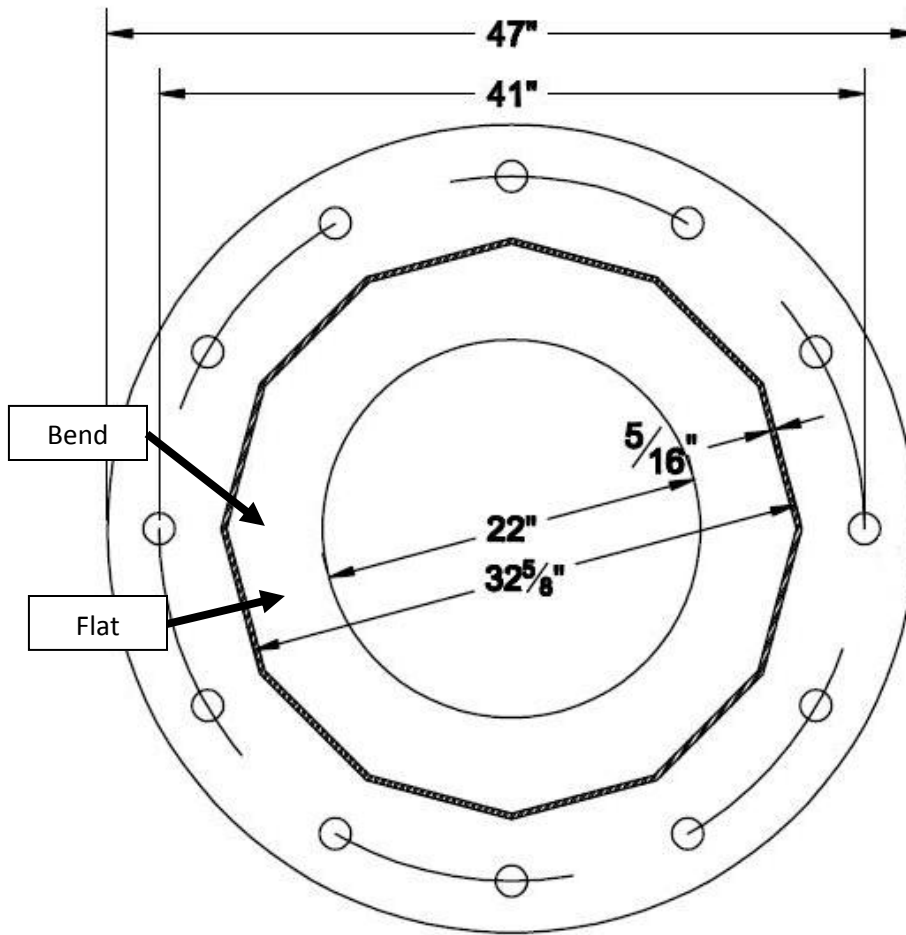


Figure 1.5 Bend and Flat Naming Convention

In Table 1.1, “Shop” represents poles that are tested at the fabrication shop, after galvanizing but before installment in the field. “Lab” represents test specimens used by the University of Texas and they are similar to “Shop” since they have been tested after galvanizing but prior to being installed and fatigue tested. Finally, “Field” denotes specimens that have been installed and were later tested for cracks. There are two ways to look at this data, either the percentage of poles with cracked bends, or the percentage of bends cracked. It should be noted that “Cracked Bends” are merely indications found from ultrasonic testing of poles, and that verification of the cracking or cause of the cracking has not been confirmed for field specimens. The percentage of bends cracked is a ratio of number of cracked bends to number of bends investigated. Looking at the



percentage of poles with cracked bends helps to identify manufacturer tendencies, but looking at the percentage of bends cracked is better for identifying how geometry acts as a variable in initial cracks.

One key variable that this table notes is the ratio of the diameter of the pole at its base to the thickness of the shaft of the pole. Previous research indicated that the weight ratio of the base plate to the first 12 inches of shaft of the pole corresponded to the likelihood of finding initial cracking (Aichinger, 2006). The ratio of the diameter of the pole to the thickness of the pole provides similar information. It can be seen that for lower ratios, in the 65-80 range, the percentage of bends with cracks is low. This percentage rises steeply once the ratios reach 95. In this table, the ground sleeve is not included as a part of this variable, but rather an independent attachment. Poles with ground sleeves consistently had lower percentages of cracked bends than their counterpart designs without ground sleeves. This data is used for comparison later in the results chapter.

### 1.3 Previous Research Conducted at the University of Texas

#### 1.3.1 Initial Fatigue Study

Fatigue testing of monotube steel structures at the University of Texas began several years ago with the testing of smaller mast arm structures, similar to what is used for the structure in traffic signals (Koenigs, 2003). The specimens tested in this investigation were initially all left uncoated in the first phase of the project to decrease the cost of the specimens. It was later decided to test two galvanized specimens in the second phase of the study to see what effect the coating has on the fatigue behavior.

Figure 1.6 shows the results of these fatigue tests for geometrically similar mast arms. All of the data shown on this chart were from 10" diameter poles with a 1.5" thick base plate. These specimens were tested in a similar fashion to this investigation's high mast tests, which is detailed in Chapter 2. It can be seen on this graph that galvanized specimens had fatigue lives less than category E' while ungalvanized specimens had fatigue lives of E' or better. The study concluded

that the galvanizing had a negative effect on the fatigue life of specimens, reducing the average fatigue life by roughly half. This study recommended that future studies should use galvanized poles for testing so that the results would not be unconservative.

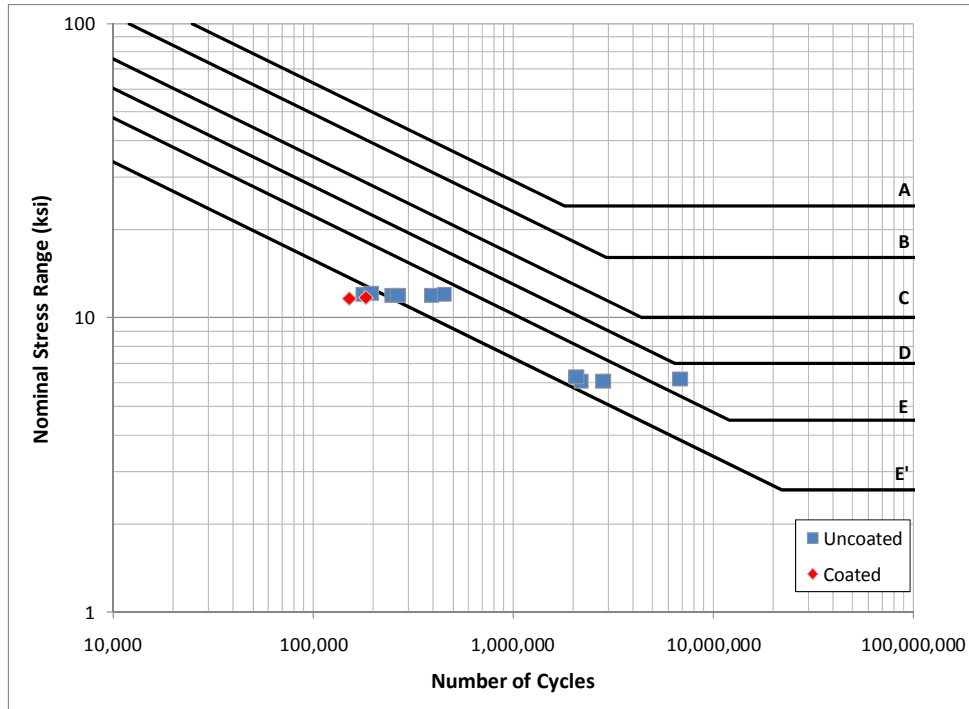


Figure 1.6 Initial Fatigue Study Results of Galvanized Specimens vs. Ungalvanized Specimens

### 1.3.2 Pooled Fund Study

Another study was conducted at the University of Texas utilizing the pooled resources of several states to help determine the variables effecting fatigue life of high masts and mast arms so that an optimal design could be determined. Utilizing Koenigs's original research, it was decided that all test specimens would be galvanized prior to testing to obtain a lower bound fatigue life (Anderson, 2007) (Rios, 2007). Only one pair of ungalvanized HMIP's was tested in this study, and these specimens used a connection that was not replicated in a galvanized specimen.

Although there were no comparable HMIP's to study, one pair of the smaller mast arm specimens from Koenigs's previous research were comparable to several mast arm specimens from this

study. Also, a few ungalvanized mast arm specimens were tested for comparison during the study. Figure 1.7, Figure 1.8, and Figure 1.9 show results of uncoated and coated galvanized specimens for three different designs. It can be seen from these graphs that, although not always outperforming the galvanized samples, the ungalvanized samples did on average perform better than the galvanized samples. The study concluded that, like in Koenigs's study, galvanizing had an impact in the fatigue life of a mast arm (Richman, 2009). No attempt was made to determine the reason for this behavior in this study.

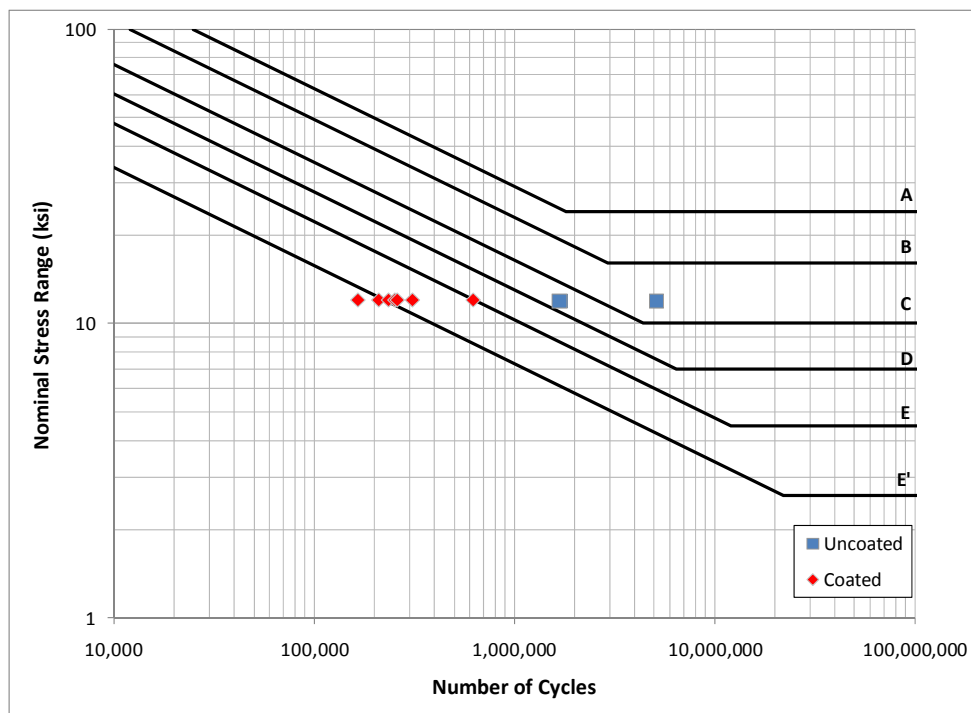


Figure 1.7 Fatigue Results of 10" Mast Arm with 2" Base Plate and Socketed Connection

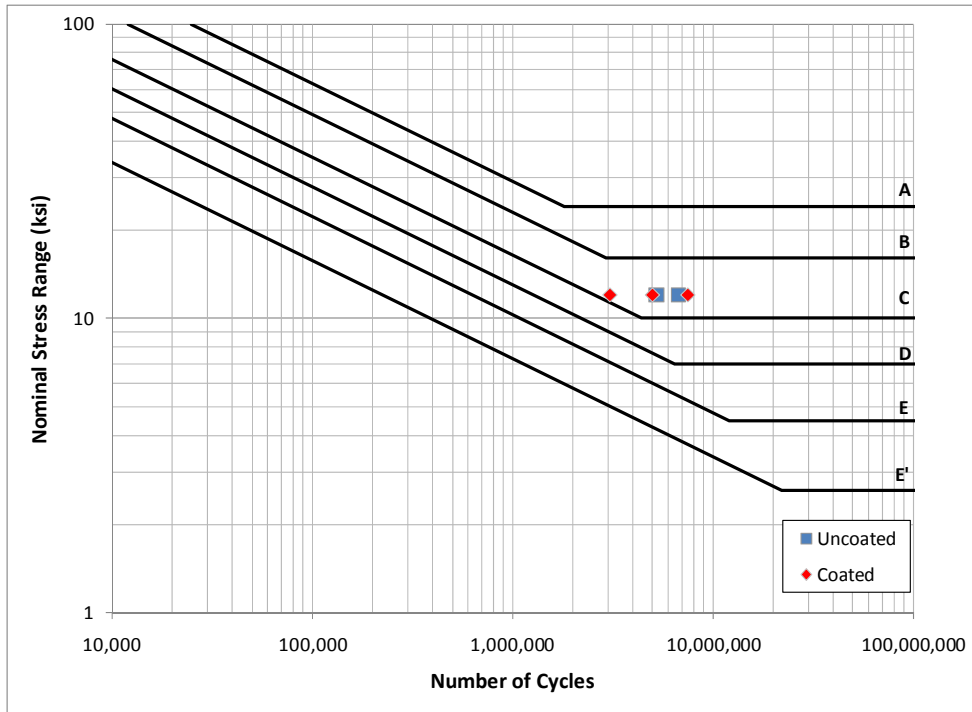


Figure 1.8 Fatigue Results of 10" Diameter Mast Arms with a 2" Base Plate and Full Penetration Weld

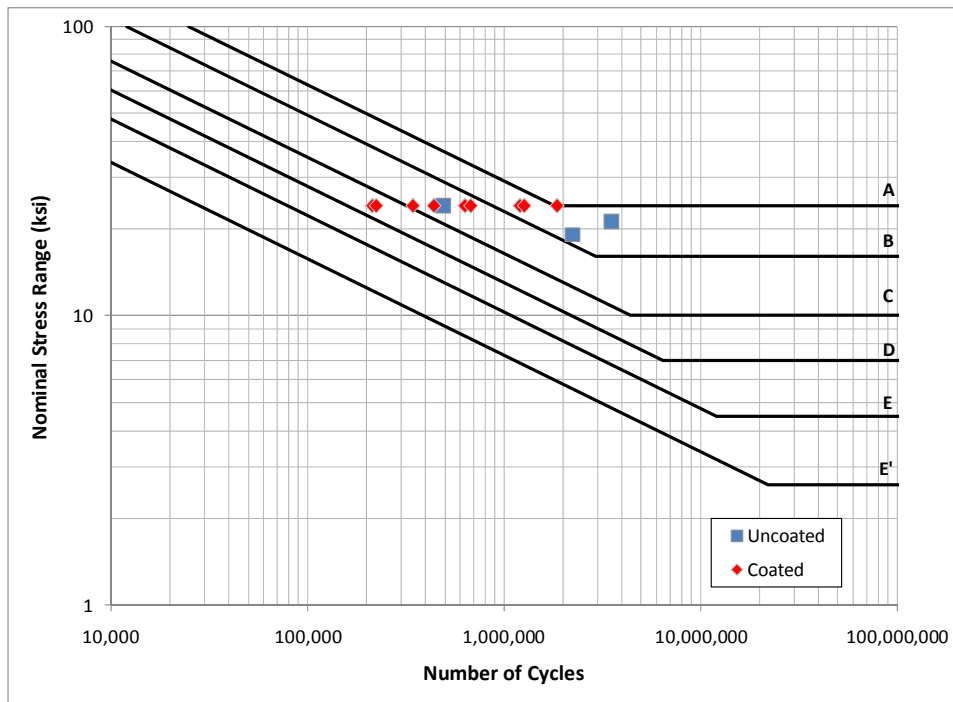


Figure 1.9 Fatigue Results of 10" Diameter Mast Arms with a 3" Base Plate and Full Penetration Weld

This study found several geometric variables that affected the fatigue life of monotube steel structures. One primary influence on the effectiveness of fatigue resistance was the stiffness of the base plate compared to the stiffness of the pole shaft wall. This is because nominal stresses at the toe of the weld are assumed using a simple cantilevered beam theory: the pole shaft is attached to a rigid fixed end support. It was soon discovered through strain gauging and finite element analyses that the base plate did not act as a rigidly fixed support, but deformed as seen in Figure 1.10. This curvature in the base plate leads to a double curvature in the pole wall which serves as a major stress amplification. The simple solution to this issue was to stiffen the base plate relative to the stiffness of the shaft, thus forcing the system to act much more like the assumed fixed end cantilever system. Since the bending in the base plate takes place through the plane of the base plate, the pooled fund study concluded one of the simplest ways to stiffen it is to make the base plate thicker (Stam, 2009)(Richman, 2009) and thus recommended a thicker base plate design for future structures. This recommendation is important because it contradicts the recommendations from previous studies on how to prevent initial cracking from galvanizing.

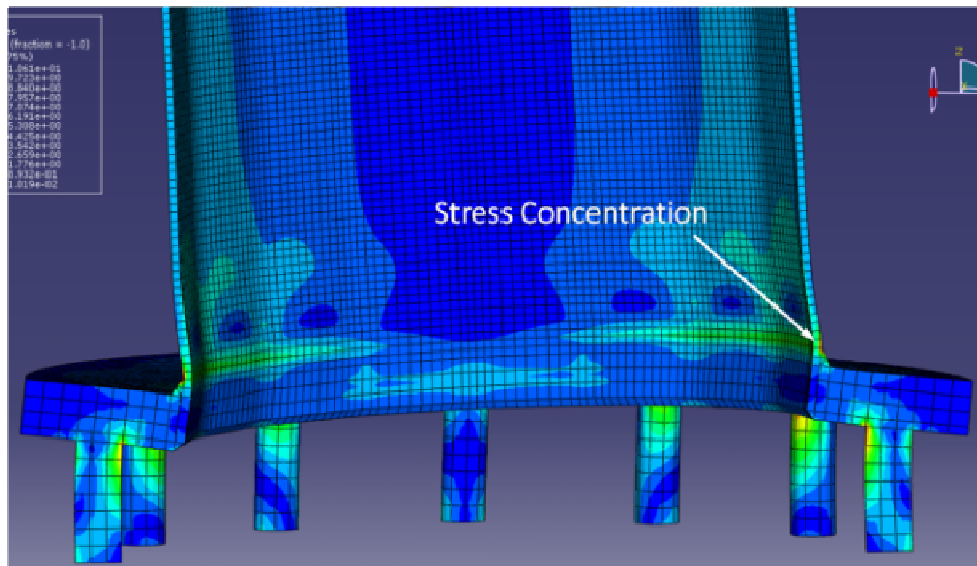


Figure 1.10 Finite Element Model of Base Plate Double Curvature Leading to Stress Concentration (Stam, 2009)

Of importance to note is that at no time during the pooled fund study were cracks found at the weld toe prior to testing. This does not mean that they were not there, only that the specimens were not inspected with the refined ultrasonic testing method developed to find these cracks. A few left over high masts were tested ultrasonically after the study ended, but no crack indications were found in bends that had not been fatigue tested. These HMIP's were smaller and made from a slightly different design from the HMIP specimens used in the current study, as well as being made from a different manufacturer. This makes it difficult to draw conclusions about whether or not the presence of initial cracks influenced the results of the pooled fund study.

#### 1.4 Literature Survey

As mentioned earlier, very little research has been undertaken to determine the cause of the weld toe cracks during galvanizing. A recent increase in the occurrences of the cracks had led to increased effort to understand their causes. Both of the studies discussed below have been undertaken by the fabrication and galvanizing industries to find ways of mitigating the cracks.

##### 1.4.1 Valmont Industries

Aichinger and Higgins of Valmont Industries (2006) reviewed a study undertaken by Valmont Industries to “better identify the causes and variables that are essential to minimize the risk of toe crack occurrences.” The study started by performing ultrasonic testing on Valmont produced poles. Two early conclusions that were reached were that the cracks were only found on galvanized products and that the cracks were less common on communication and department of transportation high mast poles. The researchers hypothesize that this might be due to the larger radius of curvature of bends usually found in those two types of poles.

The study then went on to look at the topic of welding and metallurgy, what they referred to as purchase (the chemical makeup of the weldment and steel), galvanizing, and project engineering (the design of the poles). The study was unable to determine a specific cause of the cracking, but rather attributed the cracking to a variety of combined factors that. The study hypothesized that the cracking is stress based, with liquid metal embrittlement possibly acting as a crack initiator.

Chemical analysis of both the metals used in the poles and the galvanizing baths do not immediately point to liquid metal embrittlement, but a correlation between higher concentrations of certain elements and the likelihood of cracking was noticed. The affects of the chemistry of the materials used will be investigated further in another phase of this study.

One particularly interesting finding by Aichinger and Higgins is a relationship between the base plate to shaft weight ratio and the incidence of cracking. The study found that their data consistently followed the trend of higher ratios that base plate weight to the first 12 inches of shaft weight lead to a higher event probability as shown in Figure 1.11.

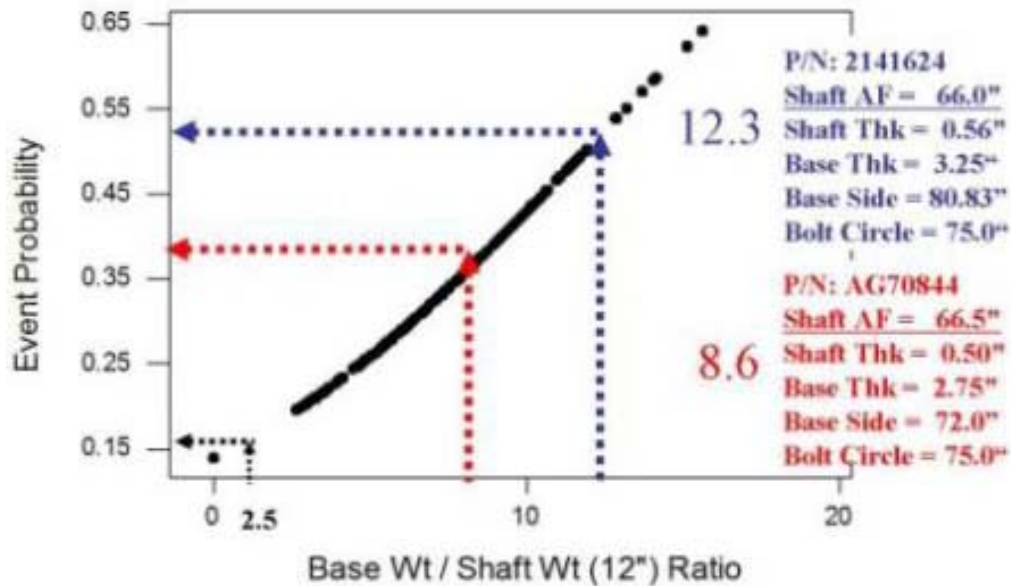


Figure 1.11 Probability of Toe Crack Appearing Compared to the Ratio: Base Plate Weight / Shaft Weight (Bottom 12") (Aichinger, 2006)

Although the paper is vague as to the exact meaning of event probability, it is believed that this describes the percentages of bends that contained cracks. This ratio is very similar to the diameter to thickness ratio shown in the TxDOT survey of poles mentioned earlier. The weight ratio variable, along with the near linear trend of weight ratio to event probability, is not

investigated in depth in the Valmont paper because, as the authors put it, the weight ratios are based on rational engineering designs and cannot be changed without affecting the efficiency of the design.

#### 1.4.2 GalvaScience Study

Kinstler (2006) provided a combination of research conducted by GalvaScience LLC research and an investigation done in Japan primarily focusing on cracks near copes and flame cuts in wide flange shapes found after galvanizing. The work generally focuses on what has caused the increase in the occurrence of the cracks within recent years.

Kinstler describes the phenomenon as liquid metal assisted cracking and breaks down the possible causes into four overlapping factors: forces acting on the member, time spent in the galvanizing bath, chemical composition of the galvanizing bath, and the condition of the steel. Kinstler found in the study that of the four, only the condition of the steel has greatly changed within the time frame of the increased appearance of these cracks. Condition of the steel is defined as the interaction of the chemical composition, thermal history, and mechanical history of the steel. The study was focused on strain age embrittlement as a leading cause of the problem. Strain age embrittlement describes the hardening of steel under strain overtime. While strain age embrittlement hardens steel slowly at normal temperatures, the effect is very rapid at temperatures such as those seen in a galvanizing plant.

Kinstler's work led to the hypothesis that the cracks formed during the galvanization of a steel member are caused by, first, cold working introducing strains into the steel. Then, while the member is in the galvanizing bath, sped up strain age embrittlement takes place at the locations of cold working causing the steel to become brittle. Finally, thermal shock introduces cracks into the brittle area. Further chemical reactions between alloys in the steel and alloys in the zinc bath also possibly exasperate the problem.

Possible solutions from Kinstler for mitigating the problem are to either use heat treatment on cold worked parts of the steel for stress relief or to decrease the time the member spend in the galvanizing bath to decrease the effects of strain age embrittlement. Kinstler noted, however, that



the latter method will not work for monotube structures with large base plates compared to the thickness of the pole wall, such as HMIP's, due to the increased thermal shock effects.

### 1.5 Research Approach

The research documented in this thesis focused on determining the influence that galvanizing has on the fatigue life of HMIP's used by TxDOT. In order to do this, tests on a galvanized specimen were compared against an ungalvanized specimen to compare fatigue performance. This investigation has also begun looking into some of the causes of cracks formed during the galvanizing process. It is focused primarily on differences in high mast design and connection design and their corresponding cracking occurrences in order to better understand some of the variables involved in causing the cracking. Finally, used different fabricators and galvanizers were used to determine whether the problem is limited to only a few producers or is an industry wide issue.

This investigation did not look into several key issues identified as variables in previous studies as causes for the cracking. The scope did not include chemical analyses of the steel or zinc bath. The work does not focus on liquid metal embrittlement or liquid metal assisted cracking, which are in part due to chemical reactions between the steel and zinc bath. Also thermal effects, although mentioned with regards to geometries, are not heavily addressed in this thesis.

Although these effects are not discussed in this thesis, several of the variables are currently being studied and will be addressed in later theses. A chemical investigation has been undertaken to identify possible reactive initiators. An extensive thermal investigation is also underway. A finite element analysis model is being developed to model the thermal effects of the galvanizing bath on the high mast. Finally, a field investigation into actual fatigue stresses and crack propagation is also being conducted.

## Chapter 2 Test Specimen Design

### 2.1 Introduction

The design choices for the test specimens used in this study are based on standard designs specified by the Texas Department of Transportation. The first two specimens, which were ordered as the final two specimens for the previous pooled fund fatigue study, were chosen to be designed similar to the TxDOT 150' – 80 mph design high mast illumination pole. This choice was due to the fact that this design contained several of the key design recommendations that were put forth at the conclusion of that fatigue study. In particular, the specimens had a large, stiff base plate relative to the pole stiffness. The TxDOT design has a three inch thick base plate with 12 bolts instead of 8, and a full penetration connection detail. The design also incorporated a much larger shaft and base plate diameter, a variable that had not been included in the high mast study.

An important difference between the first two specimens and the rest of the specimens tested in this study is that one was galvanized and the other was left ungalvanized which is referred to as a black specimen. This was done for direct comparison purposes of a galvanized pole versus a black pole in fatigue.

Later specimen design choices were expressly made for the purposes of looking for initial cracks in the poles and to test their effects on the fatigue strength of the structures. The next two specimens were chosen to be designed similar to the first two, but by a different fabricator and galvanizer to help evaluate what might be causing the cracks.

The next two specimens tested were not new specimens but rather two previously tested specimens that had undergone weld repairs. These were tested to study the efficiency of weld repairs as a way of mitigating crack problems found in poles.

The last two specimens are an alternative design to the original 150' – 80 mph design with a ground sleeve included in the connection. Previous research at the University of Texas indicated the benefits of ground sleeves, or external collars as they are sometimes called, as a way of increasing the fatigue life of monotube structures (Stam, 2009). This ground sleeve connection

design was chosen to test what affects the ground sleeve has on the formation of initial cracks, and to measure the effect of the ground sleeve on the fatigue performance.

## 2.2 Naming Scheme

The naming scheme for the specimens was adopted from the previous fatigue study (Stam, 2009).

Figure 2.1 below decodes the information displayed in the name of each specimen.

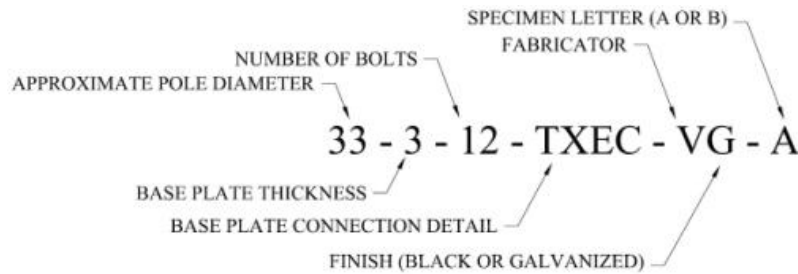


Figure 2.1 Specimen Naming Scheme

Table 2.1 below is a list of all the different specimens along with a summary of the details of the specimen.

Specimen Code	Arm Diameter (in)	Arm Thickness (in)	Base Plate Thickness (in)	# of Bolts	Connection Detail	Galv.	Peened	Manufacturer
33-3-12-TX-SG-A	32.625	0.3125	3	12	Texas	Yes	No	Structural Metals
33-3-12-TX-SB-B	32.625	0.3125	3	12	Texas	Yes	No	Structural Metals
33-3-12-TX-VG-A	32.625	0.3125	3	12	Texas	Yes	No	Valmont
33-3-12-TX-VG-B	32.625	0.3125	3	12	Texas	Yes	No	Valmont
33-3-12-TX-VG-A (flip)	32.625	0.3125	3	12	Texas	Yes	No	Valmont
33-3-12-TX-VG-B (flip)	32.625	0.3125	3	12	Texas	Yes	No	Valmont
Field Repair	32.625	0.3125	3	12	Texas FCAW Repaired	Yes	No	Valmont
Shop Repair	32.625	0.3125	3	12	Texas SMAW Repaired	Yes	No	Structural Metals
33-3-12-TXEC-SG-A	32.625	0.3125	3	12	Texas w/ External Collar	Yes	No	Structural Metals
33-3-12-TXEC-SG-B	32.625	0.3125	3	12	Texas w/ External Collar	Yes	No	Structural Metals

Table 2.1 Specimen Testing Matrix

### 2.3 Typical Specimen Design

High mast specimens tested at the University of Texas were composed of three main components: base plate connection, pole shaft, and end reaction plate as shown in Figure 2.2. In this study most of these components were kept constant throughout the specimens with some intentional variations in connection and an unintentional variation in taper in one set of specimens. Also, the endplates in all three different sets of fabricated samples varied in response to new testing criteria.

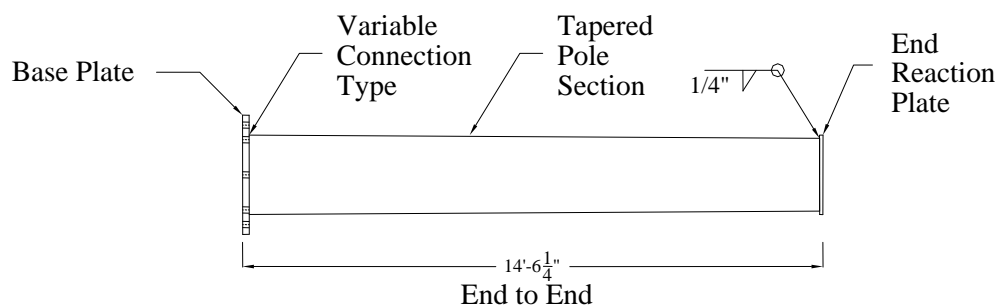


Figure 2.2 Specimen Typical Details (Rios, 2007)

Two identical, matched-paired specimens were used in each test and are referred to as specimens A and B. The need for this is due to the test setup requiring symmetric stiffness, and hence identical specimens, for uniform distribution of load. In theory, this could also yield another data point from the fatigue tests, but, as will be discussed in Chapter 3, the specimens generally failed at the same number of cycles.

In general, the specimens were designed according to the Standard Plans for High Mast Illumination Poles provided by the Texas Department of Transportation. These design specifications are provided in Appendix A. Specifically, the specimens were designed to reflect the 150' – 80 mph design for 12 sided poles. This design was initially chosen due to it containing variables that needed to be tested at the end of the original pooled fund fatigue study. This design also later proved to be the design most likely to have initial crack indications.

The specimens were not designed exactly to the specifications. Some changes to the design, such as specimen length and the addition of an end plate, were made to facilitate the testing of the specimens. Other changes to the design were made to test certain variables or eliminate others. For example, the bolt hole arrangement was made in such a pattern as to create a “worst case” fatigue condition, while some components of the poles, such as access hatches, were removed to force stress concentrations and failures at the base plate.

One change, specimen length, was dictated by the test setup length of 32-ft, which, as will be discussed in Chapter 3, was fixed. The specimen length of 14'-6 ¼" resulted after subtracting from the overall setup length the width of the loading box, the anchor rod stand-off lengths, and the end support lengths.

End plates were also added to allow testing of the specimens. These end plates allowed for a location to create a connection to the end supports in the test. In general, all end plates were one inch thick steel plates with holes drilled into it and the shaft connected to the end plate using a socket connection and a fillet weld. However, the overall design of each endplate varied from one specimen design to the next.

All three specimen designs contained similar base plate designs. These base plate designs are nearly identical to the TxDOT specified design for 150' – 80 mph HMIP's. The three inch thick base plates have a 47 inch diameter with a 22 inch diameter hole cut out of the middle. They also contain bolt holes spaced equally around the circumference of a 41 inch diameter circle. The main difference between the specimen design and the specification design is the bolt holes. The specification calls for 10 - 2¾" diameter bolt holes. The original test setup used 1¾" threaded rods, smaller than those called for by the specification and thus requiring smaller holes to be drilled. Also, twelve bolt holes instead of ten were used to place a bolt directly over every one of the twelve bends of the pole, a design that would create the worst possible fatigue condition and allow the specimen to be rotated into position the desired bend at the top highest stress location. Figure 2.3 below shows this typical layout.

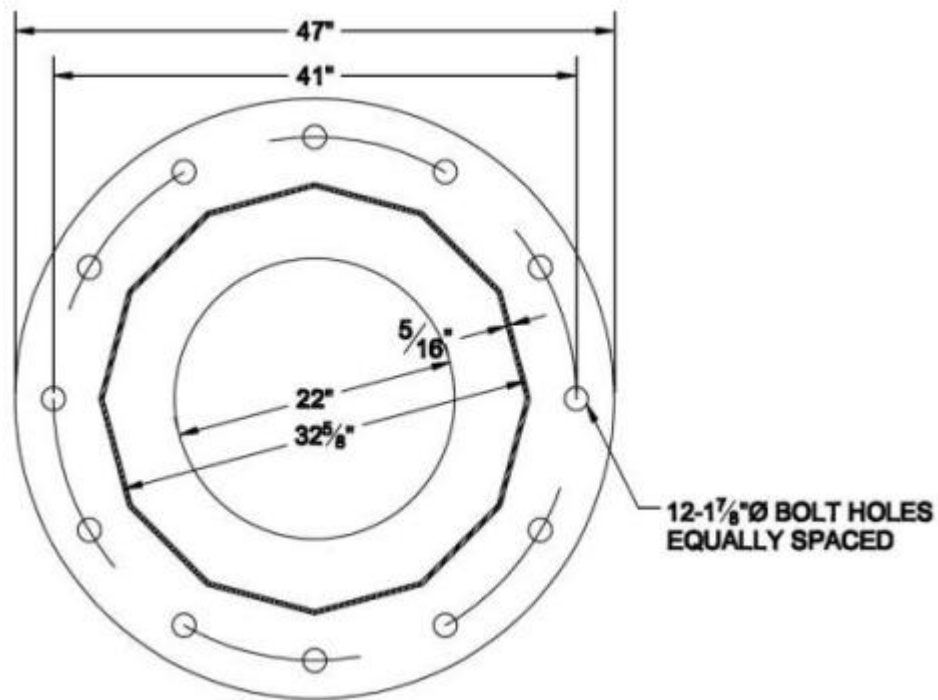


Figure 2.3 Specimen Typical Base Plate Layout

All pole shafts are dodecagons (12-sided polygon) with base diameters measured to  $32\frac{5}{8}$ " from out to out across the flats. The pole shaft walls, not including the addition of the external collar, were all  $\frac{5}{16}$ " thick. Finally, all three specimens contained a taper down from the base diameter to the diameter at the connection to the end plate.

The bends of the polygonal section, which are formed over a shaped mandrel with a press-brake device, varied only slightly between specimens. Nearly all specimens had bends with close to a four inch bend radius, with minor average variances from specimen to specimen. The previous investigation conducted at the University of Texas found that differences in bend radii do not have a large effect on the stress concentrations at the bend or the fatigue life (Stam, 2009).

All high masts were tested with a bend, rather than a flat face, in the top position. Due to the flow of stresses from the anchor rod to the bend in the shaft, this orientation was determined to cause a higher amplification in the stresses and was, in turn, worse for the fatigue life of the samples.

Also, initial cracks found in the samples were always concentrated at the bends of the pole, creating an even higher stress concentration at this location.

In the previous study, all masts were positioned with their longitudinal weld seam in the top position. This was seen as a more fatigue-critical scenario given that inherent imperfections in the weld metal were more likely in these areas. For this investigation, however, typically the bend with the largest initial crack was positioned in the top position.

All three specimens were designed utilizing full penetration welds around the circumference of the shaft to connect the pole to the base plate. The weld is created by beveling the pole wall, filling the bevel with weld material, and then topping the cavity with a fillet weld around the inside of the pole wall. Full penetration welds had been proven in the previous study to provide a better fatigue connection than the more conventional socket connection because of the more direct load path that the stress is able to take through the weld and because of the increased stiffness provided in the base plate by the smaller inner hole (Stam, 2009). The addition of the external collar slightly changes the detail of the full penetration weld. Figure 2.4 below is a picture of the cross section through the weld for a specimen without an external collar. A small lack of fusion was found in this weld. The next picture, Figure 2.5, is through the cross section of the weld of a sample from the Pooled Fund Study with an external collar. Both cross sections have been acid etched to help identify weld passes. The individual details of the welds can be seen in Figure 2.6, Figure 2.7, and Figure 2.9 shown in the following sections.

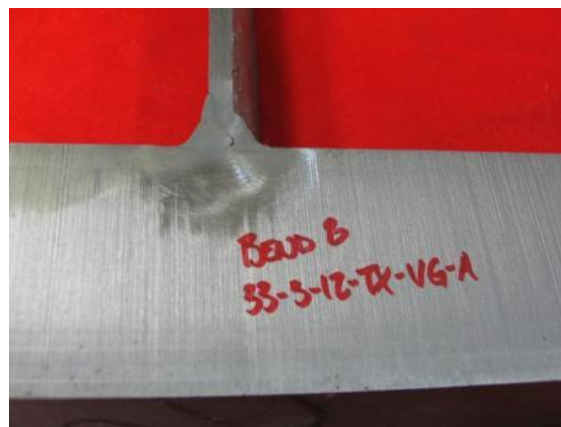


Figure 2.4 Cross Section of Full Penetration Weld without Collar

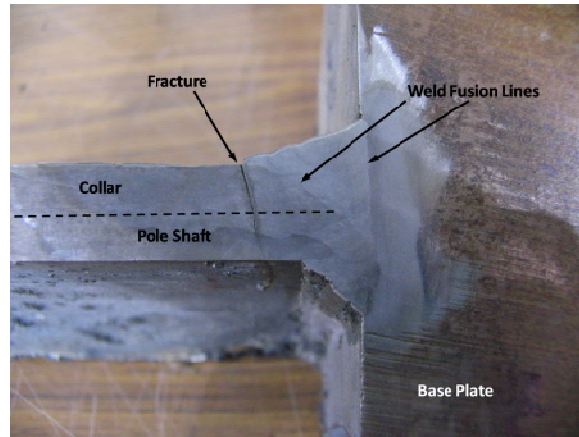


Figure 2.5 Cross Section of Full Penetration Weld of Sample with Collar (Stam, 2009)

#### 2.4 Specimens 33-3-12-TX-SG-A and 33-3-12-TX-SB-B

The first two specimens tested in this investigation were chosen specifically to test the design recommendations of the pooled fund fatigue study. These recommendations included using thick 3" base plates as well as full penetration welds for connecting the pole to the base plate. Also, since the previous project had only tested 24" diameter poles, larger diameter poles were needed to increase the applicability of the design recommendations on these larger poles. The Texas Department of Transportation specified design for the 150' – 80 mph high mast illumination poles fit these requirements and was chosen as the base design for the specimens for that reason, as well as because of the prevalence of poles of that design throughout the state. Figure 2.6 below shows the drawings for the first two specimens tested in this study.

A comparison of this design to the TxDOT specification design found in Appendix A shows that they are very similar. The key differences, which were noted earlier, are the increase in number and decrease in size of the bolt holes, the shorter length of the specimen, the end plate added onto the specimen and the removal of components such as the access hatch from the specimen.

Although the end plate in the design in Figure 2.6 is square with normal holes, a change order was issued that made the end plate circular with 12 slotted holes. This was done for alignment reasons, as it allowed the specimen to be tested in more orientations. The design was again used for the specimens with the external collars and is shown in Figure 2.9.



One accidental difference between the specimen and the specified TxDOT design is the taper of the pole shaft. The drawings do not explicitly specify what the taper is supposed to be and so the manufacturer had a change in diameter per foot length in the pole of nearly 0.25 inches, while the TxDOT design calls for only a 0.175 inch per foot taper. Previous finite element analysis investigations into the effect of the pole taper on the fatigue life of the pole had shown that the taper did not change the life of the structure significantly. Since the stress levels at the base plate are changed little by the increased taper, the relevancy of the results is not affected. Later specimens included an explicitly labeled taper to prevent this problem.

A key difference between these two specimens and any tested before or afterwards is that one was galvanized and one was not. The decision to do this arose from the concerns of initial cracking coming from TxDOT. Although similar samples of galvanized and ungalvanized (black) samples had been tested before, a head to head test of a black and galvanized sample had never been done. The theory behind testing the samples head to head was that it would remove all other variables aside from the galvanizing in a direct comparison test. These results are discussed in Chapter 3.

# HIGH MAST ILLUMINATION POLES TEST SPECIMENS

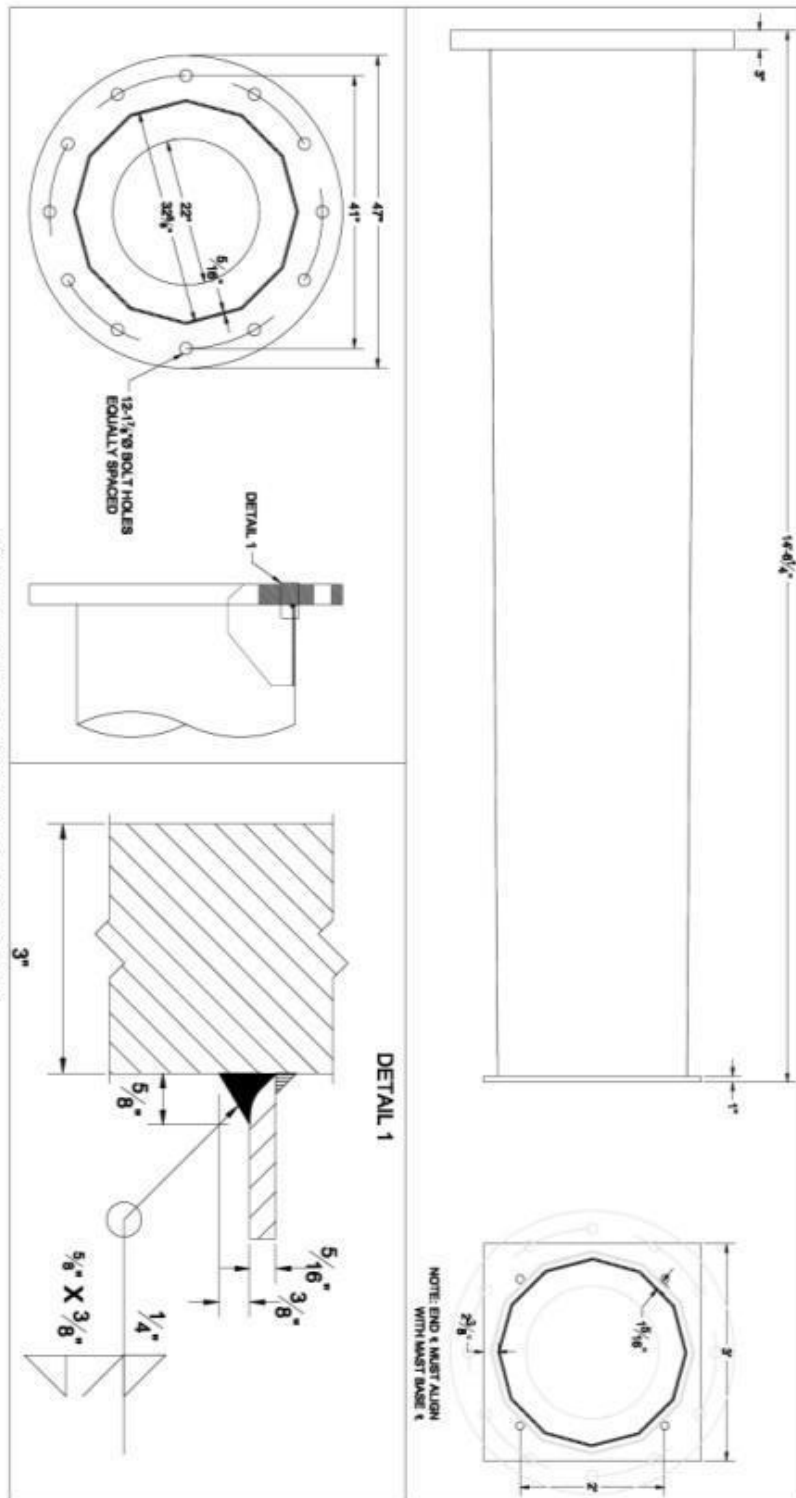


Figure 2.6 First Specimen Design

## 2.5 Specimens 33-3-12-TX-VG-A and 33-3-12-TX-VG-B

The next two samples tested were essentially identical to the galvanized specimen in the first set of specimens. The design of these two specimens was also based on the specified TxDOT design for the 150' – 80 mph wind high mast illumination poles. The design for these poles can be seen in Figure 2.7.

Similar to the previous two specimens, the key differences between these specimens and the TxDOT design are the number and size of the bolt holes, as well as the addition of the base plate at the end of the specimen and the shorter length of the specimens. Also the access hatch has been removed from the design for simplifying purposes.

There were some slight differences between the two these specimens and the first two specimens. Unlike the previous two specimens, the taper for this design was explicitly called out on the plans and was, in turn, fabricated correctly. As mentioned before, this should have little effect on the fatigue life comparisons.

Also the end plate was a different design. It was decided to go back to the square end plate for these samples. This decision was made to facilitate alignment and erection in the test setup, which was easier, though less flexible, with the square end plate. As long as the pin connection is maintained, the stress level at the base plate should not change, so this change should have any noticeable effect on the fatigue life of the specimens.

Finally, both specimens were galvanized. This decision was made because at by this point in the study it had been determined that galvanizing does affect the fatigue performance. Also, an increase in the initial cracks was desired to help in determining how they originate.

The fabrication and galvanization of these two specimens were done by a different fabricator and galvanizer than the previous pair. This was done for comparative purposes, to see if the initial cracks were a function of the fabricator or galvanizer.

# HIGH MAST ILLUMINATION POLES TEST SPECIMENS

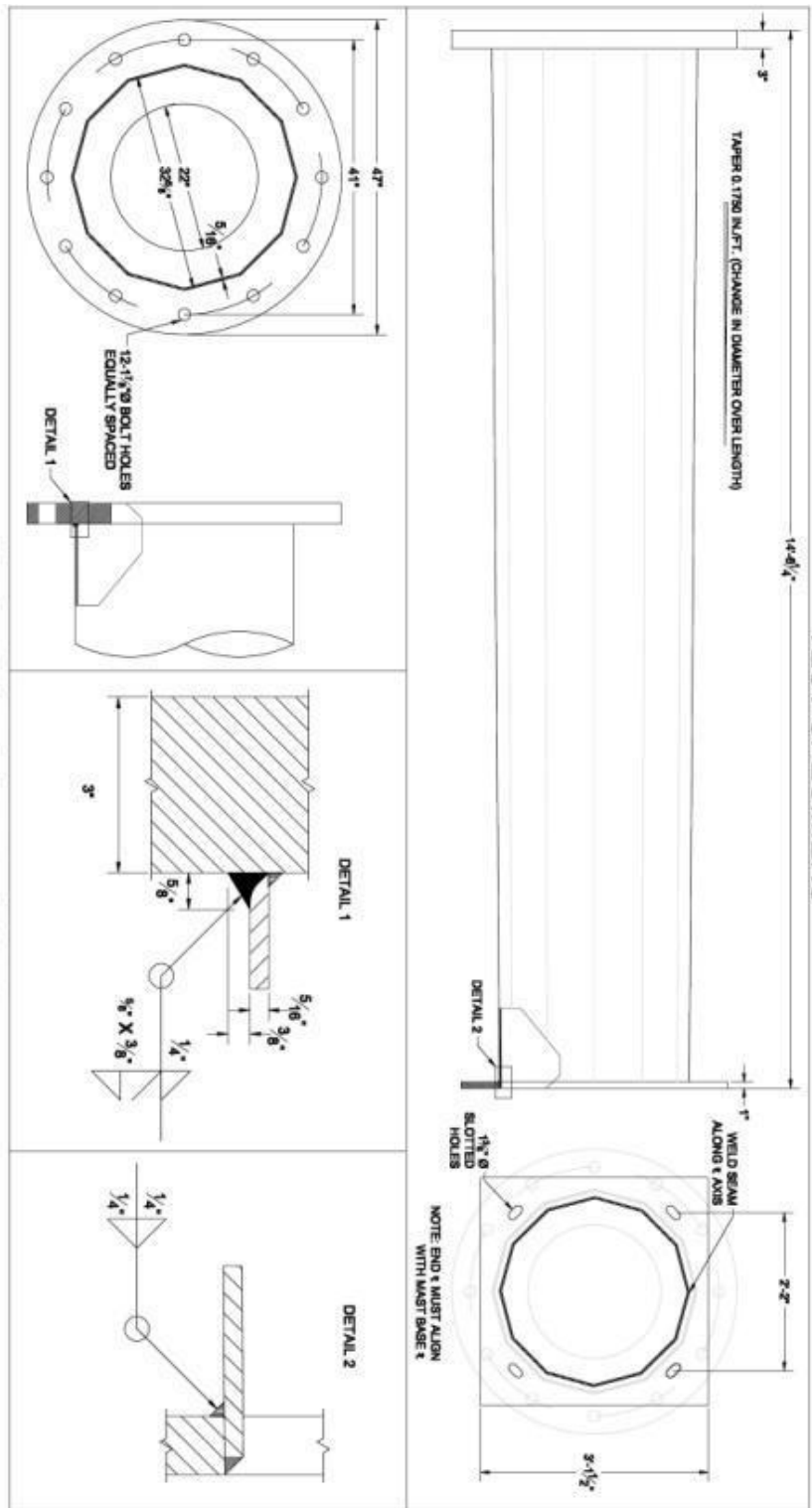


Figure 2.7 Second Specimen Design

## 2.6 33-3-12-TXEC-SG-A and 33-3-12-TXEC-SG-B

The final specimen design incorporated an external collar, also called a ground sleeve by TxDOT, around the base of the pole. This addition to the pole had been shown in the Pooled Fund Study to increase the fatigue life of the poles (Stam, 2009). It's also a design option available in the TxDOT specifications (as seen in Appendix A) for high mast illumination poles, making the addition of an external collar a possible viable solution to mitigate the issue of initial cracking. A typical in-situ high mast with an external collar is shown in Figure 2.8.



Figure 2.8 Typical High Mast Illumination Pole with External Collar

The two external collar specimens have the same differences from the TxDOT design as the previous specimen design. These differences include the addition of an end plate, a shorter section length, and changes in the size and number of bolt holes. Similar to the previous specimens, these changes in design were made to accommodate testing requirements. Once

again, accessories such as the access hatch and winch mounting channel were left out to simplify the design and analysis.

There were two main differences between this design and the previous. The first is the end plates on this design were made circular with 12 slotted holes. The square base plate only allowed for four different bends to be placed in the top high stress location (this will be further discussed in Chapter 3). By using a round base plate with multiple holes, any bend could be placed in the “up” position. This allowed for greater control over testing decisions than there had previously been. Similar to previous discussions of changes in end plates, this change in design has little effect on the fatigue life of the pole.

The other major change in this specimen design was the addition of the external collar. The external collar was a  $\frac{3}{8}$ " thick by one foot tall plate wrapped around the base of the pole. As can be seen in the design provided in Figure 2.9, the detail for welding this plate on with the pole shaft is different than the previous weld details. For this design, the full penetration weld was made through both the external collar and the shaft wall. Also, an unequal leg fillet weld was provided around the top of the external collar to connect the collar to the shaft.

It is important to note that the external collar is not included as part of the cross section for stress calculations in this study. It is viewed merely as an accessory that is in place to enhance the fatigue life of the pole. This, in turn, means that all of the designs have the same cross section for analysis at the base plate, which allows for easier analysis and comparison between designs.

The fabrication of these specimens was performed by the same fabricator as the first pair of specimens. Galvanization was done by two separate galvanizers; the original galvanizer that galvanized specimen 33-3-12-TX-SG-A also galvanized specimen 33-3-12-TXEC-SG-B. Specimen 33-3-12-TXEC-SG-A was galvanized by a new galvanizer. This was done so that comparisons between different galvanizers could be obtained.

# HIGH MAST ILLUMINATION POLES WITH GROUND SLEEVE TEST SPECIMENS

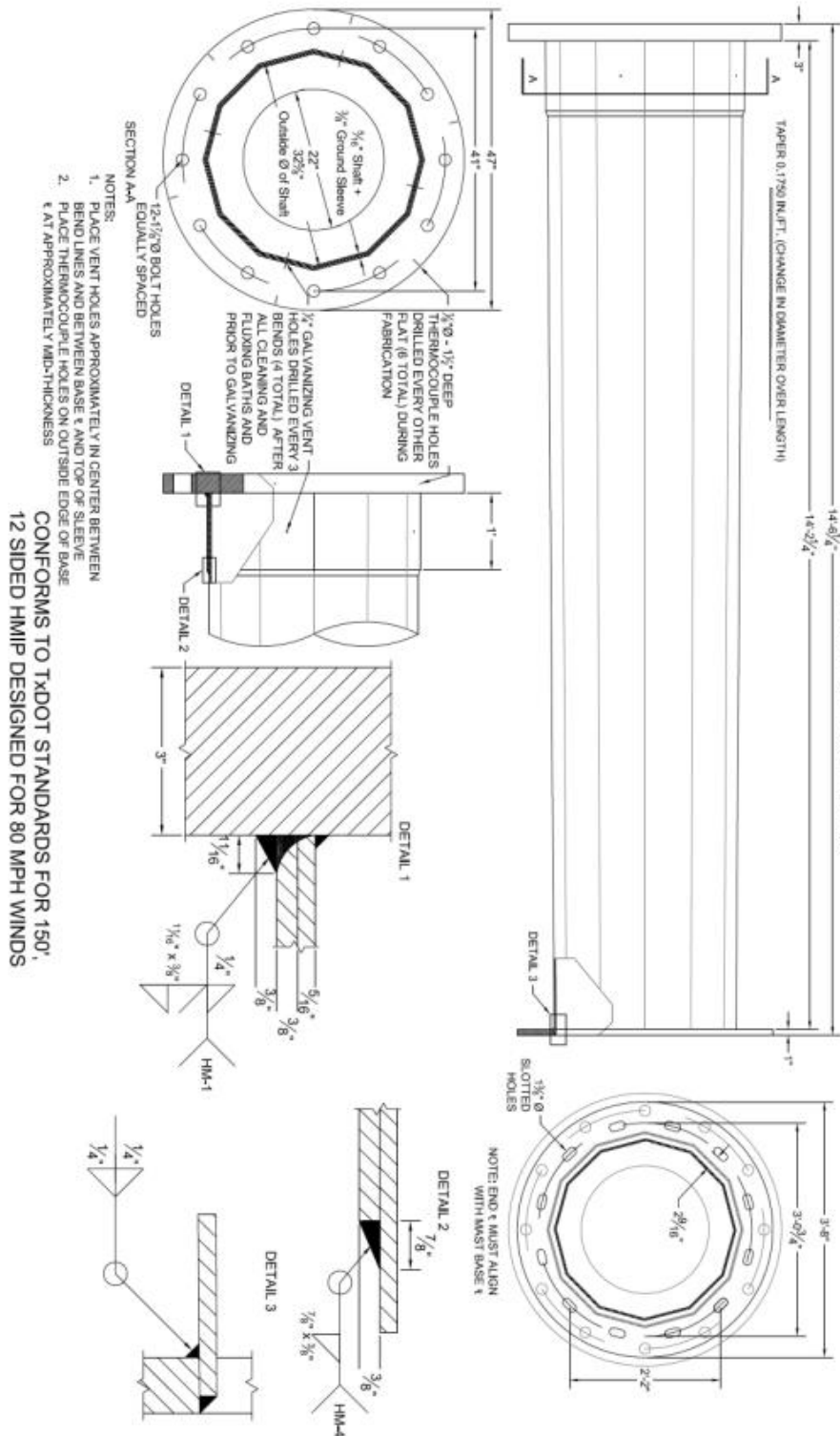


Figure 2.9 External Collar Specimen Design

Fabricators have traditionally avoided the external collar option due to added difficulties created by it. In addition to the added cost of fabrication and the difficulty of fitting the external collar to the shaft of the pole, extra precautions have to be taken during the galvanizing of the poles. Vent holes must be drilled through the external collar into the pocket between the collar and the shaft wall to allow expanding air to escape during galvanizing. This process must be done before galvanizing but after pickling, because if the acidic pickling solution were to get into the holes a severe corrosion hazard would be created. This adds an additional step in the middle of the normal galvanizing procedure, which slows down output. Figure 2.10 below is a picture of a pole from the Pooled Fund Study that shows what can happen to a pole with an external collar but no vent holes.

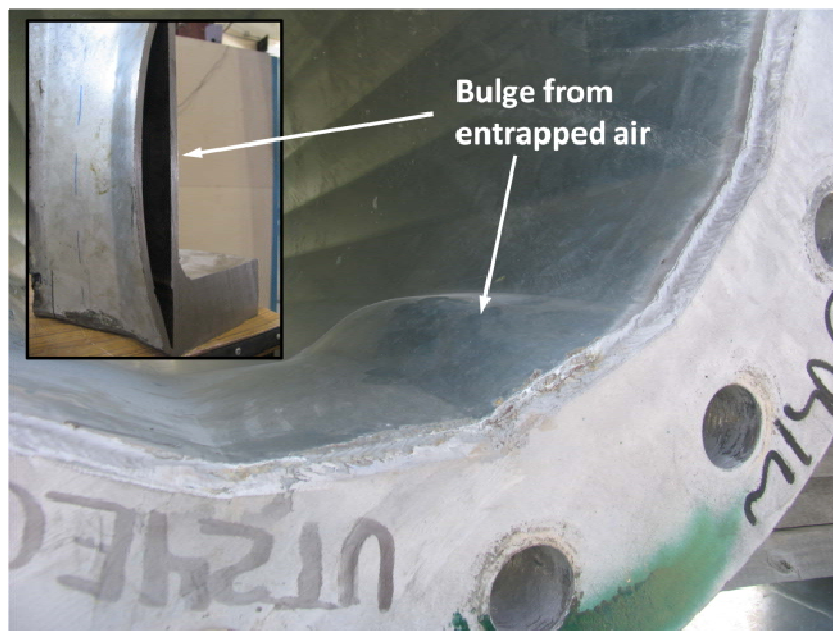


Figure 2.10 Bulge Caused by Entrapped Air between Collar and Pole (Stam, 2009)

## 2.7 Weld Repair Specimens

TxDOT and its suppliers have been finding cracks in both in-situ high mast illumination poles and in poles that have just been galvanized. The procedure for conducting a toe crack weld repair



is primarily dependent on location, due to the constraints of welding equipment, access, and machinery available. Because of the difference in circumstances for a pole in the field and a pole coming out of the shop, two different procedures have been defined for weld repair. Consequently, these weld procedures separately address the issues of fatigue cracks and initial cracks caused by galvanizing. A further investigation was done to check the ability of weld repairs to mitigate the effects of cracking on the fatigue life of high masts.

The weld repair specimens were not newly designed specimens, but were rather specimen 3-33-12-TX-SB-B and 3-33-12-TX-VG-B. For the purposes of differentiating between tests and cataloguing results, the specimens will be referred to as Shop Repair and Field Repair, respectively. Since the specimens were being reused for this portion of the study, there are very few differences between their original design and their weld repair design.

The weld repairs were only performed at bends that contained crack indications. Figure 2.11 below shows where the crack indications were on the two specimens prior to weld repair. The bend number is followed by the crack length. Specimen 33-3-12-TX-SB/G-B was initially tested prior to galvanizing. The specimen contained no fatigue cracks. The crack lengths shown were found after the specimen was galvanized.

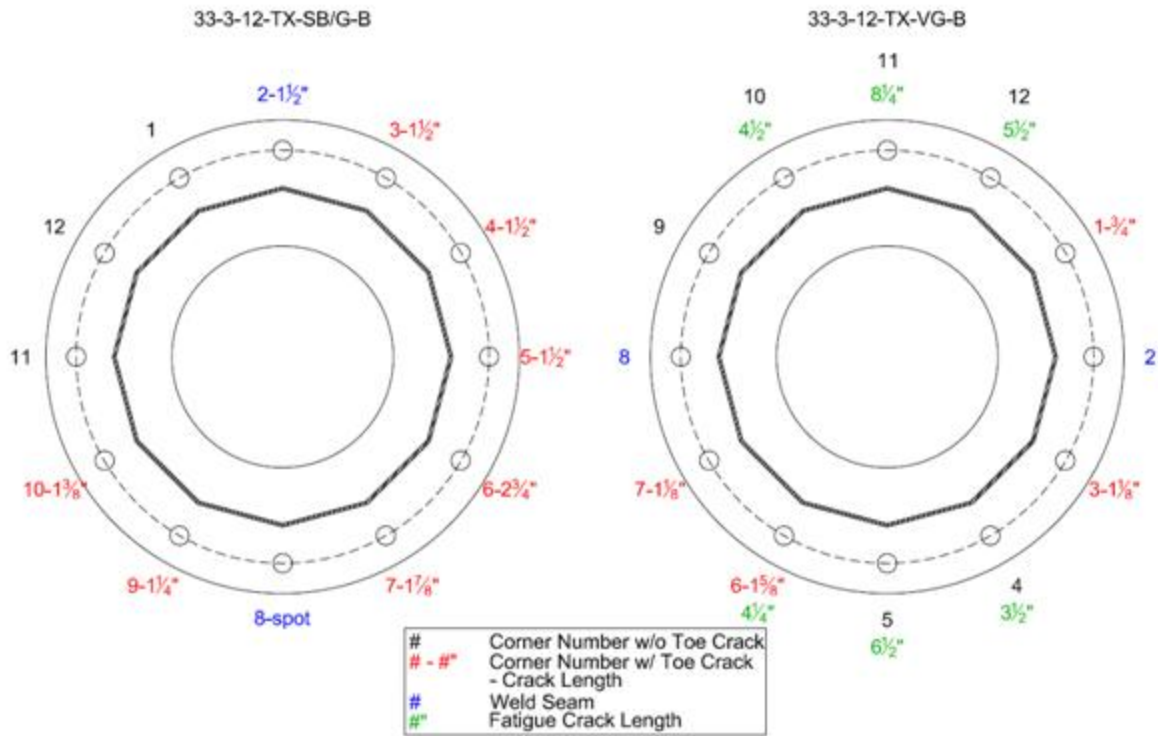


Figure 2.11 Cracks in Weld Repair Specimens Prior to Repair

### 2.7.1 Shop Repair Specimen

A “shop repair” weld procedure was developed to address poles that contain cracks after galvanizing but before installation, which means that this repair will replicate the repair of initial cracks found in the shop. The Shop Repair specimen was originally specimen 3-33-12-TX-SB-B, the black specimen from the first set of two specimens. As will be discussed in the results chapter, the original specimen did not fail under fatigue cycling. After fatigue testing, ultrasonic tests confirmed that there were no fatigue cracks present in the pole. Since the specimen appeared to be relatively undamaged, it was decided to have the specimen galvanized.

A flux core arc welding procedure (FCAW) was chosen as the shop repair procedure due to its ease of implementation in a fabrication shop. The ability of the shop to orient the high masts in the horizontal position as well as provide protected shield gasses makes FCAW a viable option.

The advantages of using FCAW are that it provides better and more consistent weld quality, with fewer likely defects compared to other available weld processes, and it can also be done at a higher rate of speed than shielded metal arc welding.

Here is an exact excerpt of the weld procedure that has been developed for the shop repair and was provided to the welder for the repair of this specimen:

*Prior to any welding, specific surface preparations must be made to ensure the removal of all parts of the initial crack. First, cracks must be identified... .. using ultrasonic testing with a seventy degree transducer to locate these shallow cracks. These cracks should be marked two inches past their extents for grinding. After ultrasonic testing, the specimen will need to be cleaned with acetone to remove any couplant, dirt, and grease. Once clean, the crack locations and two inches beyond their extents shall be ground out. The depth of the grind shall be one half of the pole wall thickness and shall have a radius of 1/4 inch. After grinding, the groove surface shall be inspected with magnetic particle testing to ensure the complete removal of the initial crack. If any indication is found, the indication shall be ground out. Then, any galvanic coating near the weld surface shall be removed with a flap wheel, or a comparable mechanical device to ensure no zinc gets into the weld. This will conclude weld preparations.*

*The weld shall adhere to the following. The weld process shall be flux core arc weld and the filler metal shall be compliant with AWS classification E71T-1 and have a diameter of 1/8 inch. The current shall be between 170 and 370 amps, DC+, with a voltage falling between 21 and 28 volts. The shield gas shall be 25% carbon dioxide and 75% argon at a flow rate of 45 cubic feet per hour. The weld technique shall be a single stringer pass.*

The repair was executed in a horizontal orientation with the high mast lying sideways on the ground. The circular base plate and end plate made rotating the specimen easy, and allowed for the easy use of the FCAW weld procedures on any bend, as it requires a relatively flat, horizontal weld surface. This is similar to what would be encountered in a fabrication shop, where cranes and mandrels make manipulating the poles much easier. Welding in this orientation, and with the capability of rotation the specimen when necessary, contributed to relatively fast, and well controlled welds.

It was also helpful that this weld procedure only necessitated grinding down to one half of the wall thickness, comparatively less grinding than the field procedure. Having a larger root face enabled the welder to use more heat without fear of burning through to the other side, and to repair the weld in one pass. Figure 2.12 below is a picture of the FCAW shop repair procedure being performed on the specimen at the Ferguson Lab.



Figure 2.12 FCAW Being Performed at the Ferguson Lab

Because only one broad pass was needed to repair the weld, the weld profile on the shop repair specimen resulted in a smooth broad parabolic shape. Previous research has indicated that this interface is critical to maintaining smooth stress flow between the stiff base plate, and relatively flexible pole wall (Stam, 2009). This shape is advantageous due to the reduction of the notch effect at the transition between the toe weld and pole wall, which, in turn, leads to a lower stress increase. A picture through the cross section of a practice weld done on another sample is provided in Figure 2.13. A small weld defect from lack of fusion can be seen in this picture.

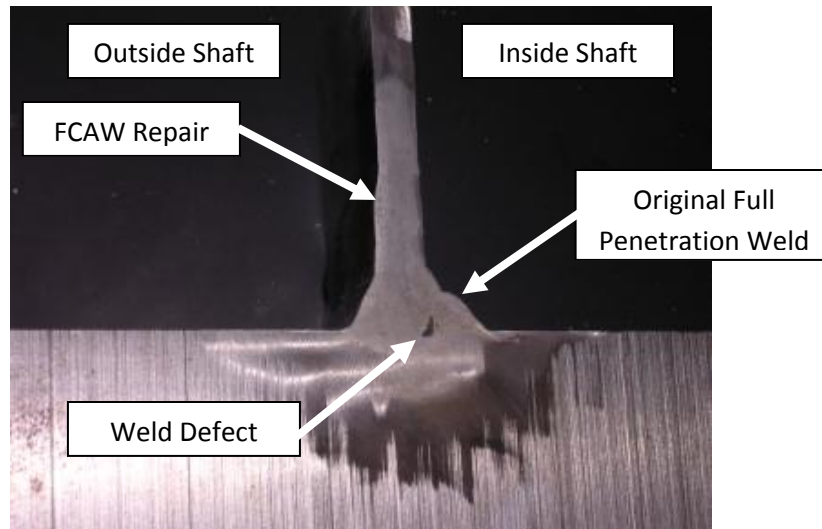


Figure 2.13 Polished Cross Section Through FCAW Repaired Weld

### 2.7.2 Field Repair Specimen

A “field repair” weld procedure was developed to address poles that were found with cracks in the field after the pole has been erected. The Field Repair specimen was originally specimen 3-33-12-TX-VG-B, one of the second set of specimens tested. The original specimen failed under fatigue loading and contained fatigue cracks for repair. After fatigue testing, ultrasonic tests confirmed the length and depth of the fatigue cracks in the pole.

Shielded metal arc welding (SMAW) was the method chosen for the repairs of the field specimen. Like the shop specimen the location and ability to manipulate the pole governed which methods were viable. SMAW was chosen because of its general ease to perform on an in-situ pole with portable equipment and no need to reorient the pole.

The repair procedure for the field specimen was described as follows:

*Surface preparations will be similar to those detailed in the flux core arc weld procedures. The only differences in procedure will be the amount of root face to be left after grinding, and the width and radius of the groove. The groove at indications, and two inches beyond, shall leave*

*1/16 inch root face, have a radius of 1/4 inch and leave a groove angle of 45 degrees. After grinding, magnetic particle inspection shall be conducted to verify the crack has been removed.*

*After surface preparations, the welder shall use filler metal adhering to AWS classification E7018 for the repair. Two different sizes of electrode will be used—3/32 inch electrode for the root pass, and 1/8 inch electrode for the other necessary passes. The weld shall be executed with a current of between 80 to 100 amps, DC+. The weld technique shall be composed of four stringer passes, using the appropriate electrodes where specified above, and a wire brush shall be used for interpass cleaning.*

To properly mimic in situ conditions, the field repair specimen was oriented vertically, elevated off the ground four inches, and mock anchor rods were inserted into bolt holes near the site of welding. The orientation, anchor rods, as well as the significantly thinner root face significantly increased the amount of time necessary to complete these repairs compared to the shop repaired specimen.

The tight controls on the depth of the grinding also added additional time into the weld repair process. Not only was it necessary for the welder to be careful to maintain the correct root face, one sixteenth of an inch, but if too much was ground off, the welder ran the risk of blowing through the root material during welding. In fact, the welder did burn through and had to fill the location of the hole, further contributing to a longer repair time, as well as risking disruption to the continuity of the surface on the inside of the pole. The welder performing the SMAW repair is shown in Figure 2.14.



Figure 2.14 SMAW Repair Procedure Performed at Ferguson Lab

To maintain the one sixteenth inch root face, the welder recommended using smaller electrodes, minimizing heat input into pole wall. This helped to maintain the root without burning through, but resulted in the larger number of passes to fill the ground opening. In doing so, the exterior of the weld had a noticeably rougher surface with many discontinuities. The roughness of this weld profile can clearly be seen in Figure 2.15, which is a section trough a test weld on another sample.

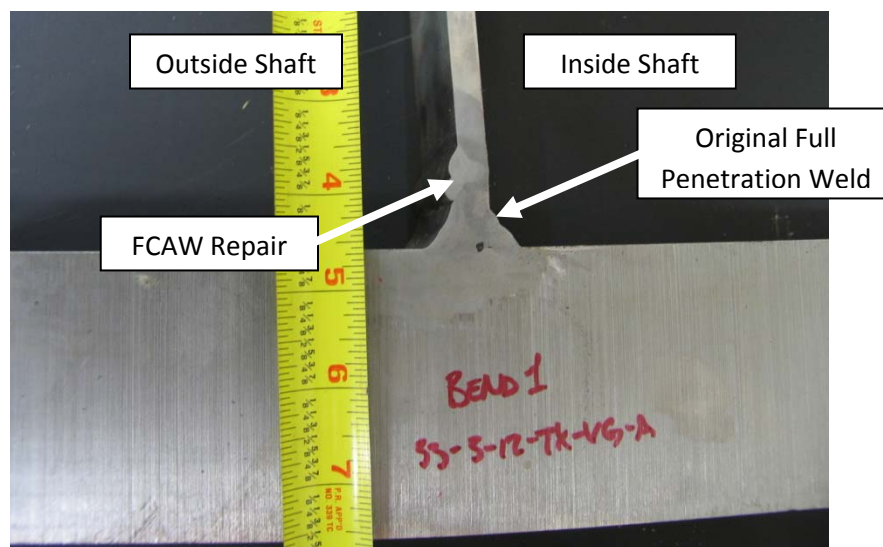


Figure 2.15 Cross Section of SMAW Repaired Weld

## Chapter 3: Testing

### 3.1 Introduction

This chapter provides a discussion of the testing setups and procedures that were used. It will follow the order of testing done on a sample, which consisted of non destructive testing, followed by fatigue testing of the samples, and ending with the destructive testing of the samples.

### 3.2 Non Destructive Testing

Non destructive testing was utilized both before and after fatigue testing for finding cracks. Before fatigue testing, non-destructive tests were administered to determine if, where, and how much initial cracking had occurred in a specimen. After fatigue testing, non destructive testing was used to verify that fatigue cracks were indeed present. Two forms of non destructive testing were employed for finding cracks: magnetic particle testing and ultrasonic testing.

#### 3.2.1 Magnetic Particle Testing

Magnetic particle testing uses a powerful electromagnet and a fine iron filing powder to locate discontinuities in a ferrous surface, such as a steel plate. The hand-held magnet is powered, adjusted for alternating current or direct current voltage, engaged to form a magnetic field through the tested material, and then the iron filing indication powder is dusted over the investigated surface. Should a crack, or discontinuity, exist in the steel surface, a disturbance propagates in the magnetic field resulting in the accumulation of these iron filings at the source of the disturbance. Figure 3.1 is an example of a crack observed using magnetic particle testing. This form of testing can be effective at accentuating small surface cracks. The observations presented below are based on the researcher's experience using this testing measure to observe fatigue and initial cracks.





Figure 3.1 Fatigue Crack Observed Using Magnetic Particle Testing

#### Advantages

The strongest advantage to magnetic particle testing is its ease of use. Magnetic particle testing is easy to perform with little training, portable, and makes tight cracks much more distinguishable. On smooth surfaces with few geometric discontinuities, and particularly on ground surfaces, operation is simple and effective. Cracks can be easy to identify under such circumstances, and a record can be made of the crack with either photography or through the use of a more advanced magnetic particle method that utilizes a hardening rubber solution.

#### Disadvantages

Unfortunately, high masts rarely present ideal conditions. When locating cracks at weld toes using magnetic particle testing, accumulation of the indicator powder follows regions of the weld toe at significant geometric discontinuities regardless of the presence of cracks. Figure 3.2 shows an example of a test specimen with strongly pronounced geometric discontinuities between a

repair weld and base metal. The black lines on the base metal show the most recent fatigue crack marks observed by visual inspection. Notice the difference between these marks, and the blurred magnetic particle indications shown by the red powder.



Figure 3.2 Poor Magnetic Particle Test Reading Caused by Geometric Discontinuity

Figure 3.2 is an exaggerated example of how false positives and incorrect indications may occur. Such weld toe discontinuities are not typical, and should be avoided by maintaining smooth transitions from weld-to-base metal for fatigue performance purposes. However, this image makes an important point—there are some situations where magnetic particle testing is not effective. Unless the crack is visible without magnetic particle inspection, it is nearly impossible to confirm that a crack is actually being observed on a surface similar to the one in Figure 3.2.

Apart from over-estimating cracks, when observing high masts under significant compressive forces, toe cracks tend to close resulting in poorly accentuated indications, which can introduce a margin of error into the reading. Figure 3.3 below is a comparison of the same bend tested for cracks using magnetic particle testing under compression and tension. Further, the experience on

this study with magnetic particle testing has shown that it is ineffective at indicating initial cracks from galvanizing or subsurface defects. Therefore, despite the usefulness in using magnetic particle testing to find cracks on smooth surfaces, the problems encountered using magnetic particle testing based on the base plate-pole wall weld profile do not justify relying on magnetic particle testing to determine crack locations.

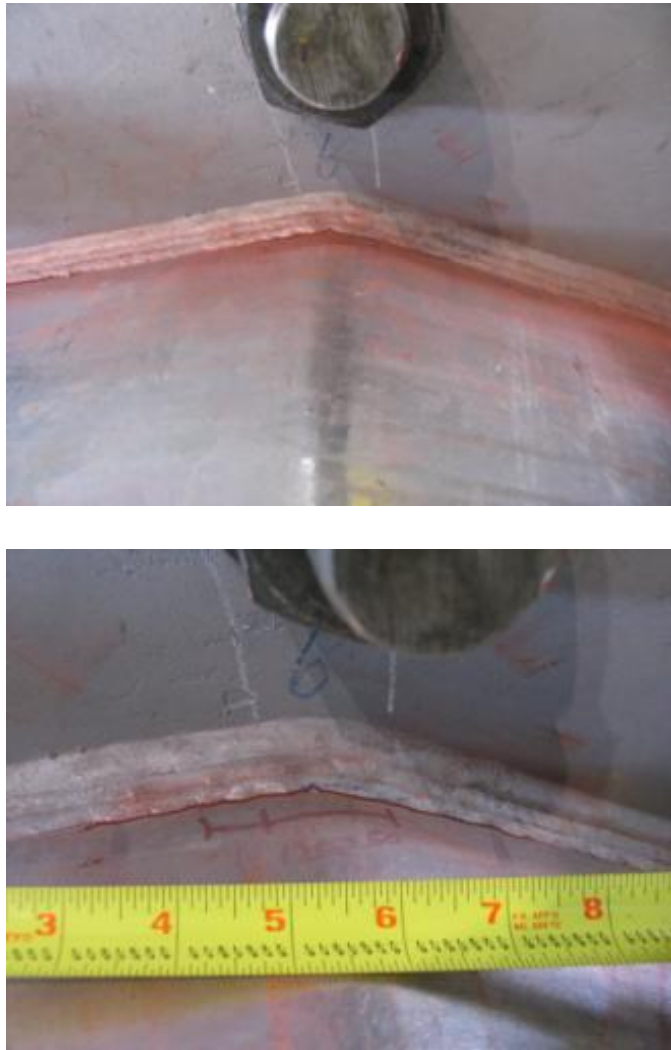


Figure 3.3 Above: Magnetic Particle Test of Bend in Compression. Below: Same Bend Tested in Tension

### 3.2.2 Ultrasonic Testing

The alternative to magnetic particle testing is ultrasonic testing. Ultrasonic testing uses sound waves emitted from a transducer to determine discontinuities in a constant material. These discontinuities are found by observing the reflection of sound waves off of surfaces orthogonal to the sound path. Ultrasonic testing is shown being performed in Figure 3.4, and a diagram of this process is provided in Figure 3.5.



Figure 3.4 Ultrasonic Test Being Performed by a TxDOT Inspector

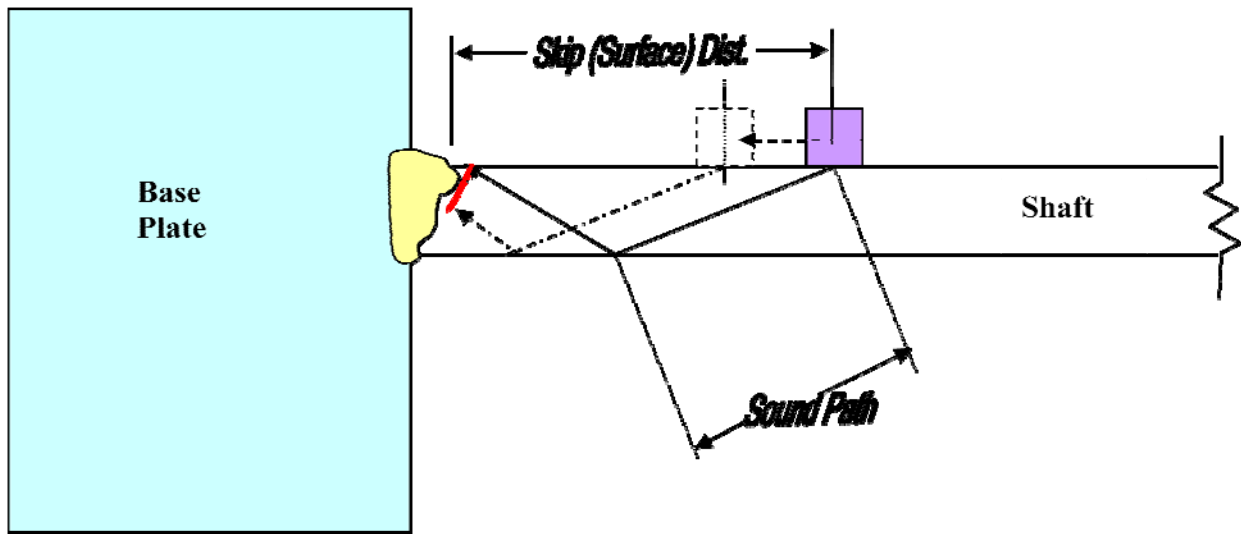


Figure 3.5 Diagram of How Ultrasonic Testing Works (diagram courtesy of Michael Smith, TxDOT)

It should be noted that the ultrasonic testing procedure to find the initial cracks in the poles is different than the procedure specified in the American Welding Society D1.1 Structural Welding Code. This is because the procedure in D1.1 was ineffective at finding the small, subsurface initial cracks. For example, the welding code specifies a rectangular transducer with minimum dimensions of  $\frac{5}{8}$ " x  $\frac{5}{8}$ ", a transducer angle of  $45^\circ$ , and a 2 megahertz to 2.5 megahertz frequency. The Texas Department of Transportation developed a procedure that employs a round transducer with a  $\frac{1}{2}$ " diameter, an angle of  $70^\circ$ , and a 3.5 MHz frequency. Also, the welding code has explicit acceptance/rejection criteria for when the testing is performed in accordance with the code, whereas the TxDOT method relies solely on detection of sharp signals from the weld toe and the interpretation by the ultrasonic technician without any codified acceptance/rejection criteria.

## Advantages

The biggest advantage of ultrasonic testing is the accuracy of the results. Ultrasonic test findings of both fatigue cracks and initial cracks have been verified to be accurate using destructive examination methods. This method has proven effective in both controlled lab settings and field settings. Not only are the testing technicians able to determine which bends are cracked, but they are able to determine the length and depth of the crack with good accuracy. This is important for eliminating cracks when paired with the weld repairs mentioned in Chapter 2.

## Disadvantages

The accuracy of ultrasonic testing comes at a price. Due to the lack of explicit failure criteria in the process used to identify initial cracks, the finding of these cracks using ultrasonic testing has been termed more of an “art” than an exacting science. While an experienced technician can easily find these cracks, a less experienced technician may be at a loss as to what identifies the crack in the signal. This problem makes it difficult to find enough well qualified inspectors to properly carry out the job of identifying initial crack issues in poles. Another problem with ultrasonic testing is that it is limited to testing certain areas of the base plate to pole connection. These limitations can be based on the distance available above the weld toe for moving the transducer and the flatness of the surface on which the transducer rests. Also, it is much more difficult to identify cracks that are in the weld itself instead of at the weld toe.

## 3.3 Fatigue Testing

The primary goal of this study is to determine the fatigue life of the high masts. To do this, fatigue testing was carried out utilizing the original test setup and test procedure from the Pooled Fund Study.

### 3.3.1 Test Setup

The setup used for fatigue testing of high mast specimens tested the masts horizontally, two at a time. This setup was designed by researchers during the first phase of the Pooled Fund Study of testing at The University of Texas at Austin (Rios, 2007). A schematic of the test setup is shown in Figure 3.6.

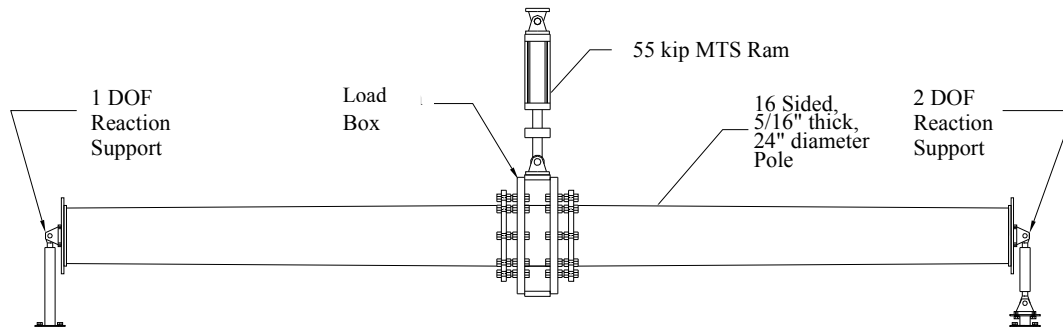


Figure 3.6 Test Setup, Depicting a 24" Diameter Pole From The Pooled Fund Study (Rios, 2007)

Although there may not be perfect rigid base restraint in high mast poles in the field, analytically they are considered as vertical cantilevers (Stam, 2009). Vertical testing is more difficult to install and only able to test one specimen at a time. For this reason, researchers designing the test setup for the Pooled Fund Study chose to test in the above horizontal fashion. Assuming this is supported by a pin end support and a roller end support, this can be modeled as a simply supported beam with length  $2L$ , or, if the rotation in the center is zero, as two back to back cantilevered beams with length  $L$ . Rotation at the center can be assumed to be zero so long as symmetry of stiffness is maintained. A rigid load box was fabricated that provided a means of connecting the two specimens to the hydraulic actuator. The reaction box is discussed further in the following section.

To preserve the simple beam assumption, proper end restraints were needed. A pin at the south end provided a single rotational degree of freedom through the use of an elevated rod-eye. The north end made use of two rod-eyes connected by a steel rod to create a roller, which offered two

degrees of freedom, rotation and longitudinal translation. See Figure 3.7 for schematics of the end supports.

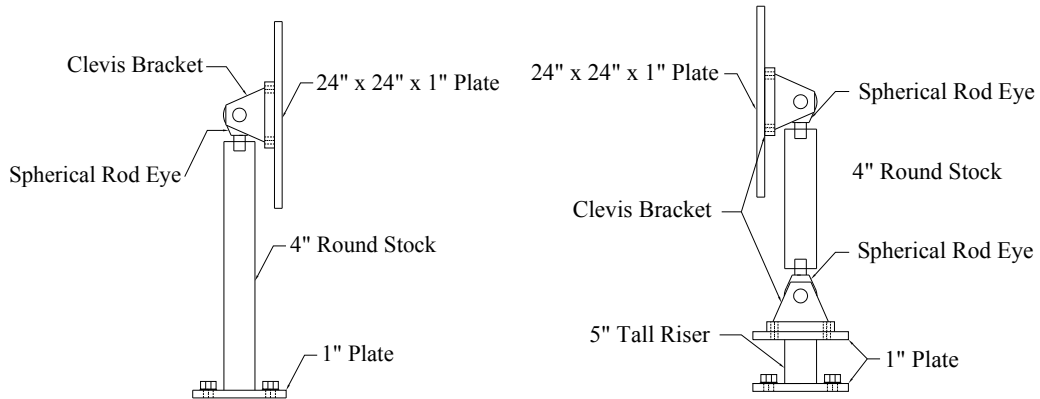


Figure 3.7 Test Setup End Supports (Rios, 2007)

A portal frame was designed at the beginning of the Pooled Fund Study to resist the loads imparted by the force in the ram. This consisted of two wide flange columns supporting a wide flange beam with diagonal braces as shown in Figure 3.8. The figure also shows the yellow load box that connected the two specimens to the hydraulic actuator.





Figure 3.8 Portal Loading Frame with Pooled Fund Study Specimen Attached (Stam, 2009)

The length of the test setup was chosen based on anchor locations in the lab floor. Since anchors were spaced every 4 feet, a length of 32 feet was chosen. This length was ideal in that it allowed the specimens to be flexible enough to be within the capacity of the ram, but stiff enough to prevent large displacements.

The 55 kip hydraulic ram was attached to the load box using ball and socket joints at the top and bottom. This was done to prevent restrictions on the center of the “simple beam” and also to facilitate easier installation of the specimens. In doing this, however, an instability occurs whenever the ram pushes down on the beam, causing the center to push outward and rotate out of plane. Because of this instability, the ram was only used to apply an upward vertical force and the top fibers on the specimens were only fatigue cycled in a tensile stress range. This is different than what would be seen in the field, since the swaying motion caused by wind induced loads would cycle the fibers from tension to compression. This testing setup still created valid lower bound results because tensile forces are considered to be more damaging in fatigue.

### 3.3.1.1 Load Box and Connection

A very stiff element to connect the ram was needed between the two poles in order to maintain the simple beam theory. It was also decided that the connection from the stiff element to the poles needed to mimic the conditions seen in the field so that an accurate representation of stress flows could be achieved. A stiff load box was designed to minimize displacements between the anchor rods and accurately represent the effect of a high mast foundation.

The stiff element connecting the two high masts together was a redesigned built up steel loading box that was different than the one used for the Pooled Fund Study. The reason for the change in load box was due to the increase in diameter of the specimens tested in this study. The diameter increase led to an increase in both the diameter of the base plate and the diameter of the bolt hole circle, which, in turn, became too large to fit on the load box from the previous study. This necessitated the design of a larger load box that could fit the larger poles tested in this study. The design of the load box is shown in Figure 3.9.

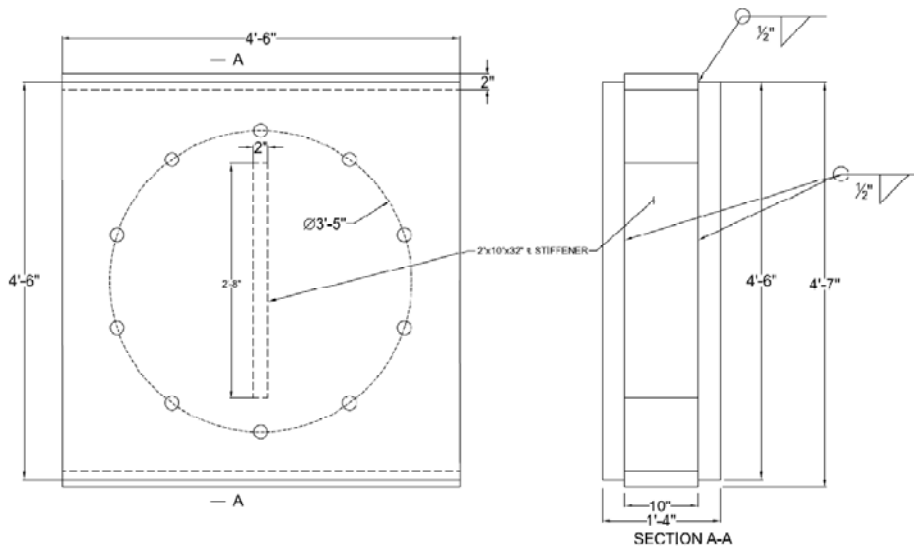


Figure 3.9 Schematic Design of Load Box

A double nut connection was used for the connection from the load box to the high mast. This connection is consistent with common field connections used to level and secure the high mast in place. See Figure 3.10 for a picture of this connection.

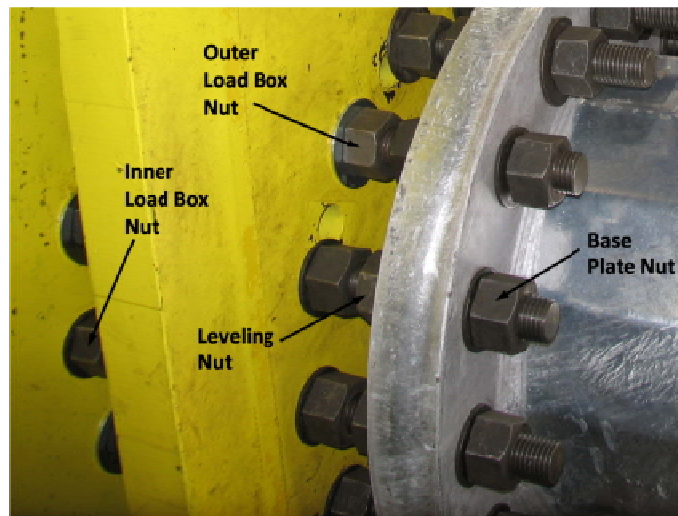


Figure 3.10 Double-Nut Connection On Pooled Fund Study Specimen (Stam, 2009)

### 3.3.1.2 Hydraulic and Control Systems

A hydraulic ram was used to cycle the specimens through a range of tensile stresses. This was done using a 55 kip MTS hydraulic actuator measured by an MTS load cell transducer. The hydraulic pressure was supplied by an MTS SilentFlo Hydraulic Power Unit connected in line with two servo valves and a manifold used to control the flow and reduce pressure fluctuations.

An MTS FlexTest SE Controller connected to a personal computer was used to control the test. The controller monitored and controlled displacement, force, and error in the ram. It was also able to set oscillation frequencies which were typically run under 2.5 Hz to avoid the natural frequency of the specimens and prevent large dynamic effects.

All the fatigue tests were performed using displacement control. This was done both to remove dynamic effects from the analysis and to prevent the system from becoming unstable as the

specimens began to fail. The use of displacement control also allowed the reduction in stiffness to be used as a failure condition.

### 3.3.2 Fatigue Testing Procedure

The testing of the specimens had three distinct pretesting phases: the measurement and inspection of the specimens, the installation of the specimens into the test setup, and the calculation of the loads and displacements necessary for the testing. Once all of this was finished the fatigue test was started.

#### 3.3.2.1 Measurement and Inspection

The first step in testing new specimens was taking measurements and inspecting the poles. The poles were checked to determine if they conformed to the specified design. Most dimensions were checked, including length, base plate thickness and diameter, weld dimensions, as well as pole thickness, diameter, and taper. Except for pole taper on the first set of specimens, all dimensions on each specimen checked conformed within typical fabrication tolerances.

After the measurements were taken on the specimens but before installation began, an inspection was performed by a trained TxDOT inspector. For most specimens this only involved performing ultrasonic testing at the bends in the pole. The second pair of specimens underwent both ultrasonic testing and magnetic particle testing. As outlined earlier, the magnetic particle testing was inconclusive and not used for further inspection of non-fatigued poles. The inspections were performed using the nondestructive testing procedures described at the beginning of this chapter.

#### 3.3.2.2 Installation Procedure

Installation of the high masts into the test setup was the next step in testing the high masts. This process was performed by the joint efforts of the researchers and lab techs at the Ferguson Lab, and all efforts were made to perform a uniform procedure that ensured the applicability of the

simple beam assumptions. A more detailed account of the installation procedure can be found in Stam (2009). A picture of a high mast being installed along with a common tightening sequence is shown in Figure 3.11. Anchor rods were tightened using a pneumatic wrench geared to a torque of approximately 1000 ft-lbs.

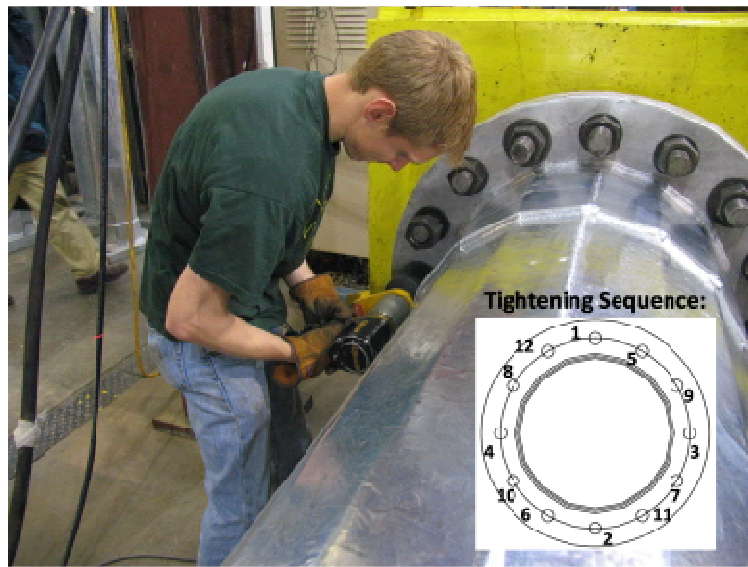


Figure 3.11 Installation of High Mast Along with Tightening Sequence (Stam, 2009)

The primary difference between this study’s installation procedure and the Pooled Fund Study’s procedure was the orientation of the high masts in the test setup. In the previous study the bend with the longitudinal weld seam on the pole had typically been placed in the “up” position (the bend pointing upwards, and also the location of the highest tensile stress) since it was believed that the weld seam in this location created the worst fatigue position. For this study, however, the “up” position was decided by the location of initial cracks found through ultrasonic testing. For most specimens, the worst initial crack location was placed up, although for the second pair of specimens the least initial cracking was put up first and then the worst cracking was rotated to the up spot for a second test.

As mentioned above, specimens were occasionally rotated after failure. This is due to the assumption that the compression cycles do not cause any (or much) fatigue damage. This was done on the first set of specimens when the galvanized sample failed before the black one, during the testing of the weld repair specimens because the field repair failed the shop repair, and on the second set of specimens as mentioned above.

### 3.3.2.3 Testing Loads and Displacements

Simple elastic bending of  $\sigma = M_1c/I$  was assumed for computing all testing loads. The moment of inertia,  $I$ , was computed by utilizing cross sectional analysis functions in the CAD program that the cross section was drawn in. The  $c$  in the equation is the distance from the center of the cross section to the extreme fiber at the top of the cross section, or half the distance from on bend to the bend directly across from it.  $M_1$  is the bending moment at the location of the weld, which was determined using simple beam analysis as shown in Figure 3.12.  $\sigma$  is the stress at the weld toe at the extreme fiber where the highest amount of tensile stress is expected.

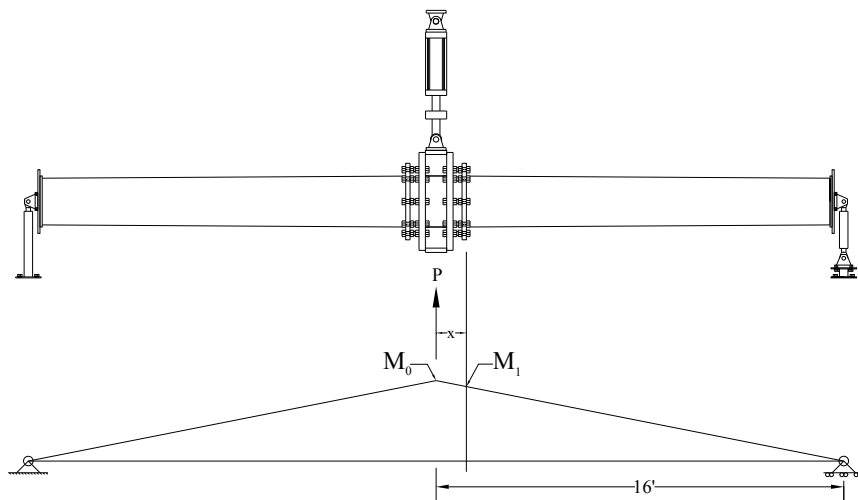


Figure 3.12 Moment Diagram for Calculating Testing Loads (Rios, 2007)

A stress range and mean stress were selected prior to testing. For all fatigue testing done except on the external collar specimens this stress range was 12 ksi and the mean stress was 10 ksi. These parameters set the maximum stress at 16 ksi and the minimum stress at 4 ksi. The external collar specimens were tested at a stress range of 6 ksi and a mean stress of 6 ksi. This was decided on based on preliminary measurements of stress ranges on in-situ poles showing much lower ranges than the 12 ksi stress range. This meant that for the external collar specimens the maximum stress range was 9 ksi and the minimum was 3 ksi. Utilizing the above simple elastic beam theory, a maximum required moment and a minimum required moment were able to be determined. A load P supplied by the ram that provided the desired moment was determined by the following equation where x is the distance from the center of the ram to the weld toe of the high mast in feet:

$$M_1 = \frac{16 - x}{16} M_0 = \frac{16 - x PL}{16 \cdot 4}$$

An important cross sectional distinction was made in the Pooled Fund Study about how to account for an external collar in the analysis. The conclusion of the researchers was that the external collar was merely an additional accessory that protected the weld, and thus its area should not be included in any cross sectional analysis (Richman, 2009) (Stam, 2009). Also, all analysis was done using nominal dimensions rather than actual measured dimensions. Because of this all specimens in this study used the same cross section for analysis and determination of testing loads.

As mentioned above, the tests were displacement controlled. Once the loads were calculated they were applied to the specimens at a low frequency of 0.1 Hz. The static displacements were measured during these pseudo static tests. These static displacements were then used to set the mean displacement and the amplitude of the displacements required for testing. Under dynamic motion during the test, the loads required to for the given displacements dropped as the frequency of the oscillations increased due to the dynamic amplification of the load, but the stress remained the same due to the displacement control.

Testing was typically begun slowly with a low frequency to allow for seating of the specimens into the test setup. During this period the displacement limits often needed to be adjusted to

maintain the desired loading. Once the specimens had settled the frequency would be increased and the test would be allowed to run until failure of one or both specimens.

### 3.4 Follow-up Inspection and Destructive Testing

Following the fatigue testing, another inspection was conducted using ultrasonic and magnetic particle testing procedures as previously discussed. This was done to verify failure conclusions drawn during the testing of the specimens, and was performed by a trained TxDOT inspector.

After the non destructive inspection was performed on all of the bends on the sample, a destructive inspection was often performed on a few selected bends. This was done to not only verify the non destructive testing results, but also to determine the nature of the cracks such as if there was evidence of initial cracking or if there might be a weld defect.

Destructive testing was performed by first separating the base plate and roughly 10” of the pole shaft above the base plate from the rest of the specimen. This was typically accomplished with torch cutting. The base plate and shortened shaft were then sectioned for easier handling using a combination of torch cutting and cuts with a chop saw. Finally, the actual bends were opened using a band saw that produced a finer and neater cut. Often times the cross sections were cleaned, polished, and even acid etched to show where weld passes were made. Several “opened” bends are shown in the next chapter.



## Chapter 4 Testing Results

### 4.1 Introduction

This chapter provides a discussion of the results of the testing done on the specimens. The first four sections discuss each individual specimen design separately. Except for Section 4.4 and Section 4.5, which cover the weld repair specimens and external collar specimens, in each section the ultrasonic testing results, fatigue testing results, and destructive testing results are discussed. The destructive testing has not been completed on the weld repair or external collar of specimens; therefore no destructive testing results are reported. The following section compares the ultrasonic testing results across the entire specimen testing matrix, as well as discussing the results of the ultrasonic tests completed on specimens from the Pooled Fund Study and on TxDOT in-situ specimens. The final section compares the fatigue test results of all of the samples, and includes fatigue test results of similar samples from the previous study as well.

### 4.2 Specimens 33-3-12-TX-SG-A and 33-3-12-TX-SB-B

The first specimens tested were specimens 33-3-12-TX-SG-A and 33-3-12-TX-SB-B. This specimen pair had one specimen galvanized and the other was left black. A description of the specimen design can be found in Section 2.4.

#### 4.2.1 Ultrasonic Test Results

Prior to fatigue testing of the specimens, ultrasound testing was performed by TxDOT personnel on both samples to check for initial cracks. Crack indications were found in all non-seam bends of the galvanized specimen and none were found in the uncoated specimen. Typical crack indications were about  $\frac{1}{8}$ " deep. Figure 4.1 shows the location of these cracks and their lengths along with the bend numbering scheme. These bend number will be consistent throughout this section.

It should be noted that at this point in the study ultrasonic tests were not performed at the longitudinal weld seams. Weld seams were not believed to provide reliable testing results and were, therefore, not tested. It was not known whether there were initial cracks located at these weld seams. In later ultrasonic tests inspectors had become more skilled at interpreting signals at weld seams and were often able to identify initial cracks in these locations.

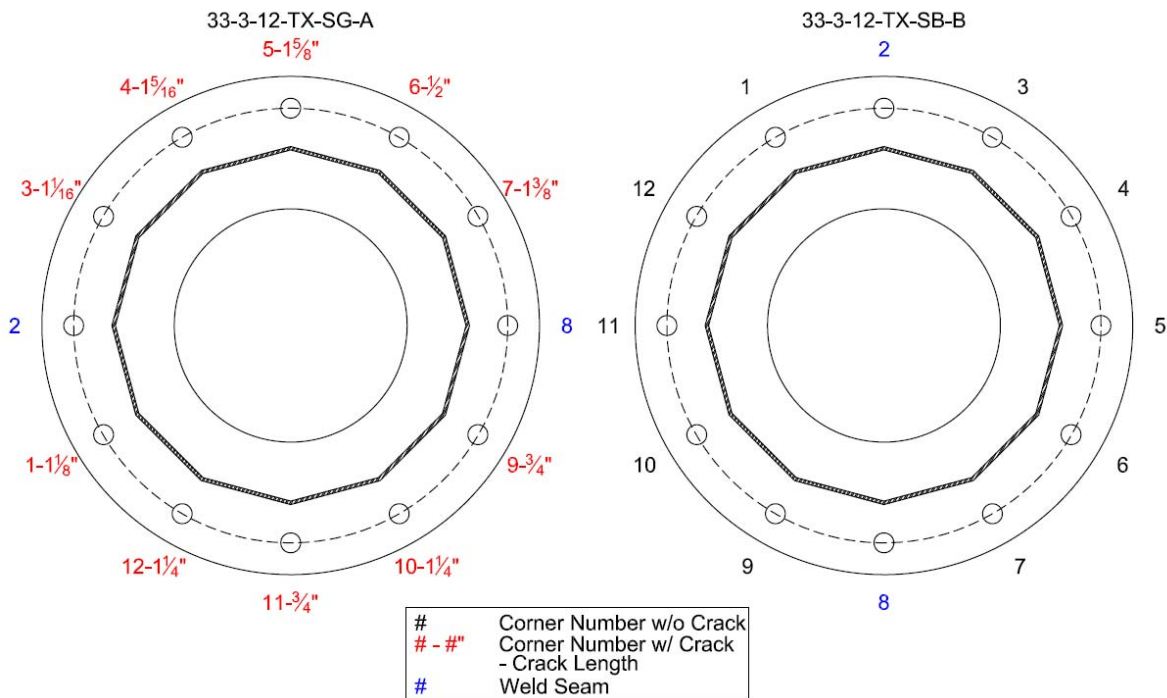


Figure 4.1 Initial Crack Locations and Lengths in Specimens 33-3-12-TX-SG-A and 33-3-12-TX-SB-B

#### 4.2.2 Fatigue Test Results

After the ultrasonic testing, fatigue testing was performed on the specimens. The load was cycled between 11.7 kips and 46.7 kips to produce a nominal stress range of approximately 12 ksi and a mean stress of 10 ksi in the mast at the base plate connection. The loading cycle was run at frequencies ranging between 0.1 Hz and 0.9 Hz, with the majority of the cycles at 0.5 Hz. Load limits were initially set to stop the testing after a 5% change in load or deflection. These testing

limits were later increased to compensate for a rapid decrease in the load carrying ability of the samples, possibly caused by slip within the test setup or propagation of cracks. The fatigue test was stopped after large fatigue cracks were found in the galvanized specimen.

The initial orientation of the galvanized sample was selected to keep the weld seams of the sample at the neutral axis. The neutral axis is located 90° from the up position discussed in Chapter 3. According to simple beam theory, the neutral axis experiences no bending stress. Figure 4.2 shows the initial orientation and rotated orientation, along with the location of bends discussed in this section. Bend 5 of the galvanized sample was selected to be placed upwards in the test setup, subjecting that bend to the maximum fatigue stress. The ultrasonic inspection of bend 5 before testing had found a crack indication roughly 1.625" long.

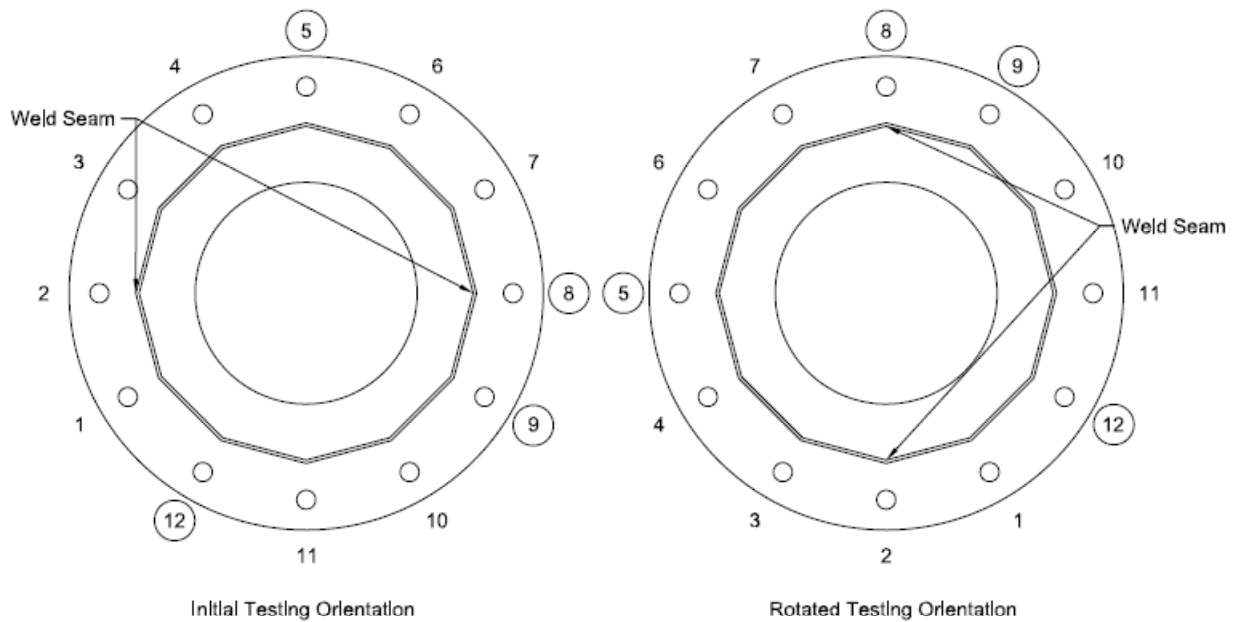


Figure 4.2 Initial and Rotated Orientation of 33-3-12-TX-SG-A with Circled Bends Further Investigated

The test was first stopped at 4,464 cycles due to loss of stiffness. There were no cracks visible upon inspection of the sample and it is believed the loss of stiffness was due to slip in the connection. A second inspection after 5,144 cycles also revealed no visible cracks. A third inspection occurred at 27,322 cycles, a very small visible crack at bend 5 was found. Testing was continued on the sample by adjusting the displacements to produce the desired fatigue loads. Testing on bend 5 was stopped at 81,326 cycles and the sample was rotated 90°, placing the bend on the neutral axis so that testing could continue. A large, visible crack had formed in bend 5, as well as smaller cracks in bends 4 and 6. No cracks had formed in the black specimen. The crack at bend 5 can be seen in Figure 4.3.

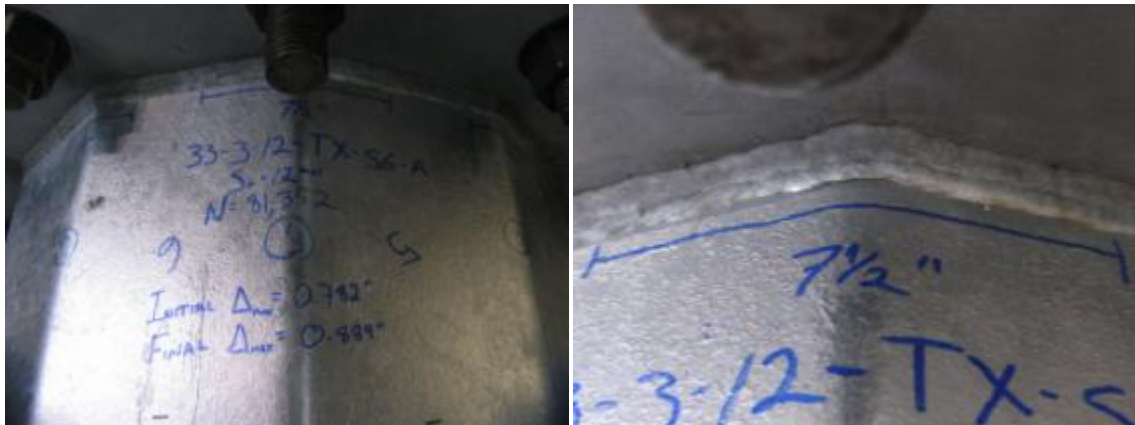


Figure 4.3 Crack Length at Bend 5 on the Galvanized Specimen after 81,326 Cycles

Considering the number of cycles run and the stress range in the specimen, the galvanized specimen failed below AASHTO's lowest fatigue category of E', as shown in Figure 4.4.

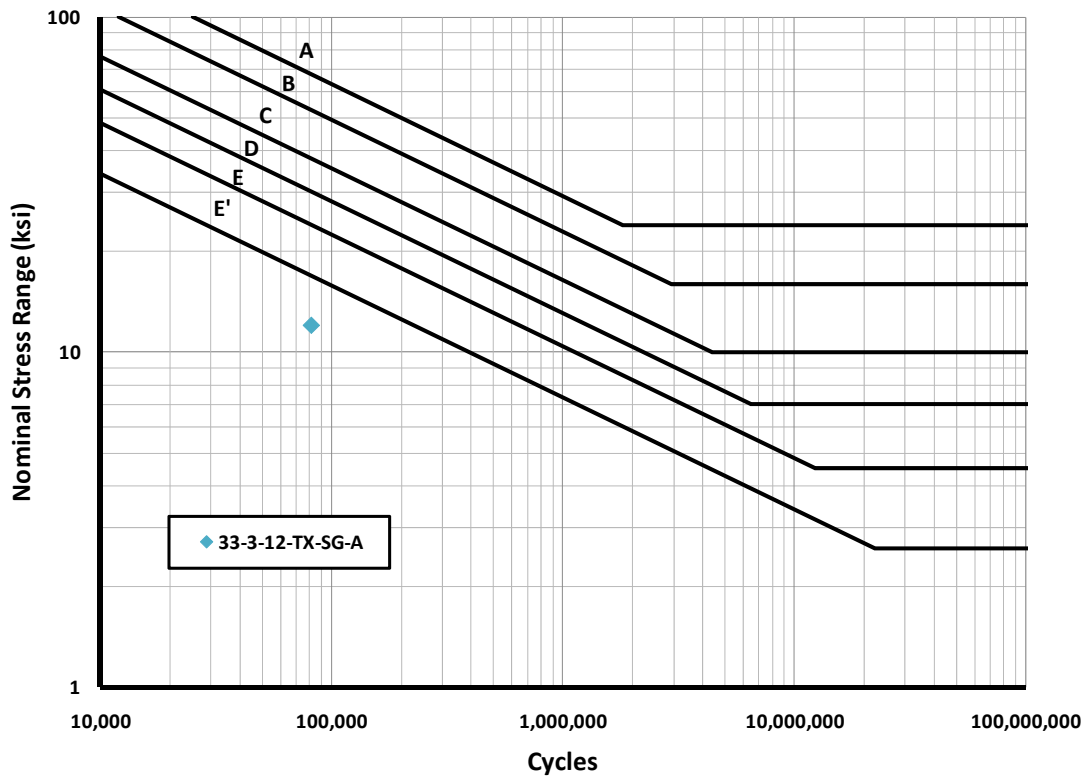


Figure 4.4 Fatigue Life of Galvanized Specimen Compared to AASHTO Fatigue Categories

The galvanized specimen was rotated 90° to allow continued testing of the black specimen that had not failed (the black specimen was left in its original orientation). Typically in the Pooled Fund Study, specimens are rotated a full 180° to put the undamaged compressive side up into tension. This was not done for this testing case because the researchers wanted to have a chance to perform a destructive test on an unfatigued bend that contained an initial crack, such as bend 12 in this case.

The same mean stress and stress range were used to test the specimens after rotation. Once again, the galvanized specimen failed after approximately 70,000 cycles and there was no apparent damage in the black specimen after the 150,000 cycles it had sustained. Because it is difficult to assess the amount of fatigue damage sustained by the bends rotated to the up position, the fatigue

results of the rotated galvanized specimen are not considered valid. There are some aspects, however, that are of interest.

The original testing orientation placed bend 8 on the neutral axis and bend 9 just below the neutral axis on the side cycled in compression. The sample was then rotated so that bend 8 was placed upwards in the highest tensile stress position with bend 9 also undergoing tensile fatigue. The results were surprising: the weld seam at bend 8, considered in the Pooled Fund Study to be one of the weakest areas in fatigue due to the intersecting welds (Stam, 2009), developed a fatigue crack later than bend 9. Upon completion of the testing, bend 8 had an approximately 3" fatigue crack and bend 9 had a 4¼" fatigue crack, despite experiencing a lower stress range.

#### 4.2.3 Destructive Test Results

Four bends from the galvanized specimen were opened using destructive methods for further investigation. These were bends 5, 8, 9, and 12. No bends were opened from the black specimen because it was decided to save the specimen for later galvanizing. This black specimen became the Shop Repair specimen used for the weld repair portion of the study.

The “opened” bends that have undergone destructive examination typically exhibit an area of initial cracking, fatigue cracking, and a ductile tear area. The ductile tear is a product of the destructive examination process: where the metal shaft has not cracked through the entire thickness the remaining connected thickness is flexed until failure. The failure surface caused by this is noticeably different from the fatigue crack area and initial crack area.

##### 4.2.3.1 Bend 5

As mentioned above, bend 5 had a 1<sup>5</sup>/<sub>8</sub>" crack indication found during ultrasonic testing and a 7½" fatigue crack found after fatigue testing. After testing, bend 5 was cut open to view the cracks. Figure 4.5 is a picture of the opened bend. A close up of the crack is shown in Figures 4.6 and 4.7.

A distinct difference in the crack is visible between the outer and inner edge of the shaft. The interior edge looks like a classic example of a fatigue crack with a smooth fracture surface. The exterior edge of the crack is darker and rougher, which does not appear to be the result of fatigue. This is believed to be an initial crack. The initial crack was approximately 3 inches long. The crack depth was approximately  $3/32$  in. deep.

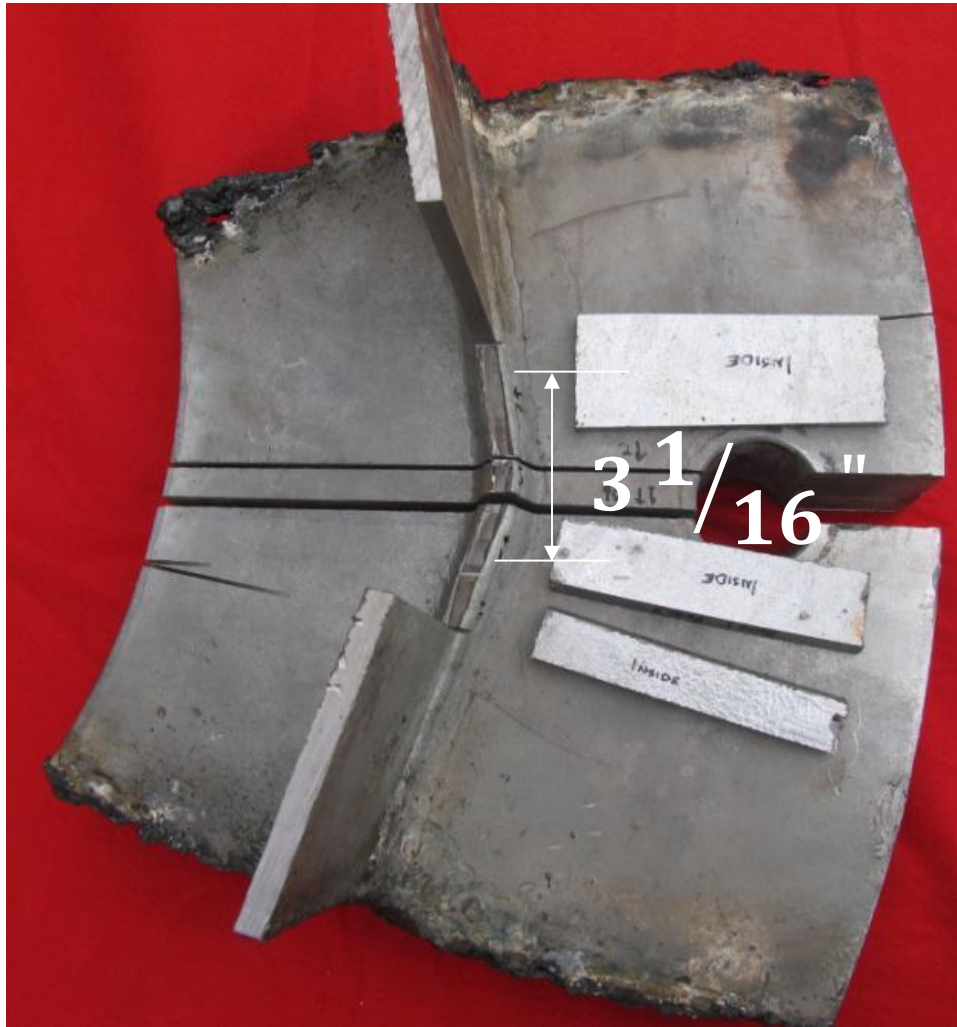


Figure 4.5 View of Bend 5 after Sectioning. Length of Observed Initial Crack is Labeled

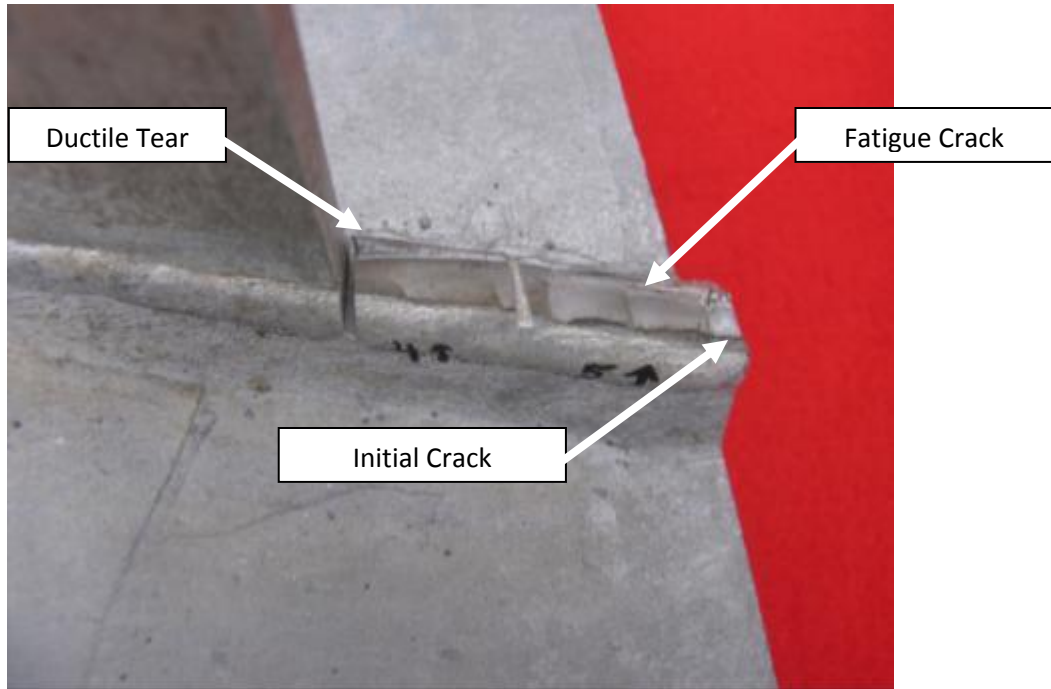


Figure 4.6 Close Up of Fracture Surface at Bend 5

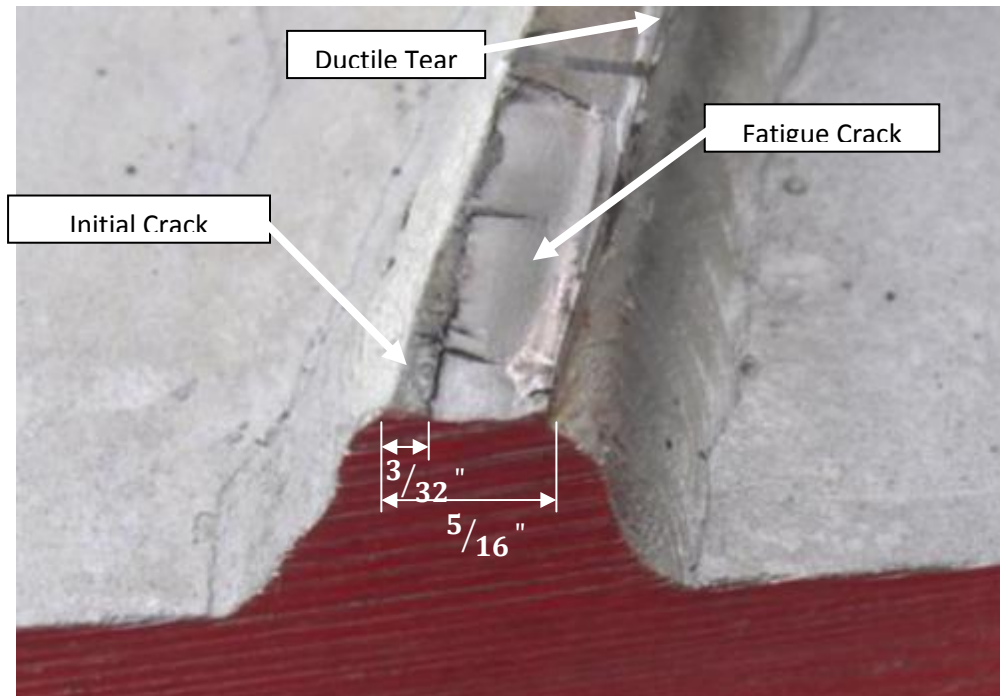


Figure 4.7 Depth of Initial Crack at Weld Toe



#### 4.2.3.2 Bend 12

Bend 12 was not subjected to tensile fatigue loading as it was placed downwards (on the compression side) and then rotated to the neutral axis. Because of this, bend 12 had no fatigue crack. Preliminary ultrasonic testing indicated a crack that was 1.25" long. Upon cutting the bend open no fatigue cracking was found but a 2.375" crack with the same rough, dark appearance that was found in Bend 5 was present. This is likely an initial crack. Figure 4.8 shows this crack.

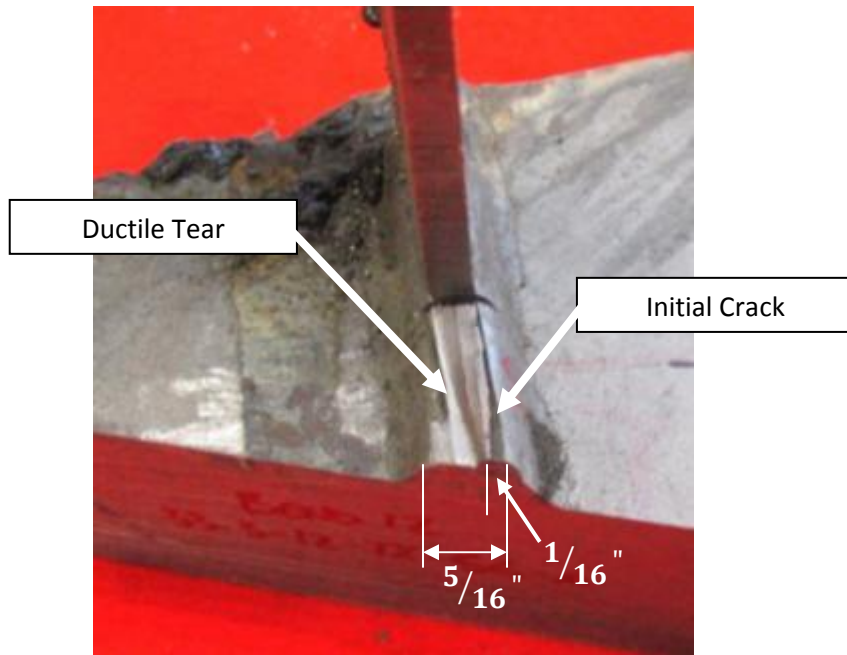


Figure 4.8 Fracture Surface at Bend 12

#### 4.2.3.3 Bend 8 and Bend 9

As mentioned before, the fatigue results at bends 8 and 9 were a little surprising. The difference in fatigue crack can be seen in Figure 4.9. After testing, the bends were cut open. Bend 8 contained what looked to be the initial crack, although in a different pattern than other bends that had been investigated. Instead of the crack being widest at the center of the bend or corner, there

was no indication of initial cracking present in the weld material at the corner. An initial crack appears to begin on either side of the weld metal and progresses outwards from the weld (approximately  $1\frac{3}{8}$ " on one side and  $\frac{7}{8}$ " on the other). The crack was about  $\frac{1}{16}$ " deep. Figure 4.10 shows close up of the cracked surface on bend 8. Bend 9 contained an initial crack similar to other bends that had been previously cut open. The crack at bend 9 was  $3\frac{1}{4}$ " long and  $\frac{1}{8}$ " deep at its deepest point.

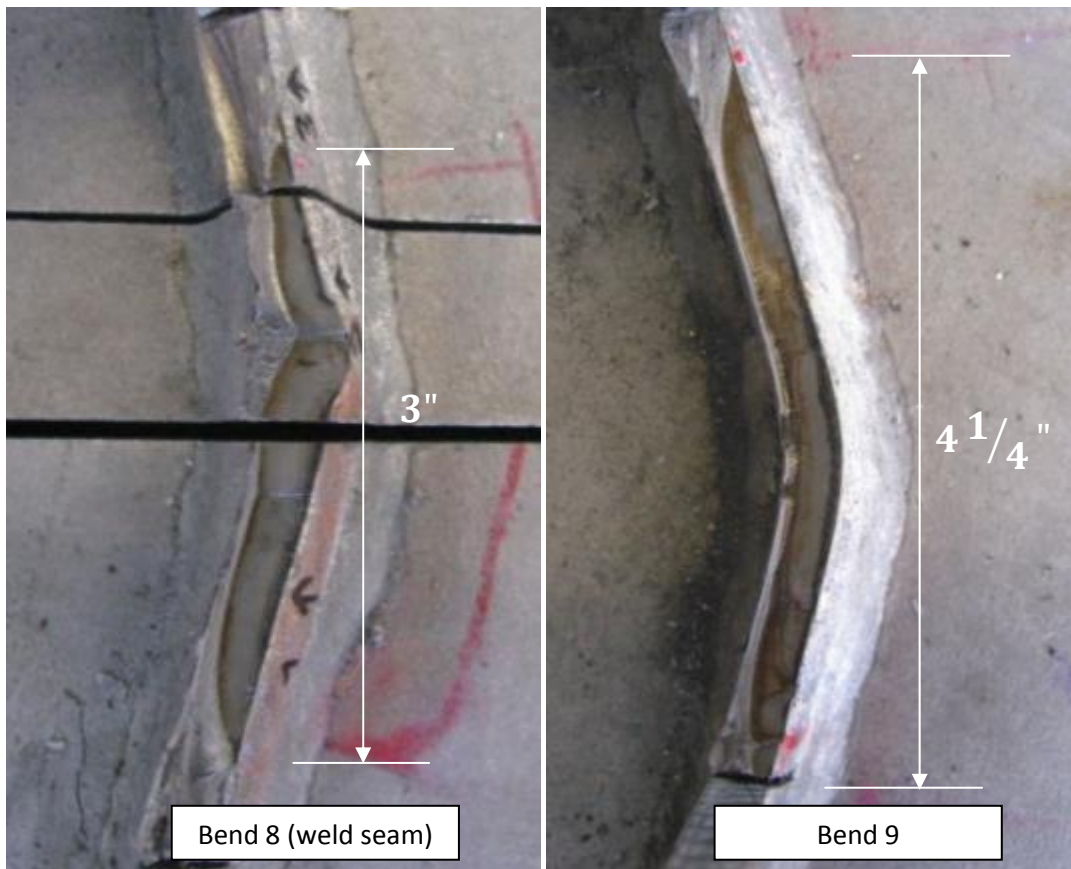


Figure 4.9 Fatigue Cracks at Bends 8 and 9

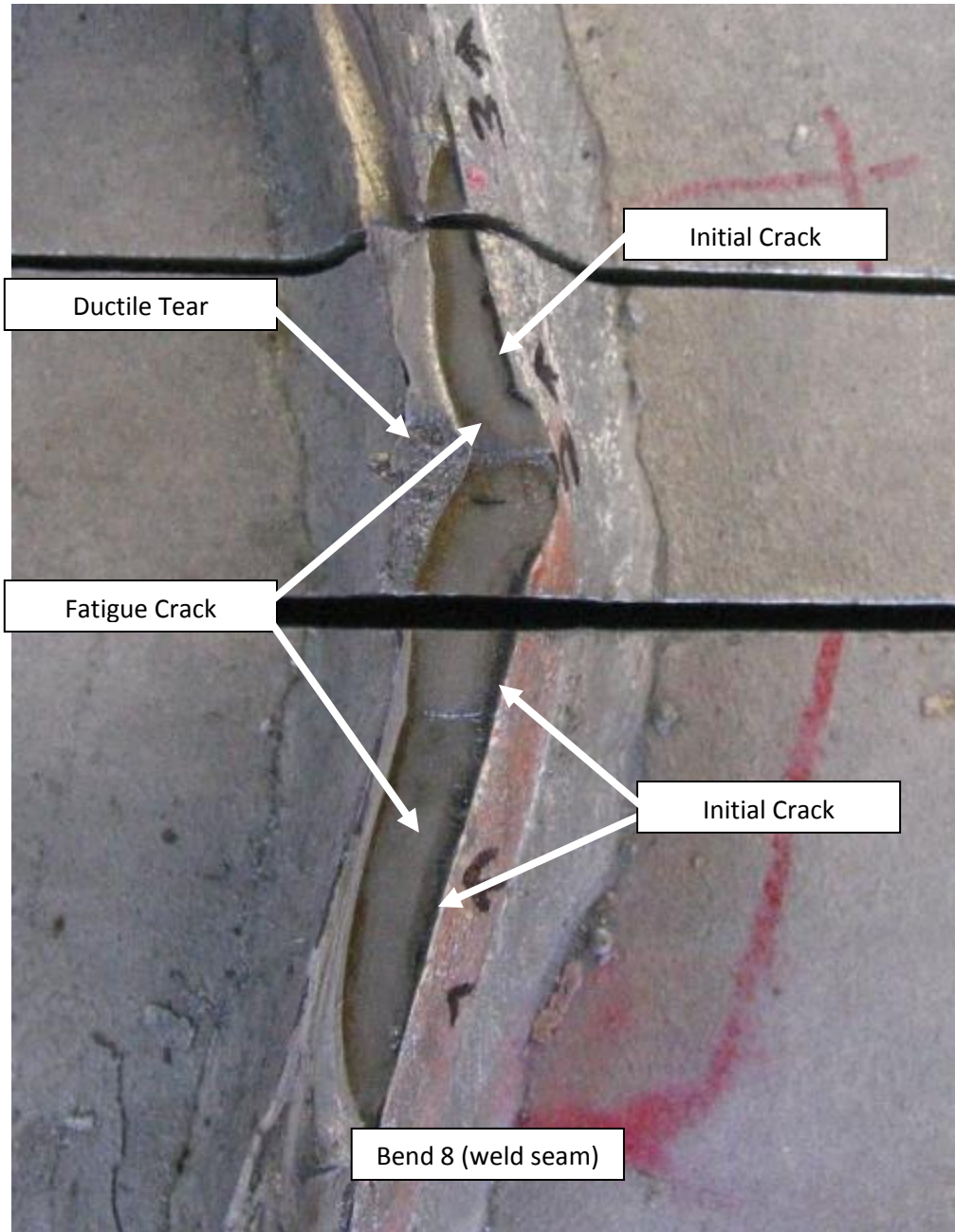


Figure 4.10 Fracture Surface of Bend 8

### 4.3 Specimens 33-3-12-TX-VG-A and 33-3-12-TX-VG-B

The following two specimens tested were specimens 33-3-12-TX-VG-A and 33-3-12-TX-VG-B. These specimens were designed similar to the previous two specimens; except in this case the specimens were fabricated by a different supplier and both specimens were galvanized at the facility of the supplier. A description of the specimen design can be found in Section 2.5.

#### 4.3.1 Ultrasonic Test Results

As before, the specimens were first submitted to ultrasonic testing prior to fatigue testing. Figure 4.11 below shows the results of the ultrasonic test along with the initial testing orientation, with bends shown at the top placed in the top of the test setup. The specimens were later rotated 180° (i.e. bend #2 placed in the upward position on specimen A) and retested (denoted in results as “flipped”). Bend numbers in black contained no crack indications, while bend numbers marked in red contain an initial crack indication with the length of the indication next to the corner number. Bends marked in blue denote weld seams and were, once again, not tested with the ultrasound.

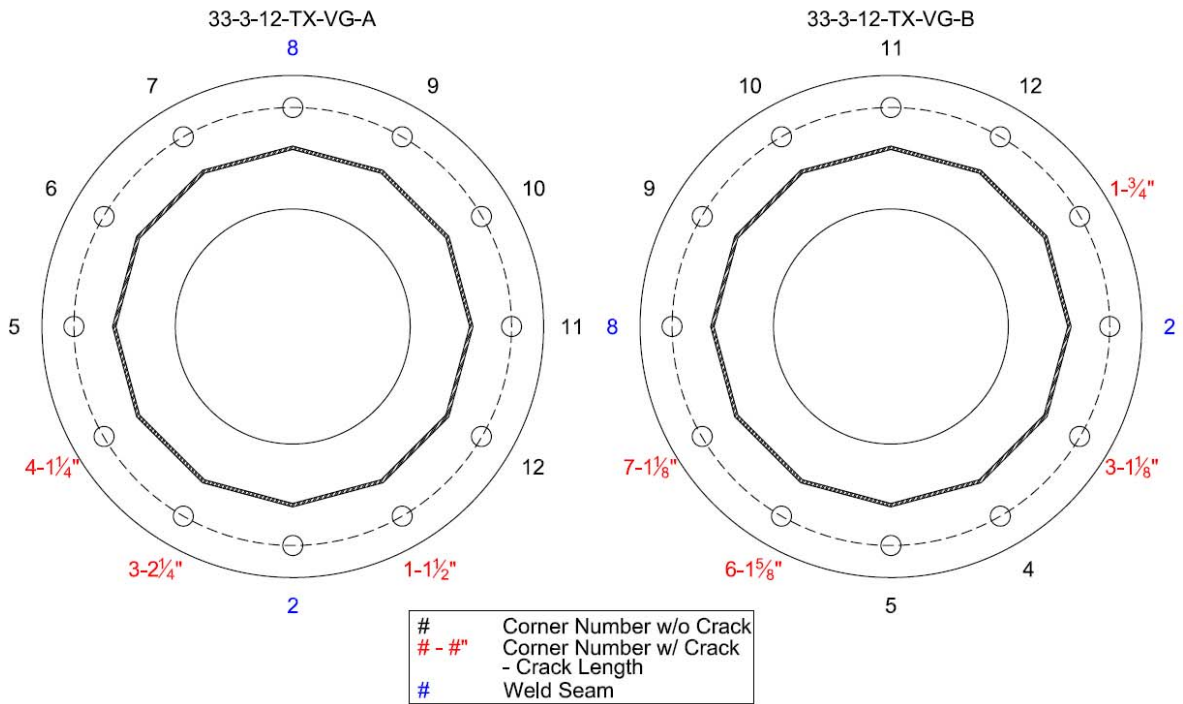


Figure 4.11 Ultrasonic Results and Initial Orientation of 33-3-12-TX-VG-A and 33-3-12-TX-VG-B

#### 4.3.2 Fatigue Test Results

It can be seen from the above ultrasonic test results that each specimen had initial crack indications primarily on one side. Because of this fortunate initial crack layout, it was decided to first test the specimens in an orientation with as few initial cracks under tensile stress as possible. After completion of the test, the specimens were rotated to test in the opposite orientation with the most initial cracks under tensile stress. This procedure was done to help compare the effects of initial cracks on the fatigue strength of a pole within the confines of the exact same specimen, eliminating many variables from the comparison.

Similar to the previous specimens, the load was cycled between 11.7 kips and 46.7 kips to produce a nominal stress range of 12 ksi and a mean stress of 10 ksi in the mast at the base plate connection. The loading cycle was run at frequencies ranging between 0.1 Hz and 2 Hz, with the majority of the cycles at 2 Hz. Failure criterion was based on an arbitrarily chosen 10% decrease in stiffness, the same failure criterion from the Pooled Fund Study. Despite this value being

arbitrary, it has been noted in previous investigations that once failure has initiated, the specimen has very little fatigue life left (Richman, 2009) (Stam, 2009).

The test was stopped after 470,711 cycles because of the loss of stiffness. Both specimens were observed to have such extensive cracking that, unlike the previous specimens, both specimens were deemed to have failed at the same time.

Figure 4.12 is a picture of specimen A immediately after failure. The specimen had a  $1\frac{7}{8}$ " crack at bend 7 and a  $5\frac{1}{2}$ " crack at bend 8. There were no initial cracks found at these bends prior to testing.

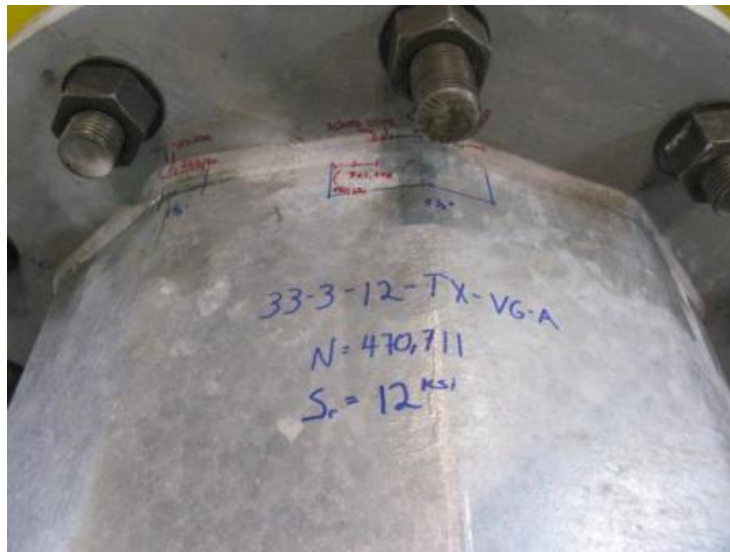


Figure 4.12 Specimen 33-3-12-TX-VG-A after Fatigue Testing

A closer picture of bend 8, seen in Figure 4.13, shows a strange cracking pattern. The crack initiated in the throat of the weld and then jumped to the shaft at the toe of the weld. Nearly all other fatigue cracks initiate and remain at the toe of the weld in the shaft. In this picture the red and black markings follow the crack progression during the test while the blue line marks the final crack length.



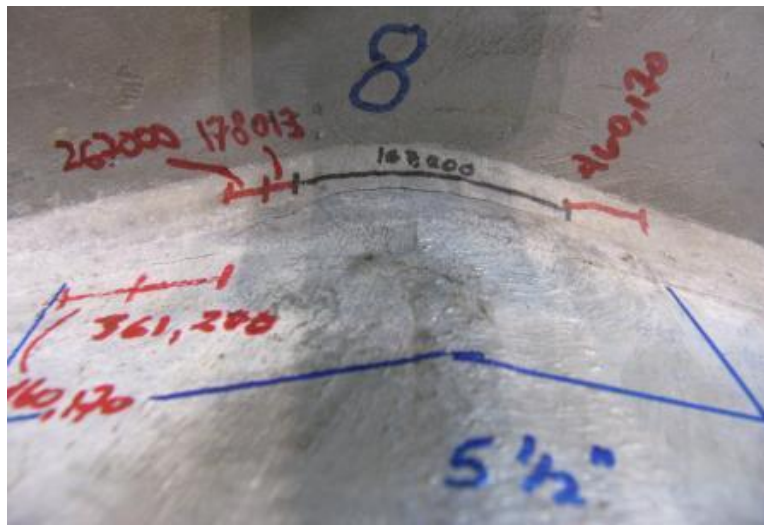


Figure 4.13 Fatigue Crack at Bend 8

Figure 4.14 is a photograph of specimen B immediately after failure. The specimen had a 4½" crack at bend 10, an 8¼" crack at bend 11, and a 5½" crack at bend 12. All cracks were located at the toe of the weld connecting the shaft to the base plate. Again, there were no initial cracks found at these bends prior to testing.

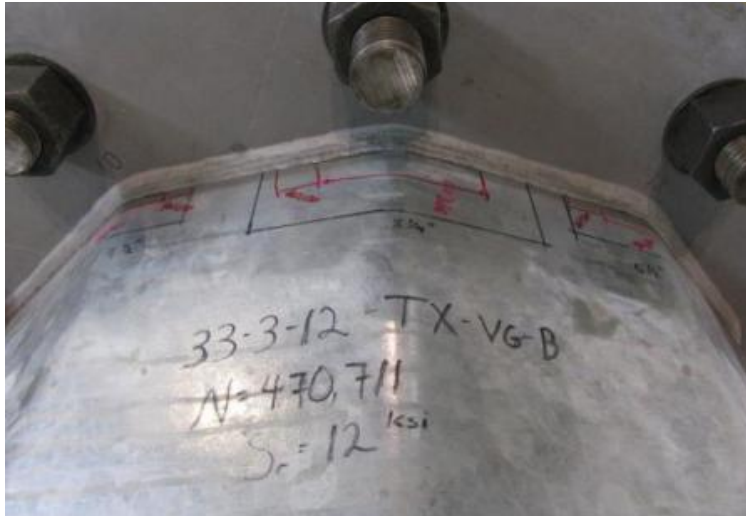


Figure 4.14 Specimen 33-3-12-TX-VG-B after Fatigue Testing

Both specimens were at this point rotated 180° to continue testing. Since the test subjects the top half of the specimen in tension and the bottom half in compression throughout testing, the bottom half of the specimen experienced no damaging cycles during the first stage of testing. When the bottom is rotated to the top, it is as if a new specimen is being tested.

The test was run using the same stress range of 12 ksi and mean stress of 10 ksi after rotation. This time the test stopped after 245,746 cycles due to loss of stiffness. Again, both specimens were observed to have large fatigue cracks and were both deemed to have failed at the same time.

Specimen A had a 1½" crack at bend 1, a 4¾" crack at bend 2, and a 3¼" crack at bend 3. All cracks were located at the toe of the weld connecting the shaft to the base plate. Both bends 1 and 3 had indications of cracks prior to testing. Bend 2 was not ultrasonic tested because it is a weld seam.

Specimen B had a 3½" crack at bend 4, a 6½" crack at bend 5, and a 4¼" crack at bend 6. All cracks were located at the toe of the weld connecting the shaft to the base plate. All three bends had indications of cracks prior to testing.



The chart in Figure 4.15 indicates how the specimens performed relative to AASHTO's fatigue ratings. Because both specimens failed at the same number of cycles, there is only one data point representing the two failures in each orientation. Both orientations of the specimens performed at an E' level, although the flipped specimens (representing the specimens tested at the 180° rotation from the initial test) only just made the E' category.

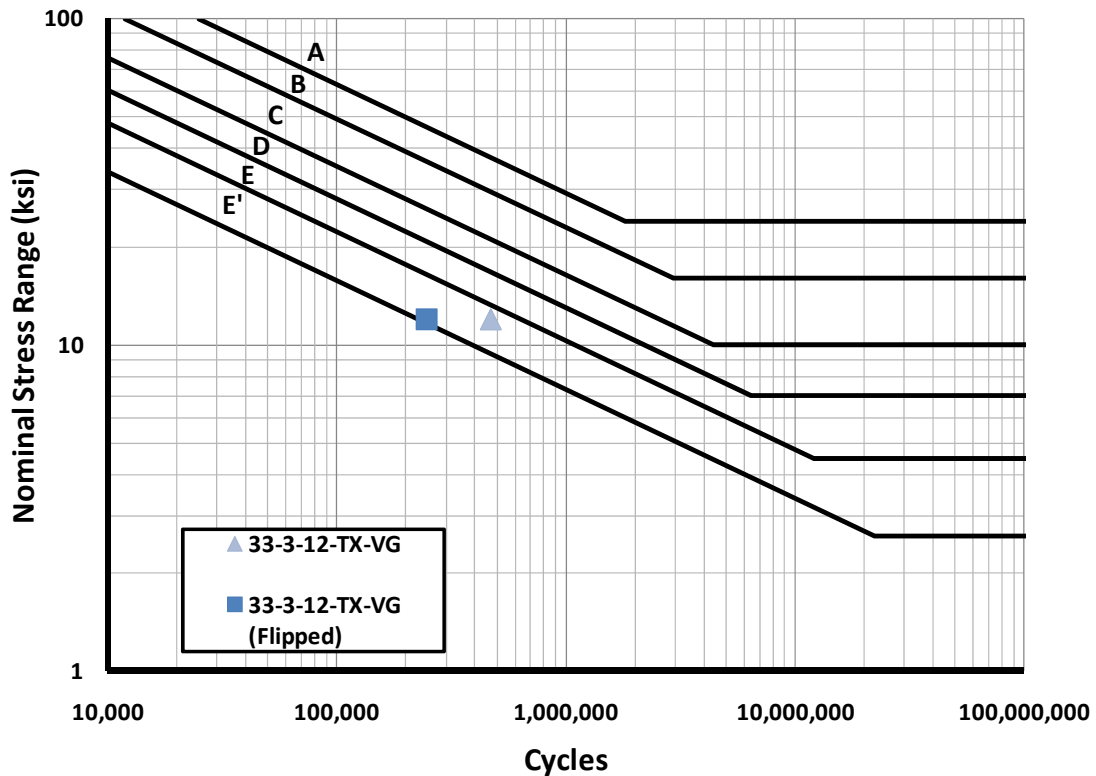


Figure 4.15 S-N Plot for Samples in Initial Orientation and Flipped Orientation

From this, it can be deduced that the initial cracks had an apparent effect on the fatigue strength of the specimens. With the initial cracks undergoing fatigue loading the specimens could handle approximately 50% fewer cycles before failure than without the initial cracks being fatigued. It is difficult to tell, however, what effect cycling the side with the initial cracks into compression has on these results.

### 4.3.3 Destructive Test Results

Only bends from specimen A were cut open using destructive testing to examine the cracks because specimen B was used for the weld repair study. Bend 3 and bend 8 from specimen A were opened for closer examination.

Figure 4.16 and Figure 4.17 are pictures of bend 3. In these pictures the red marker line drawn on the sample denotes the length of the fatigue crack and the blue marker line denotes the initial crack indication found before testing. Although it is difficult to see in these pictures, there appears a darker portion of the crack along the outside edge of the fatigue crack. This is the initial crack and it corresponds well the length of the crack indications.

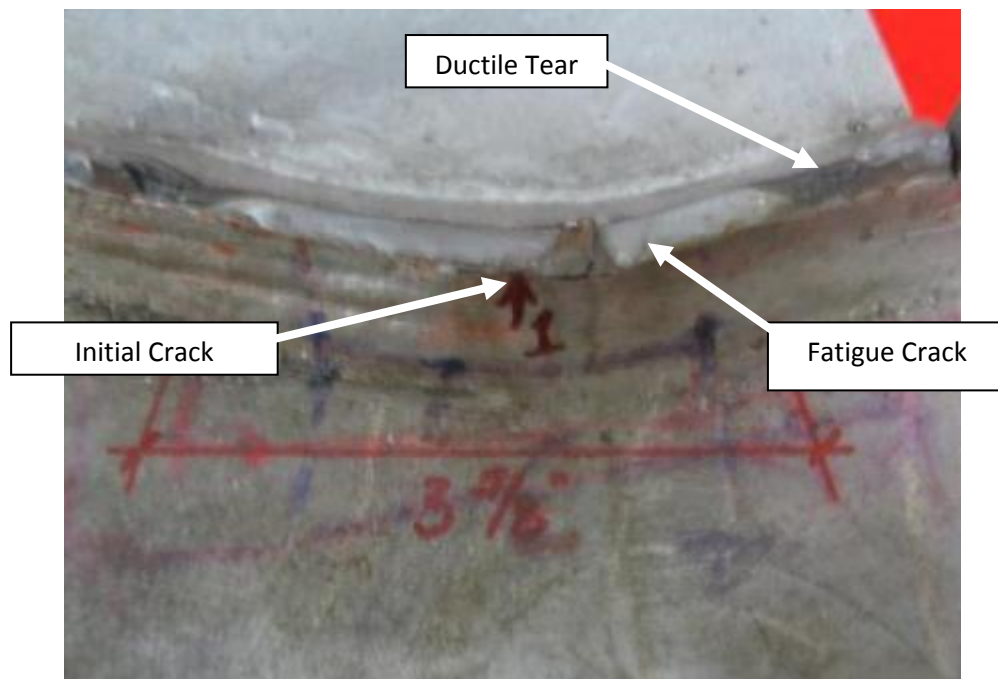


Figure 4.16 Bend 3 of Specimen 33-3-12-TX-VG-A

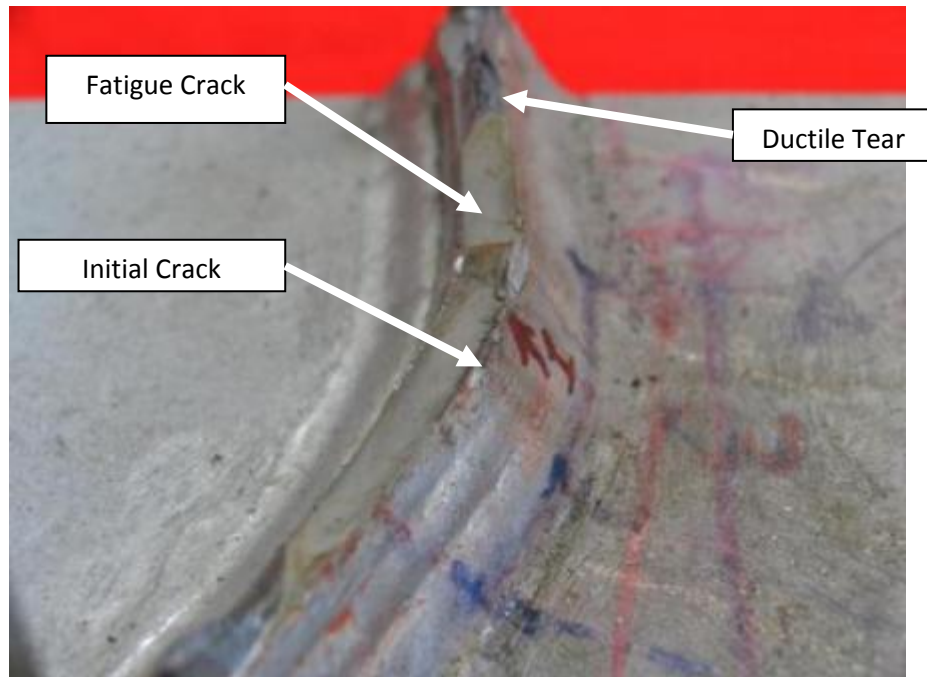


Figure 4.17 Bend 3 of Specimen 33-3-12-TX-VG-A

The following two pictures, Figure 4.18 and Figure 4.19, are of bend 8 on specimen A. This bend was cut open due to the unusual nature of the fatigue crack, as noted above, which failed through the weld rather than at the toe of the weld. Figure 4.18 shows the same darker cracking on the outer edge of the fatigue crack, similar to what was observed with previous initial cracks. There was no initial crack indicated at this bend during the ultrasonic testing. These findings are unusual in that this was the only indication of the initial cracking forming in another location other than the toe of the weld. Figure 4.19 shows the cross section through the weld, where an apparent defect is visible. It is not known what part, if any, this defect played in causing the unusual crack formation.

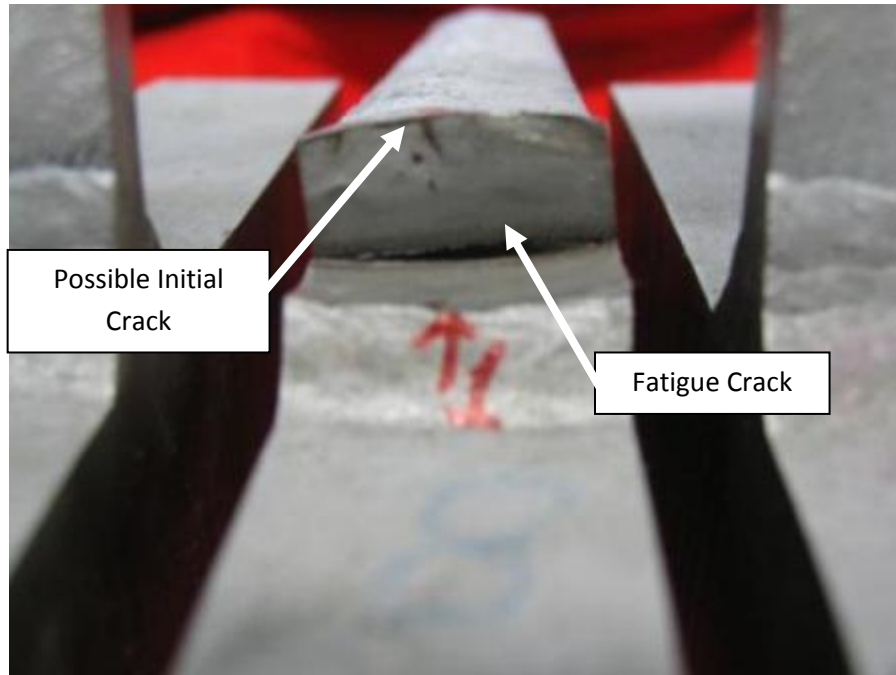


Figure 4.18 Bend 8 of Specimen 33-3-12-TX-VG-A with Fatigue Failure through Weld

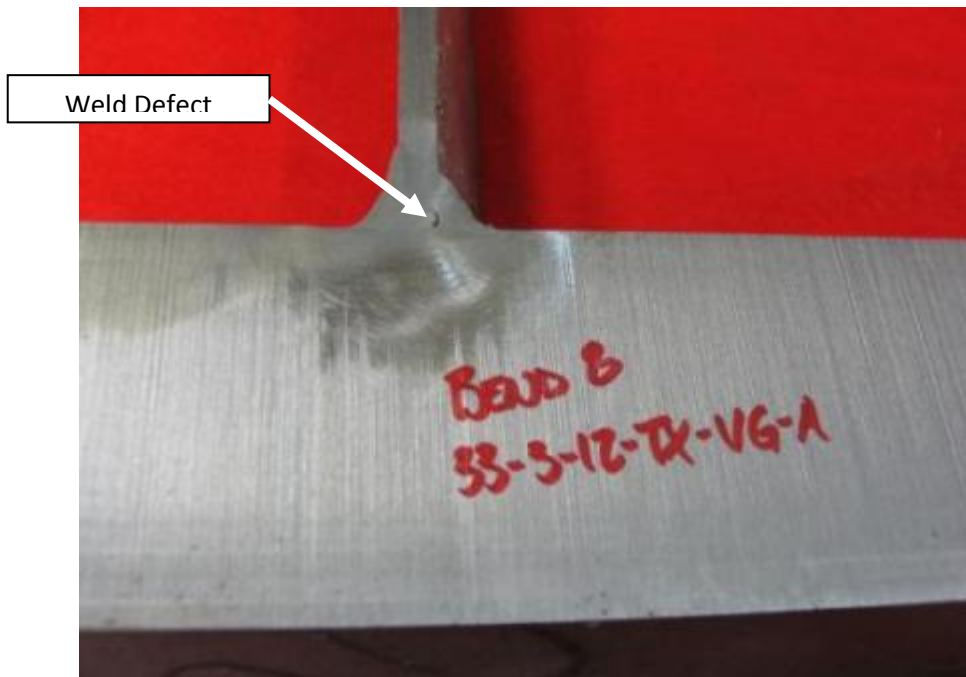


Figure 4.19 Cross Section of Bend 8 of Specimen 33-3-12-TX-VG-A Showing Apparent Weld Defect

#### 4.4 Weld Repair Specimens

The following specimen pair tested was the two weld repair specimens. As discussed in Chapter 2, the specimen referenced as Shop Repair refers to the original specimen 33-3-12-TX-SB-B that was galvanized and repaired using the FCAW weld procedure. The Field Repair specimen refers to the original specimen 33-3-12-TX-VG-B that was repaired using the SMAW weld procedure.

##### 4.4.1 Ultrasonic Testing Results

Both specimens were tested using ultrasonic testing before the weld repair. These results can be found in Figure 2.11 in Chapter 2. After the weld repair, both specimens were retested and no crack indications were found.

##### 4.4.2 Fatigue Testing Results

After the weld repair and ultrasonic testing, the two specimens both were reinstalled into the test setup. The test was performed like previous tests, with a 12 ksi stress range and a 10 ksi stress mean.

The Field Repair specimen failed first due to a loss of stiffness, though it also failed differently than in typical fatigue tests. Instead of failing in the typical manner, where the toe of the weld meets the shaft of the pole, this specimen failed in the middle between two weld passes. Figure 4.20 shows this failure. Bends 10, 11, and 12 all had large fatigue cracks exhibiting this failure through the weld.

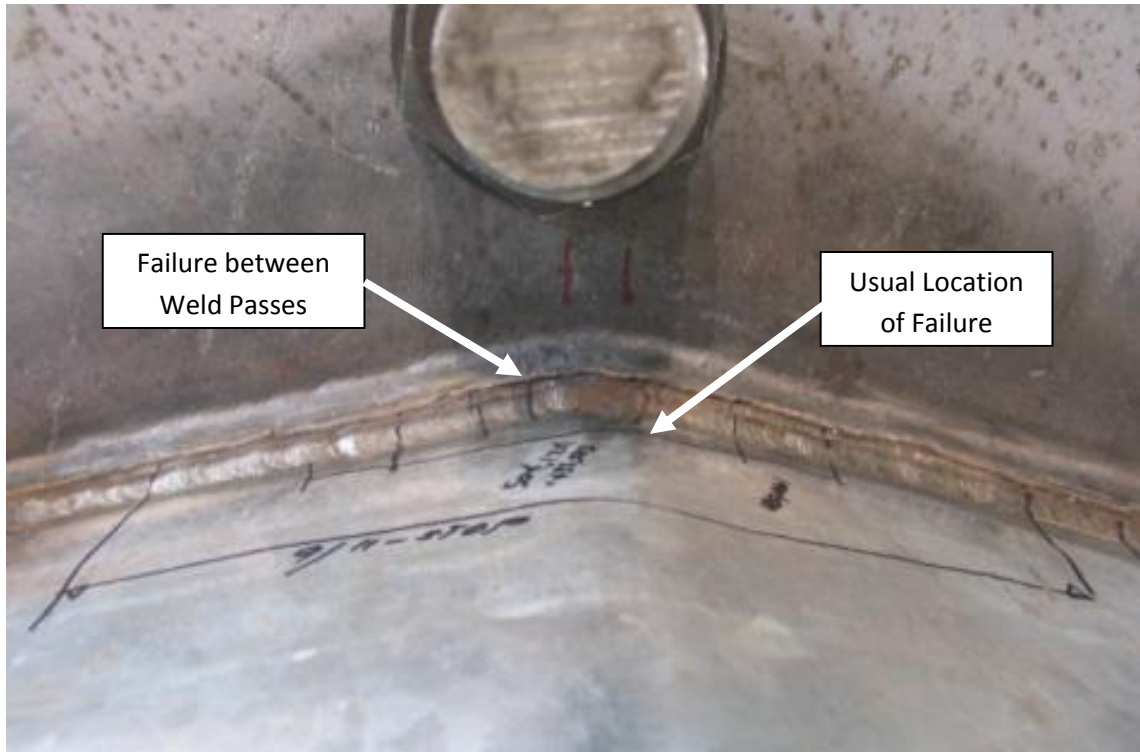


Figure 4.20 Bend 11 of Specimen Field Repair with Failure through Weld

This failure occurred after 1,467,734 cycles, which places the Field Repair specimen in the D category, and shows a substantial improvement from the fatigue strength of the specimen prior to weld repair. This type of failure also progressed much slower than previous failures. The crack became visible after approximately 600,000 cycles, but no substantial loss in stiffness occurred until just before failure. The slow rate of propagation is possibly due to the fatigue cracks progressing through the thicker weld profile instead of the thinner shaft. This slow loss of stiffness highlights another advantage to the use of the weld repairs: visible cracks can be found long before the system is likely to fail.

The Field Repair specimen was rotated and testing was restarted. Testing was stopped after 1,893,306 total cycles had been applied to the Shop Repair specimen. No cracks were found in the shop repair specimen when ultrasonically inspected at the end of the test. The test was stopped because the number of cycles to which the specimen had been subjected indicates a

substantial improvement in the fatigue strength compared to the galvanized specimen without the weld repair. It was also believed that the stress range that the test was running at was too low to fail the specimen, which would lead to the specimen being termed a “run out” and would indicate that the specimen is at least a category D, if not better. Figure 4.21 displays these results on an S-N plot.

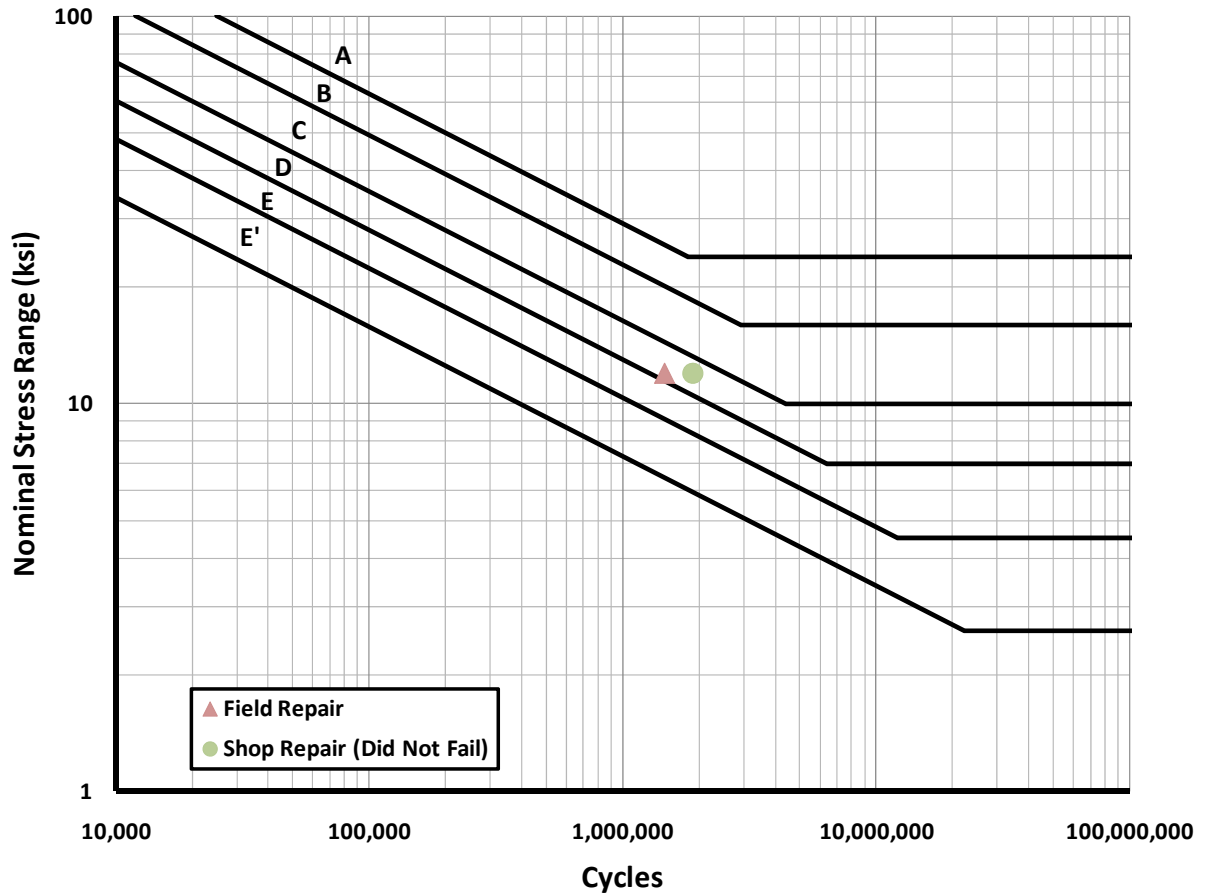


Figure 4.21 S-N Plot of Weld Repair Specimens

#### 4.4.3 Destructive Testing Results

Destructive examination is currently underway for these samples. No bends have been opened yet; therefore there are no destructive testing results. The results from these destructive tests will likely be written up in Kleineck (2011).

#### 4.5 Specimens 33-3-12-TXEC-SG-A and 33-3-12-TXEC-SG-B

The final pair of specimens tested was the pair designed with an external collar. This pair of specimens was fabricated by the same fabricator as specimens 33-3-12-TX-SG-A and 33-3-12-TX-SB-B. The galvanizing of each specimen, however, was performed by two different galvanizers. This was done to check the influence of galvanizer upon the initial cracking.

##### 4.5.1 Ultrasonic Testing Results

Ultrasonic testing was first performed on the specimens by a trained TxDOT inspector. Both the connection of the collar to the base plate and the connection of the collar to the pole were inspected. No crack indications were found at the connection of the external collar to the pole. Figure 4.22 shows the locations that were inspected and Figure 4.23 displays the results of this inspection. The inspector did note that typical crack depths were around  $\frac{1}{16}$ " , shallower than on the specimens without external collars.



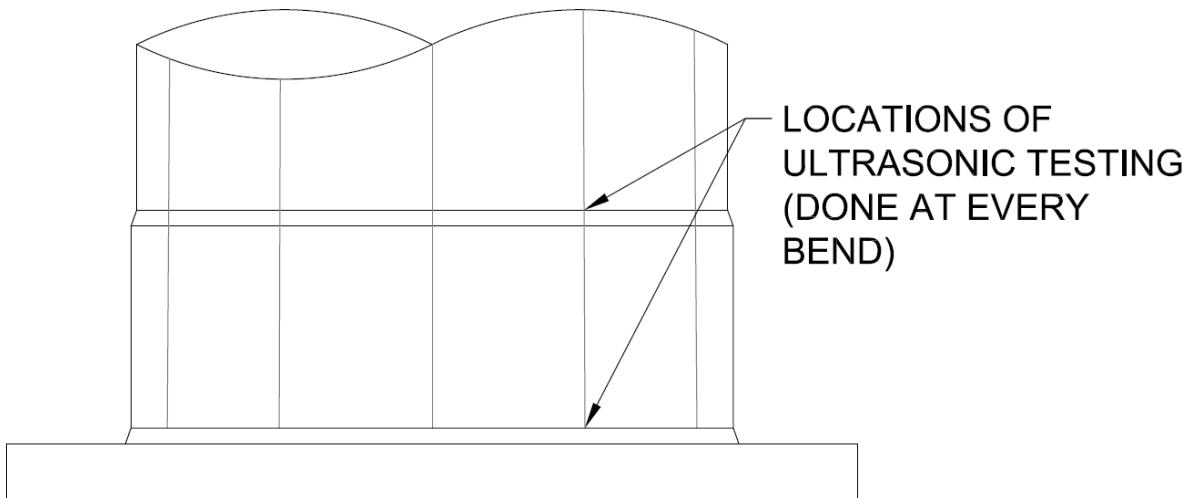


Figure 4.22 Locations Inspected Using Ultrasonic Testing on External Collar Samples

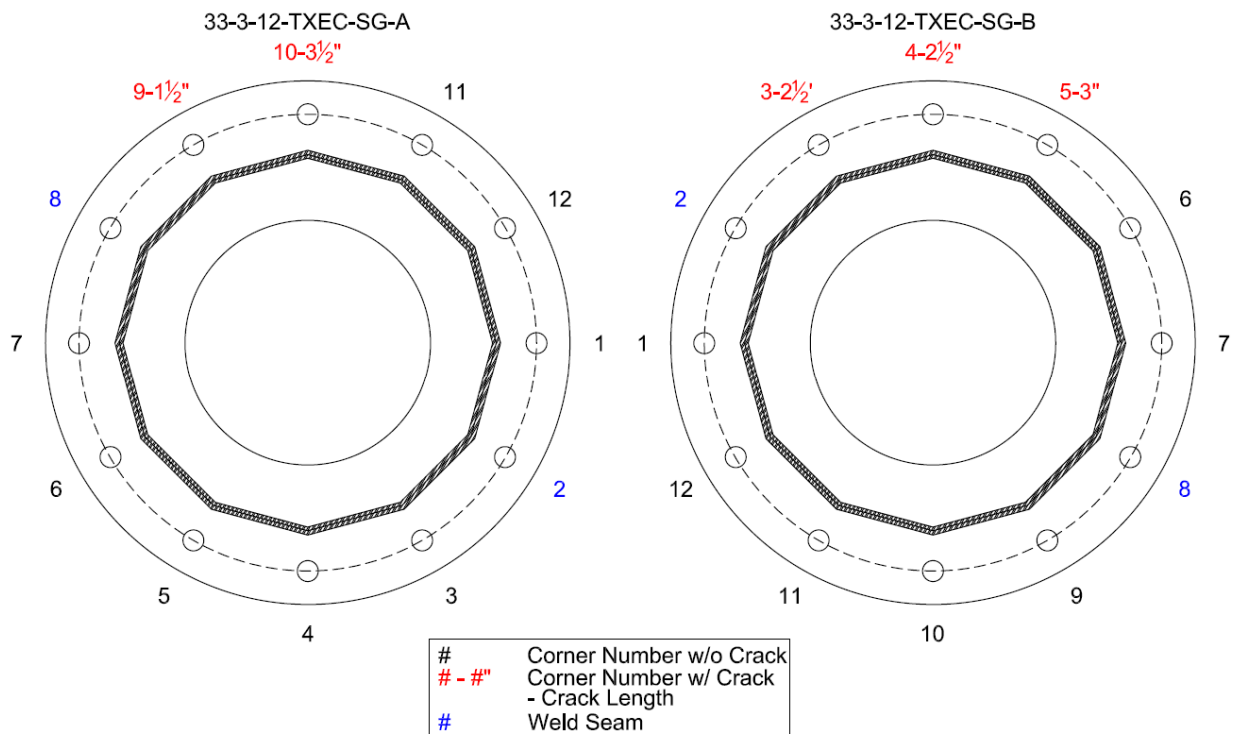


Figure 4.23 Crack Indications, Lengths, and Initial Orientation of External Collar Samples

#### 4.5.2 Fatigue Testing Results

After ultrasonic testing both samples were installed into the fatigue test setup. Unlike previous samples, these samples were run at a mean stress of 6 ksi and a stress range of 6 ksi. This lower stress range and mean stress was chosen to test more closely to stresses that are likely to occur in the field.

The samples ran for 7,374,384 cycles. There was no noticeable drop in stiffness or visible cracks. The test was stopped and determined to be a “run out”, meaning that the stress range was too low to cause fatigue damage on the specimens and giving the specimens at least a Category E rating. Ultrasonic testing afterwards confirmed this as only the original initial crack indications were found. Figure 4.24 shows where these specimens fall on an S-N plot. Note that, as before, both specimens are denoted by a single data point.

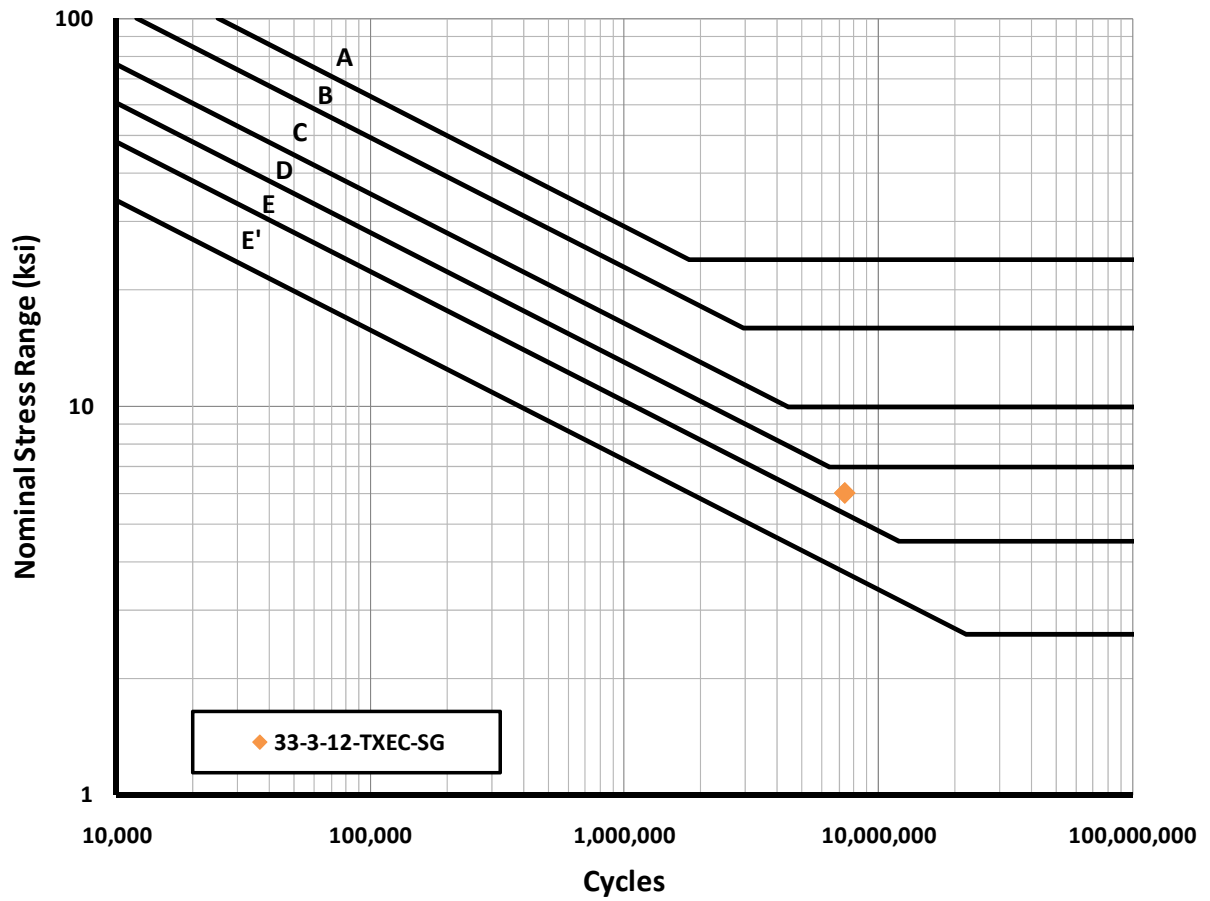


Figure 4.24 S-N Plot of External Collar Samples

#### 4.5.3 Destructive Testing Results

Destructive testing has begun on this specimen pair but has not been completed. Because of this, no destructive testing results are reported. The results from the destructive tests will likely be written up Kleineck (2011).

## 4.6 Ultrasonic Testing Results Comparison

This section compares the results of the ultrasonic inspections of high masts for initial cracks only. This comparison is the beginning of an attempt to determine what variables have an effect on the likelihood of initial cracks appearing. Due to how few specimens have been tested and the inherent variability of the initial cracks, it is difficult to perform a statistical analysis of the results.

The variables that are compared are the fabricator, galvanizer, detail design, and volume ratio. The fabricator and galvanizer variables are checked to determine if the cracks are manufacturer related. The detail design variable, such as what type of connection and what TxDOT design, can help determine geometric variables. Finally, the volume ratio variable is based on information taken from previous research into this phenomenon and discussed in Chapter 1. The volume ratio is derived by taking the volume of the base plate and dividing it by the volume of the first 12 inches of the shaft. For poles with external collars this includes the area of the external collar.

### 4.6.1 Specimen Comparison

First, specimens within this study are compared amongst each other. The results of its ultrasonic test before galvanizing of the black specimen, 33-3-12-TX-SB-B, is not included because it did not contain any cracks. However, the results after this specimen was galvanized are included. Also, the results of the ultrasonic testing of the weld repair specimens are not included since the weld repairs removed all initial cracks. Table 4.1 shows the specimen matrix from this study along with ultrasonic testing results and variables that may impact initial cracking.

Specimen Code	Detail	Volume Ratio	Fabricator	Galvanizer	Bends Tested	Crack Indications	% Bends Cracked
33-3-12-TX-SG-A	Full Penetration	10.16	A	A	10	10	100.0%
33-3-12-TX-SB-B (after galvanizing)	Full Penetration	10.16	A	A	12	9	75.0%
33-3-12-TX-VG-A	Full Penetration	10.16	B	B	10	3	30.0%
33-3-12-TX-VG-B	Full Penetration	10.16	B	B	10	4	40.0%
33-3-12-TXEC-SG-A	External Collar	4.57	A	C	12	2	16.7%
33-3-12-TXEC-SG-B	External Collar	4.57	A	A	12	3	25.0%
24-3-16-TX-PG-A	Full Penetration	9.21	C	D	8	0	0.0%
24-3-16-WY-PG-B	Full Penetration (with backing bar)	9.21	C	D	8	0	0.0%

Table 4.1 Ultrasonic Testing Results for All Specimens

Two specimens from the previous Pooled Fund Study are included in table above. The two specimens are a similar design to those used in this study, with the major exceptions being that they have a smaller shaft diameter and base plate diameter and are 16 sided. They were also fabricated and galvanized by different suppliers than the specimens from this study. These specimens were ultrasonic tested after fatigue testing had already been completed, therefore only bends that had not been fatigued (on the compression side during testing) were checked for initial cracks. No cracks were found in either of these specimens.

As can be seen from the above figure, it is difficult to draw many conclusions from the data present. It appears both fabricator A and galvanizer A have higher rates of incidence than the others. Also, external collars appear to decrease the number of instances of initial cracking. Again, more data is required to verify these results.

#### 4.6.2 Detail Comparison Including TxDOT Inspections

There is an ongoing inspection of TxDOT's inventory of high mast poles and, to provide more data for comparison, the results of TxDOT ultrasonic inspections on both in-situ masts, denoted as "Field", and masts prior to erection, denoted as "Shop", are included in this section. Poles tested in this study are denoted as "Lab" and are placed under the TxDOT detail category they are meant to replicate, typically the 150'-80 mph full penetration or external collar design. The two

specimens tested from the Pooled Fund Study discussed above are also included; their design is similar to the 100'-80 mph full penetration TxDOT design.

It is important to note that the ultrasonic results of the “Field” poles may be skewed by the presence of fatigue cracks. This is because the poles were erected prior to testing and have undergone cycles of fatigue loading. Whether or not the stress range of this fatigue loading has been high enough to cause fatigue cracks is difficult to tell without destructive analysis. Future research may help refine these results.

The data provided by TxDOT does not include fabrication information; therefore only detail information and the volume ratio are compared. Also, two field tested poles did not include how many bends were tested and how many were cracked, only that the poles contained cracks. Table 4.2 displays this information.

Design	Detail	Location	Volume Ratio	# Poles Tested	# Poles Cracked	% Poles Cracked	# Bends Tested	# Bends Cracked	% Bends Cracked
175'-80 mph	Full Penetration	Field	8.54	17	9	52.9%	-	-	58.0%
	External Collar	Field	4.23	1	1	100.0%	-	-	-
150'-80 mph	Full Penetration	Field	10.16	13	13	100.0%	-	-	52.0%
		Lab	10.16	4	4	100.0%	42	26	61.9%
	External Collar	Field	4.57	1	1	100.0%	-	-	17.0%
		Lab	4.57	2	2	100.0%	20	7	35.0%
		Shop	4.57	2	2	100.0%	-	-	21.0%
125'-80 mph	Full Penetration	Field	9.78	3	1	33.3%	-	-	11.1%
	External Collar	Field	4.39	1	1	100.0%	-	-	-
100'-80 mph	Full Penetration	Field	9.91	3	2	66.7%	-	-	8.3%
		Lab	9.21	2	0	0.0%	16	0	0.0%

Table 4.2 TxDOT and Study Specimen Ultrasonic Testing Results

From these results it can be seen that, compared to the TxDOT poles, the study specimens had a higher percentage of bends with initial cracks. This holds true except for the 100'-80 mph design, where no cracks were found in lab specimens but a small percentage of bends were cracked in field specimens. Aside from this discrepancy, the some of the same trends are apparent in both

the TxDOT poles and the study specimens. For example, for the 150'-80 mph designed poles the external collar detail consistently contains fewer cracks than the detail without the external collar. Also, the smaller 100'-80 mph design contains fewer cracks than the larger design sizes.

A comparison of volume ratio to crack probability is shown in Table 4.3. "EC" on the graph stands for poles with an external collar. Included in this is a linear approximation of the probability of toe cracks vs. volume ratio from Aichinger and Higgins (2006) discussed in Chapter 1. From this graph, a slight trend can be seen following what the Valmont paper had predicted. This is evident in the larger 150' and 175' design poles, but the trend is not followed by the two smaller designs.

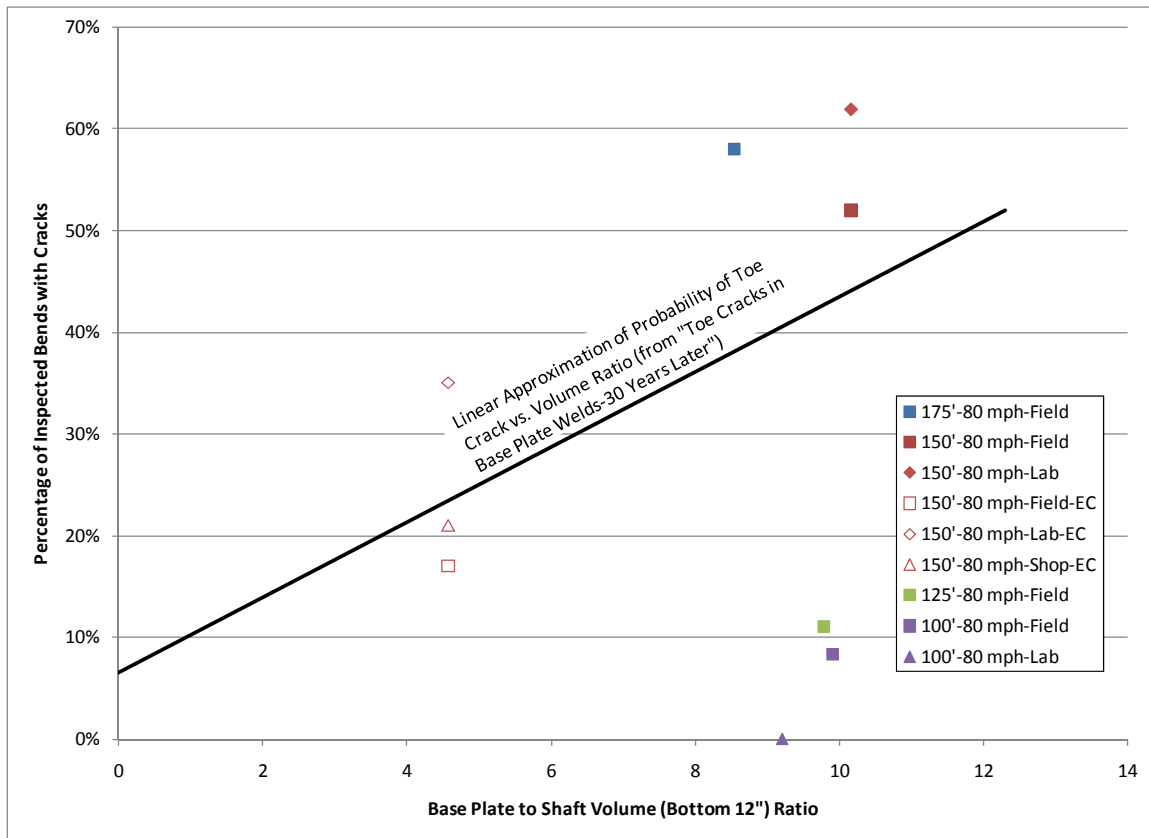


Table 4.3 Percentage of Cracks Found Compared to Ratio of the Volume of the Base Plate to the Volume of the Shaft

#### 4.7 Fatigue Test Comparisons

This section compares the fatigue test results of the specimens. It also utilizes fatigue test results of specimens from the Pooled Fund Study for comparison.

Figure 4.30 shows the results of all of the specimens' fatigue tests plotted on one S-N plot. AASHTO fatigue design curves are included for reference. The AASHTO Specification places these details as Category E fatigue details. It is evident from curve that only the repaired specimens and the external collar specimens were able to attain this fatigue life, indicating that the AASHTO Specifications are possibly unconservative.

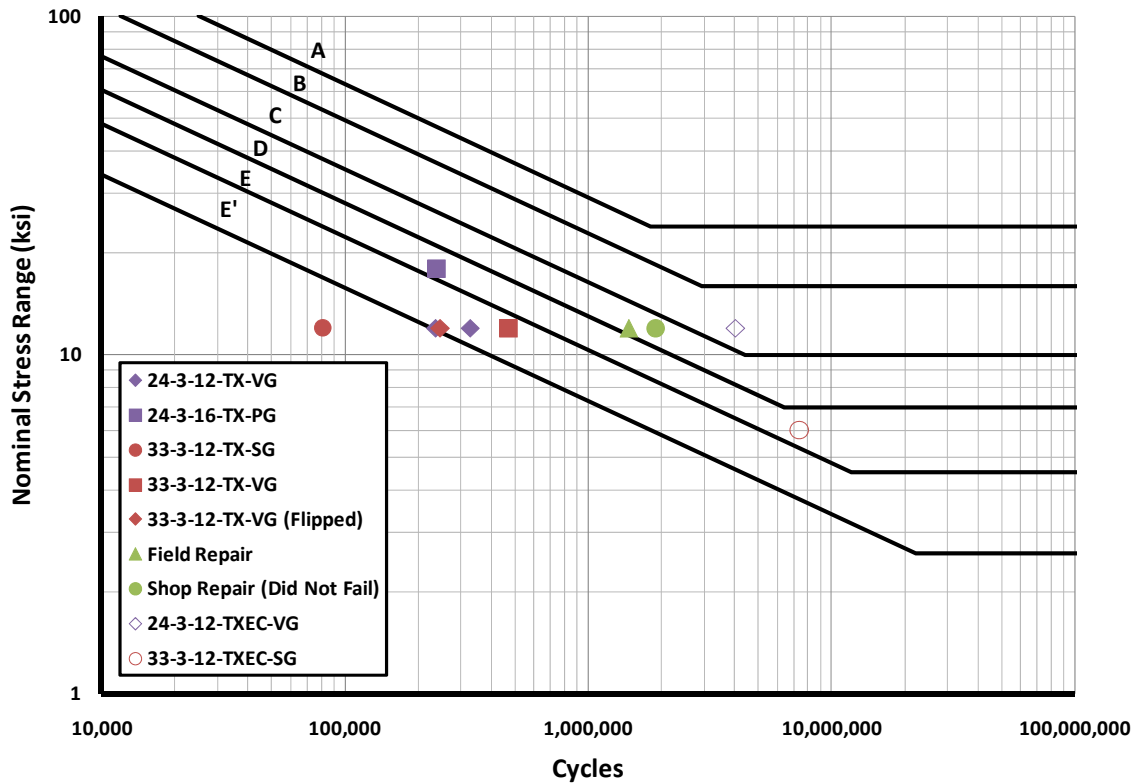


Figure 4.30 S-N Plot of All Specimens

The bar chart in Figure 4.31 is another way of showing these results. The number of cycles has been normalized for a 12 ksi stress range to aid in comparison between specimens. From this chart the beneficial effects of adding an external collar or performing weld repairs can clearly be seen.



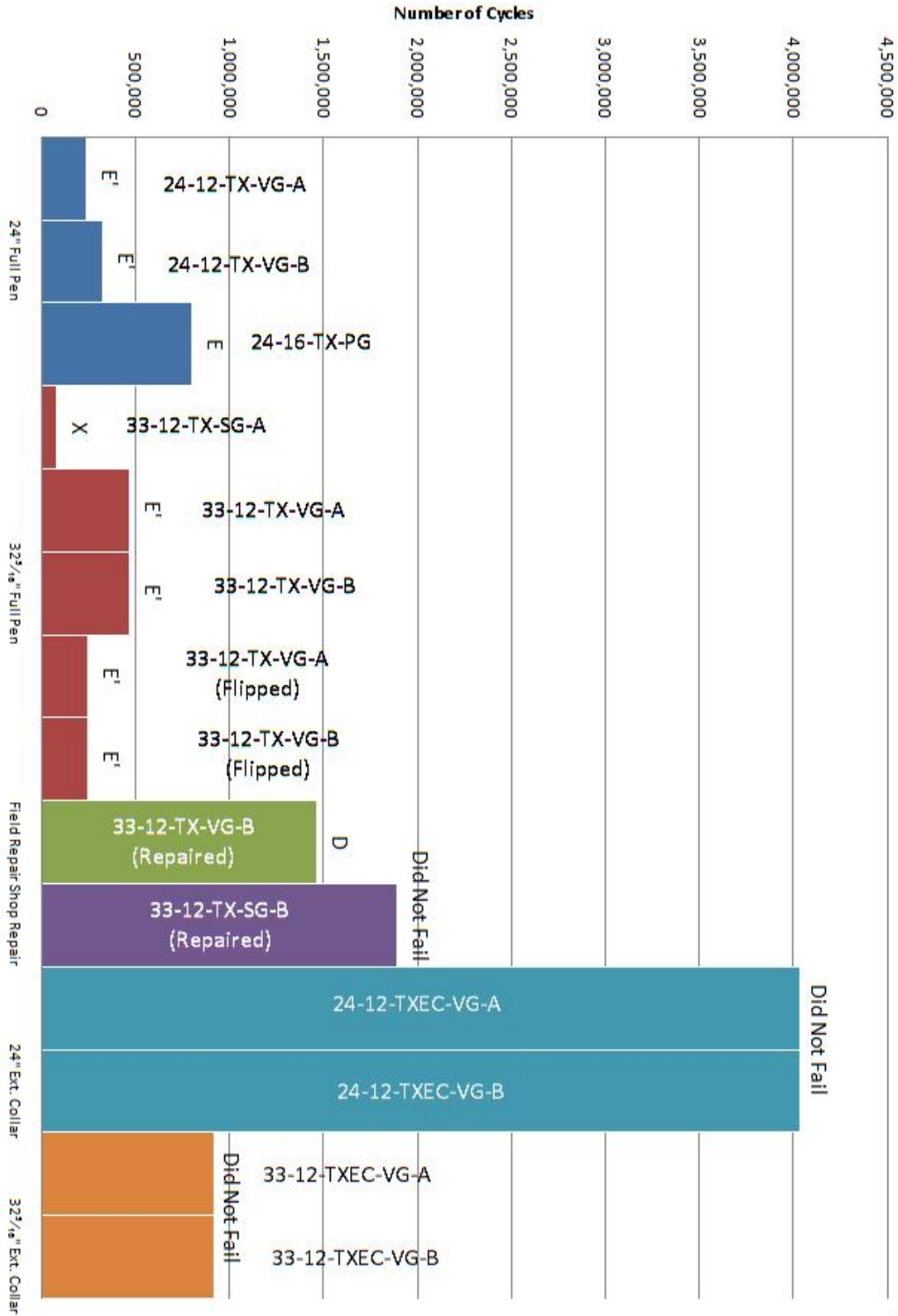


Figure 4.31 Fatigue Results by Specimen Normalized for 12 ksi Stress Range

## Chapter 5 Conclusions

### 5.1 Introduction

This thesis has provided a summary of tests conducted on high mast illumination poles commonly used in the state of Texas. The study consisted of preliminary inspection testing, fatigue tests, and destructive tests to investigate the sizes of initial cracks and the extent of crack growth that occurred during the fatigue tests. A total of 8 HMIP's were tested. Based upon the results of the study, a number of conclusions can be made. These conclusions are divided into three sections based on what portion of testing allowed for the conclusion to be drawn.

### 5.1 Ultrasonic Testing Conclusions

- Only poles that have been galvanized appear to contain initial cracks.
- No correlation can be drawn as yet between fabricator or galvanizer and the likelihood of an initial crack occurring. More data on this will help with comparing the results between different suppliers.
- Larger diameter poles, such as the 175' and 150' TxDOT designs, are more likely to have initial cracks than smaller diameter poles
- The cracking occurrences increase in larger poles as the ratio of the volume of the base plate to the volume of the first 12 inches of shaft increases.
- Similarly, poles with external collars, and in turn lower volume ratios, are less likely to contain initial cracks.

## 5.2 Fatigue Testing Conclusions

- Galvanized poles have a lower fatigue life than ungalvanized poles.
- Initial cracks lower the fatigue life on poles that do not have external collars
- External collars provide protection to the weld on the pole. This increases the fatigue life of the pole.
- Weld repairs drastically increase the fatigue life of a pole. This is true for both shop repairs utilizing the FCAW procedure and the field repair utilizing the SMAW procedure.

## 5.3 Destructive Testing Conclusions

- Initial crack indications are consistent with cracks found during destructive examination. Although the indications do not always accurately measure the entire length of the crack, they do not overestimate crack size.
- Initial cracks form from a different fracture mechanism than fatigue cracks.

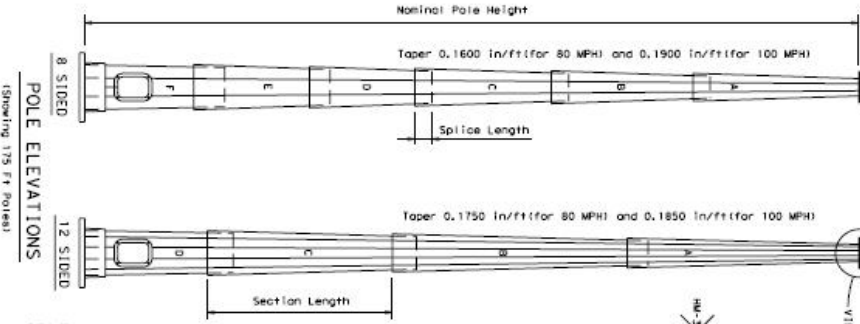
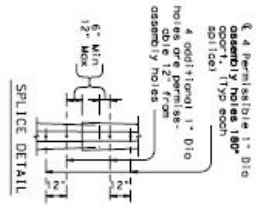
## 5.4 Future Work

Currently, work is underway to continue studying the effects of galvanization on the fatigue life of HMIP's. A thermal analysis is in progress. This involves taking thermal readings to determine temperature changes in poles during galvanizing. Two poles were instrumented with thermal couples and monitored through the galvanizing process that was conducted at two different galvanizers. The thermal couple data provided valuable information on the temperature gradients that occur during the galvanizing process. The data was used to validate a three dimensional finite element model. Also, more specimens with varying connections and geometries are currently being designed for additional thermal tests. Similar to the previous two specimens, thermal couples will be applied to the base plate and shaft to measure the thermal gradients during the galvanizing process. These specimens will have a shorter pole shaft length than the

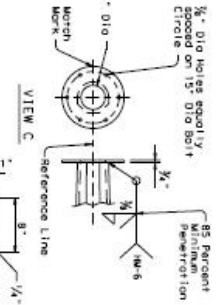
specimens fatigue tested and discussed in this thesis. The new specimens will only be subjected to ultrasonic testing and destructive testing to determine whether they contain initial cracks.

Finally, a separate study into the wind loading conditions on an HMIP is started. In-situ poles are being instrumented with anemometers and strain gages to record the wind history as well as the corresponding strains induced in the HMIP. The anemometer measures both the wind speed and the direction. The data from these studies will provide valuable information on the actual stress history that the poles experience so that a picture of what type of fatigue damage typical poles may see can be made. This data will be utilized to help determine which poles are in particular trouble and in need of repair.

Appendix A: Texas Department of Transportation's Standard Plans for High Mast  
Illumination Poles

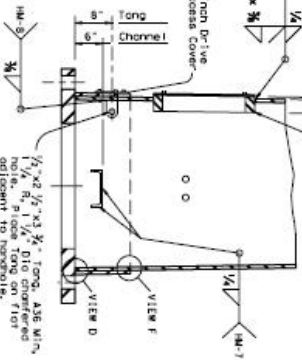


POLE ELEVATIONS (Showing 175 Ft Pole)



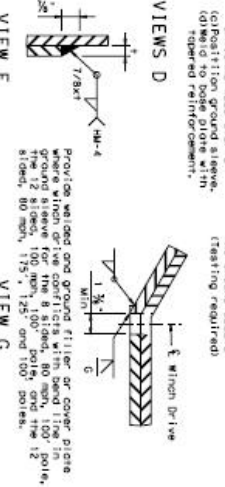
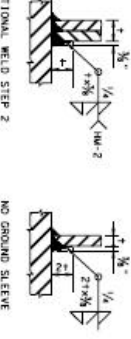
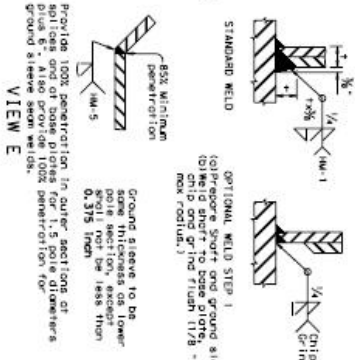
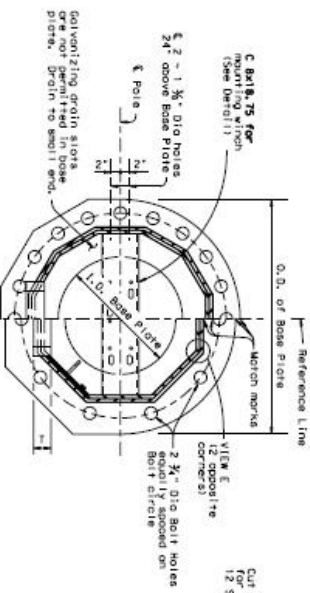
WINCH DRIVE ACCESS COVER

Provide 3- 1/2\"/>

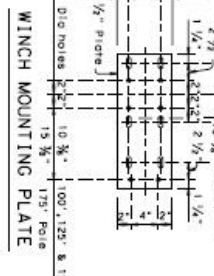
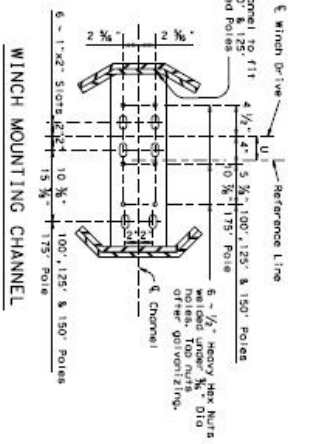


SECTION B-B

SECTION A-A



WINCH MOUNTING CHANNEL



WINCH MOUNTING PLATE

STANDARD PLANS ILLUMINATION DEPARTMENT OF TRANSPORTATION TRAFFIC OPERATION DIVISION

**HIGH MAST ILLUMINATION POLES**

100' - 125' - 150' - 175'

100' - 125' - 150' - 175'

HMIP(1)-98

SHEET 1 OF 2

DATE	DESIGNER	CHECKER	APPROVER

**TABLE OF VARIABLE POLE DIMENSIONS**

Hi Section (ft)	8 SIDED POLE				12 SIDED POLE						
	Diameter (Inches)	Height (feet)	Length (feet)	Splice (Inches)	Diameter (Inches)	Height (feet)	Length (feet)	Splice (Inches)			
175	A	13,083	7,750	250	33,33	19	16,792	7,750	250	51,67	24
	B	17,792	12,205	375	34,92	25	24,858	15,817	313	51,67	36
	C	22,250	16,583	375	35,42	32	32,625	23,583	313	51,67	48
	D	25,375	20,948	438	27,67	36	36,250	31,175	375	29,00	-
	E	28,375	23,895	500	28,00	41	-	-	-	-	-
	F	31,250	26,703	500	28,42	-	-	-	-	-	-
150	A	13,083	7,750	250	33,33	19	16,792	7,750	250	51,67	24
	B	17,792	12,205	375	34,92	25	24,858	15,817	313	51,67	36
	C	22,250	16,583	375	35,42	32	32,625	23,583	313	51,67	48
	D	25,375	20,948	438	27,67	36	36,250	31,175	375	29,00	-
	E	28,375	23,895	500	28,00	41	-	-	-	-	-
	F	31,250	26,703	500	28,42	-	-	-	-	-	-
100	A	13,083	7,750	250	33,33	19	16,792	7,750	250	51,67	24
	B	17,792	12,205	375	34,92	25	24,858	15,817	313	51,67	36
	C	22,250	16,583	375	35,42	32	32,625	23,583	313	51,67	48
	D	25,375	20,948	438	27,67	36	36,250	31,175	375	29,00	-
	E	28,375	23,895	500	28,00	41	-	-	-	-	-
	F	31,250	26,703	500	28,42	-	-	-	-	-	-

Diameters are measured across the flange.

**TABLE OF VARIABLE BASE DIMENSIONS**

Hi Section (ft)	O.D. (Inches)	I.D. (Inches)	8 SIDED POLE		12 SIDED POLE	
			Bolt Cir. (Inches)	No. Bolts	No. Bolts	5 (Inches)
175	47	22	41	16	2,00	3,75
	44	18	38	12	2,00	4,00
	41	16	35	8	2,00	4,50
	37	14	31	6	2,00	5,00
	34	12	28	4	2,00	5,50
	31	10	25	3	2,00	6,00
150	52	27	46	20	1,75	3,50
	49	23	43	16	1,75	4,00
	45	21	39	12	1,75	4,50
	41	17	34	10	1,75	5,00
	37	14	30	8	1,75	5,50
	34	12	27	6	1,75	6,00
100	52	27	46	16	1,75	3,50
	50	25	44	12	1,75	3,50
	48	22	40	10	1,75	3,75
	46	20	38	8	1,75	4,00
	44	18	36	6	1,75	4,25
	42	16	34	4	1,75	4,50

NOTE: Base plate may be found or with 8 or 12 round segments matching the pole.

**GENERAL NOTES:**

Design conforms to ASCE Standard Specifications for Steel Structures and Light Towers, Luminaires, and Traffic Signals and Interiors - Signs, etc. The design wind speed is 80 mph or 100 mph as shown elsewhere in the plans.

Each pole section, top flange plate and base plate shall be permanently marked on the reference end with the manufacturer's name, the baseplate, top plate, and foundation pin details. These marks shall be used in pole assembly to ensure proper orientation and alignment of the pole section and its components at the center of the pole unless otherwise shown on lighting layouts.

**STANDARD PLANS**  
**TEXAS DEPARTMENT OF TRANSPORTATION**  
*Traffic Operations Division*

**HIGH MAST ILLUMINATION POLES**

100' - 125' - 150' - 175'

SHEET 2 OF 2 HMIP (2) - 98

5-88 - Revised 1995  
 5-88 - Revised 1995  
 5-88 - Revised 1995

DATE	BY	CHKD	APP'D

## References

1. Aichinger, R., Higgins, W., Toe Cracks in Base Plate Welds – 30 Years Later. Valmont Industries, Nebraska, 2006
2. American Association of State Highway and Transportation Officials, AASHTO Standard Specifications for Structural Supports for Highway Signs, Luminaries and Traffic Signals. Fourth Edition, AASHTO, Washington, D.C., 2001.
3. American Welding Society, AWS D1.1/D1.1M:2008 An American National Standard: Structural Welding Code – Steel. Twenty First Edition, AWS, Miami, Florida, June 2008
4. Anderson, T.H., Fatigue Life Investigation of Traffic Mast-Arm Connection Details. M.S. Thesis, Department of Civil Engineering, The University of Texas at Austin, August 2007.
5. High Mast Illumination Poles. Standard Plans, Texas Department of Transportation (TXDOT), August 1995.
6. Kinstler, T.J., Current Knowledge of the Cracking of Steels During Galvanizing. GalvaScience LLC, Springfield, Alabama, 2006
7. Koenigs, et al., Fatigue Resistance of Traffic Signal Mast-Arm Connections. Texas Department of Transportation, Research Report 4178-2, Center for Transportation Research, August 2003.
8. Richman, N.B., Fatigue Life Investigation of High Performance Mast Arm Base Plate Connections. M.S. Thesis, Department of Civil Engineering, The University of Texas at Austin, May 2009
9. Rios, C.A., Fatigue Performance of Multi-Sided High-Mast Lighting Towers. M.S. Thesis, Department of Civil Engineering, The University of Texas at Austin, May 2007.
10. Stam, A.P., Fatigue Performance of Base Plate Connections Used in High Mast Lighting Towers. M.S. Thesis, Department of Civil Engineering, The University of Texas at Austin, May 2009



## Vita

Charles Stephen Pool was born in Euless, Texas on June 14, 1985 to Mike and Linda Pool. After completing his primary education at Trinity High School in 2004, he went on to attend the University of Texas at Austin. He graduated with a degree Bachelors in Science in May, 2008. Afterwards, he enrolled in the University of Texas at Austin to pursue a Master's Degree.

**Permanent Address:** *3832 Ashbury Lane*  
*Bedford, TX 76021*  
*cspool12@gmail.com*

This thesis was typed by the author.